

Air Force Institute of Technology

AFIT Scholar

Theses and Dissertations

Student Graduate Works

6-1994

Mixed H_2 - H_∞ Optimization with Multiple H Infinity Constraints

Julio C. Ullauri

Follow this and additional works at: <https://scholar.afit.edu/etd>



Part of the [Aerospace Engineering Commons](#), and the [Controls and Control Theory Commons](#)

Recommended Citation

Ullauri, Julio C., "Mixed H_2 - H_∞ Optimization with Multiple H Infinity Constraints" (1994). *Theses and Dissertations*. 6638.

<https://scholar.afit.edu/etd/6638>

This Thesis is brought to you for free and open access by the Student Graduate Works at AFIT Scholar. It has been accepted for inclusion in Theses and Dissertations by an authorized administrator of AFIT Scholar. For more information, please contact AFIT.ENWL.Repository@us.af.mil.

AD-A280 572



DTIC
ELECTE
JUN 23 1994
S B D

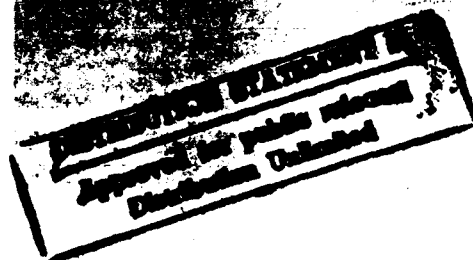
MIXED H_2/H_{∞} OPTIMIZATION WITH
MULTIPLE H_{∞} CONSTRAINTS

THESIS

Julio C. Ullauri, B.S.

1Lt, Ecuadorian Air Force

AFIT/GAE/ENY/94J-04



DTIC QUALITY INSPECTED A

DEPARTMENT OF THE AIR FORCE
AIR UNIVERSITY

AIR FORCE INSTITUTE OF TECHNOLOGY

Wright-Patterson Air Force Base, Ohio


AFIT/GAE/ENY/94J-04

MIXED H_2/H_∞ OPTIMIZATION WITH
MULTIPLE H_∞ CONSTRAINTS
THESIS

Julio C. Ullauri, B.S.

1Lt, Ecuadorian Air Force

AFIT/GAE/ENY/94J-04

1368 94-19303


Approved for public release; distribution unlimited

94 6 23 127

AFIT/GAE/ENY/94J-04

MIXED H_2/H_∞ OPTIMIZATION WITH MULTIPLE
 H_∞ CONSTRAINTS

THESIS

Presented to the Faculty of the Graduate School of Engineering
of the Air Force Institute of Technology
Air University

In Partial Fulfillment of the Requirements for the Degree of
Master of Science in Aeronautical Engineering

Julio C. Ullauri, B.S.
1Lt, Ecuadorian Air Force

June 1994

Accession For	
NTIS GRA&I	<input checked="checked" type="checkbox"/>
DTIC TAB	<input type="checkbox"/>
Unannounced	<input type="checkbox"/>
Justification	
By	
Distribution/	
Availability Codes	
Dist	Avail and/or Special
A-1	

Approved for public release; distribution unlimited

Acknowledgment

I wish to thank the many people that have helped me on this thesis, at AFIT and at Ecuador Air Force. Most important, the faculty members that I wish to thank are my thesis committee, consisting of Dr. Oxley and Lt. Col. Kramer, and my advisor, Dr. Ridgely. Also the support I have received from Lt. Col. Dave Walker has been incredible.

Lastly, and most importantly, I want to thank the persons that I love and have helped me so much, my wife Sandra, who I love with all my heart; and my little son Julio Jr. who helped me erasing some important files from the computer.

Con todo mi amor para ustedes my familia, que me soportó moralmente en todo momento a pesar de la distancia, nuestros corazones estuvieron unidos, gracias. A mi linda esposa, Sandra, y a mi adorable hijo Julito, los amo.

Dedicated to my wife Sandra and my son Julito.

Dedicado a mi esposa Sandra y a mi hijo Julito.

Julio C. Ullauri

Table of Contents

	Page
Preface	ii
List of Figures	vi
List of Tables	x
Notation	xi
Abstract	xiv
 I. Introduction	 1-1
 II. Background	 2-1
2.1 H_2 Optimization	2-2
2.2 H_∞ Optimization	2-4
2.3 Structured Singular Value	2-6
2.3.1 Structured Singular Value in Control Systems	2-8
2.3.2 Structured Singular Value Analysis	2-9
2.3.3 Structured Singular Value Synthesis	2-11
2.4 Nominal Performance, Robust Stability, and Robust Performance tests	2-12
2.5 Guaranteed MIMO Gain and Phase Margins using T and S	2-13
 III. Mixed H_2/H_∞ Optimization with a Single H_∞ Constraint	 3-1
3.1 Nonsingular H_∞ Constraint	3-2
3.2 Singular H_∞ Constraint	3-5
3.2.1 General Formulation	3-5
3.2.2 Numerical Solution	3-9

IV. Mixed H_2/H_∞ Optimization Problem with Multiple H_∞ Constraints	4-1
4.1 Development of Multiple Constraints	4-2
4.2 Multiple H_∞ Constraints: Numerical Methods	4-8
4.2.1 Grid Method	4-8
4.2.2 Direct Method	4-9
4.3 Feasible Solutions	4-11
4.3.1 Trade off between H_2 design and the $H_{\infty i}$ design	4-12
4.3.2 Trade off between $H_{\infty i}$ designs ($i=1,2$)	4-13
V. Numerical Validation through a SISO example	5-1
5.1 Problem Set-Up	5-1
5.2 H_2 Design	5-2
5.3 Mixed H_2/H_∞ Design with a Single H_∞ Constraint	5-5
5.3.1 Sensitivity Constraint Design ($H_2/H_{\infty 1}$)	5-5
5.3.2 Complementary Sensitivity Constraint ($H_2/H_{\infty 2}$)	5-7
5.3.3 Boundaries on the mixed H_2/H_∞ surface	5-9
5.4 Mixed H_2/H_∞ Optimization Problem with Multiple H_∞ Constraints	5-12
5.4.1 Grid Method	5-12
5.4.2 Direct Method	5-14
5.5 Conclusions for the Multiple H_∞ Constraints SISO case	5-17
VI. HIMAT Problem: a MIMO example	6-1
6.1 Problem Set Up	6-1
6.2 H_2 Design requirement	6-2
6.2.1 Weight Selection	6-2
6.2.2. H_2 Results	6-4

6.3 Mixed $H_2/H_{\infty,1}$ problem: H_{∞} Design to a multiplicative uncertainty at the input of the plant	6-7
6.4 Mixed $H_2/H_{\infty,2}$ problem: H_{∞} Design for Nominal Performance	6-12
6.5 Trade off between weighted Output Sensitivity and weighted Input Complementary Sensitivity	6-18
6.6 Multiple H_{∞} Constraints: H_{∞} design for Nominal Performance and Robust Stability: Weighted Input Complementary Sensitivity and Weighted Output Sensitivity	6-21
6.7 Mixed H_2/H_{∞} with Multiple Singular H_{∞} Constraints and Robust Performance: μ -Synthesis versus Mixed H_2/H_{∞} -Synthesis	6-27
6.8 Mixed H_2/H_{∞} design with three H_{∞} constraints	6-35
6.9 Summary	6-39
 VII Summary, Conclusions and Recommendations	 7-1
 Appendix A: The HIMAT problem (Data)	 A-1
A.1 Weighted Input Complementary Sensitivity Constraint	A-1
A.2 Weighted Output Sensitivity Constraint	A-2
A.3 Weighted Output Sensitivity and Weighted Input Complementary Sensitivity Constraints	A-3
A.4 Weighted Output Sensitivity ,Weighted Input Complementary Sensitivity and Weighted Output Complementary Sensitivity Constraints	A-5
Bibliography	BIB-1

List of Figures

Figure	Page
2-1 Closed Loop system T	2-1
2-2 H_2 Design Diagram	2-3
2-3 H_∞ Design Block Diagram	2-5
2-4 M- Δ feedback connection	2-8
2-5 Robust Performance Diagram	2-9
2-6 Nominal and Robust Performance specifications Diagram	2-10
 3-1 Mixed H_2/H_∞ Design Diagram	 3-1
3-2 H_2/H_∞ Boundary Plot	3-10
 4-1 Mixed H_2/H_∞ with Multiple H_∞ Constraints Design Diagram	 4-2
4-2 Grid Method	4-9
4-3 Direct Method	4-10
4-4 Direct method 3D and 2D projections	4-11
4-5 H_2/H_∞ feasible planes	4-12
4-6 Trade-off among H_2/H_∞ (feasible solutions)	4-13
4-7 Design region in the $\ T_{ed_1}\ _\infty / \ T_{ed_2}\ _\infty$ plane	4-14
4-8 H_2/H_∞ Projection of feasible solution	4-15
4-9 H_2/H_∞ Surface of Optimal and Suboptimal solutions	4-16
 5-1 H_2 Block diagram (F-16)	 5-3
5-2 Magnitude of Sensitivity and Complementary Sensitivity (dB)	5-4
5-3 Mixed H_2/H_∞ Block Diagram (Sensitivity Constraint)	5-5

5-4	$\ T_{zw}\ _2$ vs. $\ T_{ed,1}\ _\infty$ curve	5-7
5-5	Mixed H_2/H_∞ Block Diagram (Complementary Sensitivity Constraint)	5-8
5-6	$\ T_{zw}\ _2$ vs. $\ T_{ed,2}\ _\infty$ curve	5-9
5-7	$\ T_{ed,2}\ _\infty$ vs. $\ T_{ed,1}\ _\infty$ curve (H_2/H_∞ design)	5-10
5-8	$\ T_{ed,2}\ _\infty$ vs. $\ T_{ed,1}\ _\infty$ curve (H_2/H_∞ design)	5-11
5-9	3D $\ T_{zw}\ _2$ vs. $\ T_{ed,1}\ _\infty$ vs. $\ T_{ed,2}\ _\infty$ curve for H_2/H_∞ design and H_2/H_∞ design	5-11
5-10	$\ T_{ed,2}\ _\infty$ vs. $\ T_{ed,1}\ _\infty$ Grid Method	5-13
5-11	3D plot Grid Method $\ T_{zw}\ _2$ vs. $\ T_{ed,1}\ _\infty$ vs. $\ T_{ed,2}\ _\infty$	5-13
5-12	$\ T_{ed,2}\ _\infty$ vs. $\ T_{ed,1}\ _\infty$ Direct Method	5-14
5-13	3D plot Direct Method $\ T_{zw}\ _2$ vs. $\ T_{ed,1}\ _\infty$ vs. $\ T_{ed,2}\ _\infty$	5-15
5-14	$\ T_{ed,2}\ _\infty$ vs. $\ T_{ed,1}\ _\infty$ for both methods	5-16
5-15	$\ T_{zw}\ _2$ vs. $\ T_{ed,1}\ _\infty$ vs. $\ T_{ed,2}\ _\infty$ for both methods	5-16
5-16	Application of the mixed problem with multiple H_∞ constraints	5-18
6-1	H_2 Regulator Diagram (HIMAT)	6-3
6-2	Maximum Singular Values of Complementary Sensitivity	6-5
6-3	Maximum Singular Values of Sensitivity	6-5
6-4	Time Responses due to a step α_c and θ_c	6-6
6-5	Block Diagram of multiplicative uncertainty at the plant input	6-7
6-6	Magnitude of Multiplicative Uncertainty Weighting Function (dB)	6-9

6-7	$\ T_{zw}\ _2$ vs. $\ W_{del} T_i\ _\infty$ (4th order controller)	6-11
6-8	H_∞ design for Nominal Performance	6-12
6-9	Inverse of Performance Weighting Function, w_o	6-13
6-10	$\ T_{zw}\ _2$ vs. $\ W_p S_o\ _\infty$	6-15
6-11	Time Response due to a step angle of attack command (* controller from Table 6-4)	6-17
6-12	Time Response due to a step pitch angle command (* controller from Table 6-4)	6-17
6-13	Weighted Output Complementary Sensitivity Block Diagram	6-18
6-14	$\ W_{del} T_i\ _\infty$ vs. $\ W_p S_o\ _\infty$ for $H_2/H_{\infty 1}$ design and $H_2/H_{\infty 2}$ design (K 4th order)	6-19
6-15	$\ W_{del} T_i\ _\infty$ vs. $\ W_p S_o\ _\infty$ for $H_2/H_{\infty 2}$ design (K 4th)	6-20
6-16	$\ W_{del} T_o\ _\infty$ vs. $\ W_{del} T_i\ _\infty$ for $H_2/H_{\infty 1}$ design (K 4th)	6-20
6-17	Objectives of the mixed problem with two H_∞ constraints	6-22
6-18	Direct Method versus Single H_∞ constraint designs (HIMAT)	6-23
6-19	Trade off between weighted T_i and S_o (4th order controller)	6-24
6-20	Trade off between weighted T_i and S_o (8th order controller)	6-24
6-21	$W_{del}(s) T_i(s)$ Maximum Singular values (K_{mix} 8th order)	6-25
6-22	$W_p(s) S_o(s)$ Maximum Singular values (K_{mix} 8th order)	6-26
6-23	Block diagram for Robust Performance	6-27
6-24	Mixed H_2/H_∞ controllers and the effects on $\ M\ _\mu$	6-29
6-25	$\mu(M)$ of the 8th order Mixed controllers from Table 6-6	6-29
6-26	$\mu(M)$ of the μ -synthesis, $H_{\infty opt}$, and mixed H_2/H_∞ Controller control design	6-30
6-27	Magnitude of $W_p(s) S_o(s)$ for μ -Synthesis, H_∞ , and the Mixed H_2/H_∞	6-31

6-28	Magnitude of $W_{del}(s)T_i(s)$ for μ -Synthesis, H_∞ , and the Mixed H_2/H_∞	6-32
6-29	Magnitude of Sensitivity Function for μ -Synthesis, H_∞ , and the mixed H_2/H_∞	6-32
6-30	Magnitude of Complementary Sensitivity for μ -Synthesis, H_∞ , and the Mixed H_2/H_∞	6-33
6-31	Time response for a step angle of attack command	6-34
6-32	Time response for a step pitch angle command	6-34
6-33	Mixed H_2/H_∞ design with three H_∞ constraints Block Diagram	6-35
6-34	Time response α command	6-38
6-35	Time response θ command	6-39
A-1	Boundary for the fourth order controller with two and three H_∞ constraints	A-7
A-2	Boundary for the eight order controller with two and three H_∞ constraints	A-7

List of Tables

Table	Page
2-1 Induced norms	2-2
2-2 Test for Nominal Performance, Robust Stability, and Robust Performance	2-12
5-1 H_2 Results (F-16)	5-4
6-1 H_2 Results (HIMAT)	6-4
6-2 Input Complementary Sensitivity Design $\ T_{zw}\ _2$ and $\ W_{del}T_i\ _\infty$	6-10
6-3 Input Complementary Sensitivity Design VGM _{i.o} and VPM _{i.o}	6-11
6-4 Output Sensitivity Design $\ T_{zw}\ _2$ and $\ W_pS_o\ _\infty$	6-15
6-5 Output Sensitivity Design VGM _{i.o} and VPM _{i.o}	6-16
6-6 Mixed H_2/H_∞ with two H_∞ Constraints: $\ T_{zw}\ _2$, $\ W_{del}T_i\ _\infty$, and $\ W_pS_o\ _\infty$	6-22
6-7 Mixed H_2/H_∞ with two H_∞ Constraints VGM and VPM	6-26
6-8 μ Analysis for the HIMAT example	6-30
6-9 Mixed H_2/H_∞ with three H_∞ Constraints: $\ T_{zw}\ _2$, $\ W_{del}T_i\ _\infty$, $\ W_pS_o\ _\infty$, and $\ W_{del}T_o\ _\infty$	6-37
6-10 Mixed H_2/H_∞ with three H_∞ Constraints: VGM and VPM	6-38
6-11 (HIMAT) Selection of Controllers	6-40
7-1 Comparison of different Control Law Designs	7-3

Notation

\mathbf{R}	field of real numbers
$\mathbf{x}^T, \mathbf{A}^T$	vector/ matrix transpose
$\mathbf{A} > 0$ (< 0)	\mathbf{A} is positive (negative) semidefinite
$\bar{\sigma}(\mathbf{A})$	maximum singular value of \mathbf{A}
$\text{tr}(\mathbf{A})$	trace of $\mathbf{A} = \sum_{i=1}^n a_{ii}$
\mathbf{RH}_2	space of all real-rational, strictly proper, stable transfer functions
\mathbf{RH}_∞	space of all real-rational, proper, stable transfer functions
$\ \cdot\ _2$	matrix norm on L_2
$\ \cdot\ _\infty$	matrix norm on L_∞

$$\left[\begin{array}{c|c} \mathbf{A} & \mathbf{B} \\ \hline \mathbf{C} & \mathbf{D} \end{array} \right] \quad \text{transfer function notation} \equiv \mathbf{C}(\mathbf{sI} - \mathbf{A})^{-1} \mathbf{B} + \mathbf{D}$$

$$\mathbf{P}_2 = \left[\begin{array}{c|cc} \mathbf{A}_2 & \mathbf{B}_w & \mathbf{B}_{u_2} \\ \hline \mathbf{C}_z & \mathbf{D}_{zw} & \mathbf{D}_{zu} \\ \hline \mathbf{C}_{y_2} & \mathbf{D}_{yw} & \mathbf{D}_{yu} \end{array} \right] \quad \text{underlying } H_2 \text{ plant}$$

$$\mathbf{P}_\infty = \left[\begin{array}{c|cc} \mathbf{A}_\infty & \mathbf{B}_d & \mathbf{B}_{u_\infty} \\ \hline \mathbf{C}_c & \mathbf{D}_{cd} & \mathbf{D}_{cu} \\ \hline \mathbf{C}_{y_\infty} & \mathbf{D}_{yd} & \mathbf{D}_{yu} \end{array} \right] \quad \text{underlying } H_\infty \text{ plant}$$

$$J_\gamma \quad \text{performance index for the mixed problem}$$

λ	penalty on the error between the desired γ and the infinity-norm of T_{ed} .
$G^*(s)$	complex conjugate transpose of $G(s) \equiv G^T(-s)$
$\text{Ric}(M)$	Riccati operator on Hamiltonian matrix M
\inf	infimum
\sup	supremum
$a \equiv b$	a identically equal to b , a defined as b
ARE	Algebraic Riccati Equation
DFP	Davidon-Fletcher-Powell
LFT	Linear Fractional Transformation
LQG	Linear Quadratic Gaussian
SISO	Single-Input, Single-Output
MIMO	Multiple-Input, Multiple-Outputs
\in	element of
s	Laplace variable
ω	frequency variable
n_∞	number of H_∞ constraints
γ_i	value of the infinity norm corresponding to the transfer function T_{ed_i} , $i=1, \dots, n_\infty$
$\gamma^* \equiv \ T_{ed}\ _\infty$	when $K(s) = K_{\text{mix}}$
$\alpha^* \equiv \ T_{zw}\ _2$	when $K(s) = K_{\text{mix}}$
$\underline{\gamma}_i$	$\inf_{K \text{ stabilizing}} \ T_{ed_i}\ _\infty$
$\bar{\gamma}_i$	$\ T_{ed_i}\ _\infty$ when $K(s) = K_{\text{opt}}$
α	value of the two norm
α_o	$\inf_{K \text{ stabilizing}} \ T_{zw}\ _2$

L	Lagrangian
K_{2opt}	the unique $K(s)$ that yields $\ T_{zw}\ _2 = \alpha_o$
K_{mix}	mixed H_2/H_∞ controller
μ	structured singular value
Δ	unstructured or structured perturbation
D-K	D-K iteration that solves μ -synthesis
$S_i, (S_o)$	input (output) sensitivity transfer function
$T_i, (T_o)$	input (output) complementary sensitivity transfer function
VGM	Vector gain margin
VPM	Vector phase margin

Abstract

A general mixed H_2/H_∞ optimal control design with multiple H_∞ constraints is developed and applied to two systems, one SISO and the other MIMO. The SISO design model is normal acceleration command following for the F-16. This design constitutes the validation for the numerical method, for which boundaries between the H_2 design and the H_∞ constraints are shown. The MIMO design consists of a longitudinal aircraft plant (short period and phugoid modes) with stable weights on the H_2 and H_∞ transfer functions, and is linear-time-invariant. The controller order is reduced to that of the plant augmented with the H_2 weights only. The technique allows singular, proper (not necessarily strictly proper) H_∞ constraints. The analytical nature of the solution and a numerical approach for finding suboptimal controllers which are as close as desired to optimal is developed. The numerical method is based on the Davidon-Fletcher-Powell algorithm and uses analytical derivatives and central differences for the first order necessary conditions. The method is applied to a MIMO aircraft longitudinal control design to simultaneously achieve Nominal Performance at the output and Robust Stability at both the input and output of the plant.

I. Introduction

Recently, there has been a great deal of interest in formulating a mixed H_2/H_∞ control methodology which can handle bounded spectrum and bounded energy inputs simultaneously. Early approaches included solving the problem for one input/one output, one input/two outputs and two inputs/two outputs ([BH89]; [KDGB90]; [DZB89]; [YBC90]; [MG88]; [MG90]; [KR91]). The general formulation of the mixed problem with two exogenous inputs and two controlled outputs was first approached for full state feedback in [KR91]. Ridgely, Valavani, Dahleh and Stein [RVDS92] developed a solution for the general mixed H_2/H_∞ problem with output feedback which results in a controller order equal to or greater than the order of the underlying system augmented the H_2 weighting and the H_∞ weighting. Also, the assumption is made that the underlying H_∞ problem is regular and has no feedforward term. Walker and Ridgely [WR94a] reformulated the general mixed H_2/H_∞ problem with the strictly proper and regularity assumptions relaxed to allow singular, proper H_∞ constraints. Furthermore, Walker and Ridgely showed strong theoretical results for controllers selected to have orders equal to or greater than the order of the underlying H_2 problem.

Multiple objective optimal control, as formulated by the above, allows the designer to determine the tradeoff between noise rejection (H_2) and some unstructured perturbation (H_∞), which embodies desired performance and margins at either the input or output of the plant (or some combination). However, the unstructured perturbation approach to the H_∞ problem is generally conservative. A better approach is to exploit the structure of the perturbations [DWS82], but the single H_∞ constraint in the mixed H_2/H_∞ setup is unable to do this. Doyle [Doy82] introduced structured singular value (μ) synthesis to design controllers which are less conservative. While this approach handles structured

uncertainties, the current μ -synthesis method generally results in a large controller order. It is desired to develop a control synthesis method which can reduce the controller order below that of μ -synthesis. One approach to this problem is to consider each perturbation as an individual H_∞ constraint and solve the problem using mixed H_2/H_∞ synthesis with multiple H_∞ constraints. An advantage of this technique is that it allows the controller order to be reduced to the order of the H_2 problem. Further, by employing mixed optimization, one can design a controller which minimizes the effect of white noise inputs as well as bounded energy inputs.

This thesis will first develop the H_2/H_∞ problem with a single H_∞ constraint. Second, the H_2/H_∞ problem is extended to allow multiple H_∞ constraints. The nature of the solution will be compared with μ -synthesis. A SISO example will represent the validation of this new technique and a MIMO example will address control design requirements (Robust Stability and Nominal Performance).

II. Background

This chapter is intended to lay the foundation for the specific compensator designs that will follow. Figure 2-1 shows the closed loop transfer function T , and it is desired to minimize an appropriate norm on T due to varying assumptions about the exogenous input signal and the exogenous output signal. For instance, if the exogenous signal is not known exactly but is known to lie in a set $(p=2,\infty)$, then a reasonable measure for performance is one which looks at the worst possible output. In particular, assume that the set of exogenous inputs is given by

$$\{w \in l_p \mid \|w\|_p \leq 1\}; \quad p = 2, \infty$$

The 2-norm is the energy, and the ∞ -norm is the maximum magnitude of the signal. A good measure of performance is given by

$$\sup_{w \in l_p} \|z\|_q$$

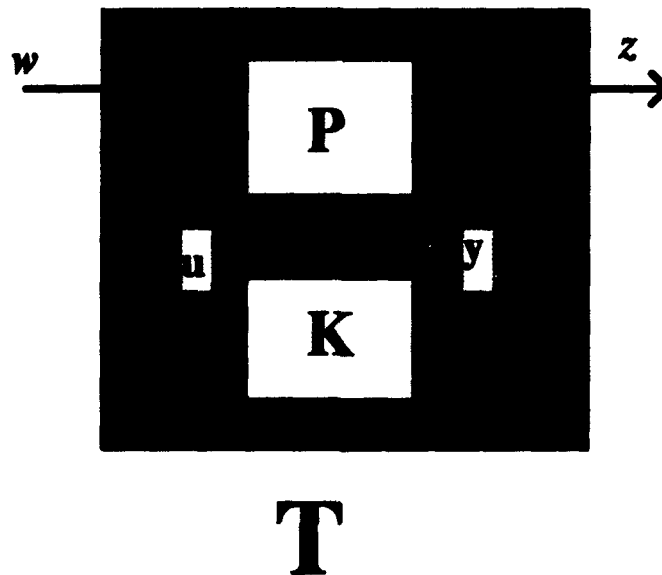


Figure 2-1 Closed Loop system T

which is the norm of the worst possible output as the exogenous signal ranges over the allowable set. The controller design problem is given by

$$\inf_{K \text{ stabilizing}} (\sup_{w \in l_p} \|Tw\|_q) = \inf_{K \text{ stabilizing}} \|T\|_{l_p \text{-induced}}$$

This performance objective is known as the minimax objective. The controller is designed to guard against all exogenous signals in the allowable set [DD93]. Table 2-1 shows the l_{pq} -induced norm for different exogenous inputs and outputs.

Table 2-1 Induced norms

input	$\ w\ _2$	$\ w\ _\infty$
output		
$\ z\ _2$	$\ T\ _\infty$	**
$\ z\ _\infty$	$\ T\ _2$	$\ T(t)\ _1$

** not induced norm exits

For more information on signal theory, refer to [DD93] and other references. When uncertainties are in the system, the minimization of $\|T\|_p$ [$p=1, \infty$ (the system 2-norm is not good for uncertainty management)] is conservative, especially when the uncertainty model is highly structured. In this case, μ -analysis is a better tool for analyzing the robustness of the system. Next, we examine the H_2 , H_∞ , and μ -synthesis design procedures. Minimization of $\|T(t)\|_1$, known as l_1 optimization, will not be covered in this thesis.

2.1 H_2 Optimization

H_2 optimization, which parallels the popular LQG problem in the optimal output feedback case, is based on minimizing the 2-norm of a transfer function matrix from white noise inputs to controlled outputs [DGKF89]. The white noise input is assumed to be zero-mean, unit intensity, and possess a Gaussian distribution. Figure 2-2 shows the basic H_2 design diagram where :

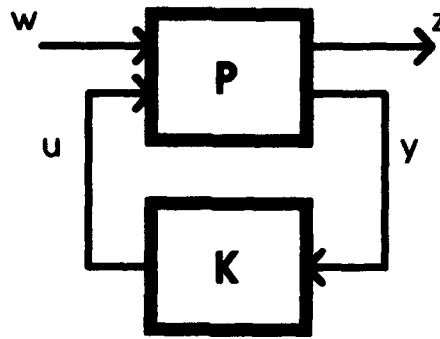


Figure 2-2 H_2 Design Diagram

z is the controlled output (exogenous output)

w is a white Gaussian noise with unity intensity (exogenous input)

u is the controller input to the plant

y is the measured plant output

P includes the design weights and the plant

K is the controller

The H_2 design objective is to find an admissible (stabilizing) $K(s)$ that minimizes the energy of the controlled output (z), which is equivalent to minimizing the two-norm of T_{zw}

$$\inf_{K \text{ admissible}} \|z\|_2 = \inf_{K \text{ admissible}} \|T_{zw}\|_2$$

The optimal $\|T_{zw}\|_2$ is represented by α_o , with the corresponding $K(s) \equiv K(s)_{2opt}$. $K(s)_{2opt}$ is unique and full order (the order of the nominal plant plus the order of the H_2 weights). In state space, the plant P is described by:

$$\begin{aligned}\dot{x} &= Ax + B_w w + B_u u \\ z &= C_z x + D_{zw} w + D_{zu} u \\ y &= C_y x + D_{yw} w + D_{yu} u\end{aligned}$$

The following assumptions are now made:

(i) $D_{zw} = 0$

- (ii) $D_{yu} = 0$
- (iii) (A, B_u) stabilizable and (C_y, A) detectable
- (iv) $D_{zu}^T D_{zu}$ full rank ; $D_{yw} D_{yw}^T$ full rank
- (v) $\begin{bmatrix} A - j\omega I & B_u \\ C_z & D_{zu} \end{bmatrix}$ has full column rank for all ω
- (vi) $\begin{bmatrix} A - j\omega I & B_w \\ C_y & D_{yw} \end{bmatrix}$ has full row rank for all ω

where assumption (i) is a requirement for the two-norm of the transfer function to be finite. The condition on D_{yu} simplifies the problem, but it is not a requirement. For a stabilizing compensator to exist, (iii) must be satisfied. Condition (iv) is required to avoid singular control problems. Finally, conditions (v) and (vi) guarantee the existence of stabilizing solutions to the algebraic Riccati equation (AREs) that are involved in the solution of the H_2 problem. For a complete description of the H_2 solution, see [DGKF89].

2.2 H_∞ Optimization

The objective of H_∞ optimization is to minimize the energy of a controlled output to a deterministic input signal that has bounded, but unknown, energy. In the H_∞ problem the controlled output is e , and the exogenous input is d ; therefore, the H_∞ problem is

$$\inf_{K \text{ admissible}} \sup_{\|d\|_2 \leq 1} \|e\|_2 \equiv \inf_{K \text{ admissible}} \|T_{ed}\|_\infty$$

where

$$\|T_{ed}(j\omega)\|_\infty \equiv \sup_{\omega} \bar{\sigma}[T_{ed}(j\omega)]$$

The optimal controller $K(s)_{\text{opt}}$ yields $\|T_{ed}\|_\infty = \underline{\gamma}$, and a family of suboptimal controllers such that $\|T_{ed}\|_\infty < \gamma$ can be defined, where $\gamma > \underline{\gamma}$. Figure 2-3 shows the block diagram for the H_∞ design. In this case, the state space matrices for P are:

$$\begin{aligned}\dot{x} &= Ax + B_d d + B_u u \\ e &= C_e x + D_{ed} d + D_{eu} u \\ y &= C_y x + D_{yd} d + D_{yu} u\end{aligned}$$

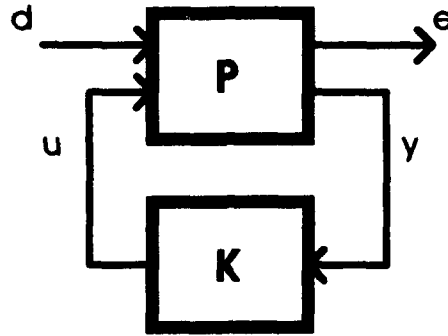


Figure 2-3 H_2 Design Block Diagram

The following assumptions on the state space matrices are made:

- (i) $D_{yu} = 0$
- (ii) (A, B_u) stabilizable and (C_y, A) detectable
- (iii) $D_{eu}^T D_{eu}$ full rank; $D_{yd} D_{yd}^T$ full rank
- (iv) $\begin{bmatrix} A - j\omega I & B_u \\ C_e & D_{eu} \end{bmatrix}$ has full column rank for all ω
- (v) $\begin{bmatrix} A - j\omega I & B_d \\ C_y & D_{yd} \end{bmatrix}$ has full row rank for all ω

Condition (i) is not required, but simplifies the problem. For stabilizing solutions to exist, condition (ii) must be satisfied. In order to avoid singular problems, condition (iii) is required. Conditions (iv) and (v) along with (ii) guarantee that the two Hamiltonian matrices in the corresponding H_2 problem belong to $\text{dom}(\text{Ric})$. Notice that there is not a

restriction on D_{ad} , because it does not make the closed loop infinity-norm infinite. For more information of the complete solution, refer to [DGKF89].

2.3 Structured Singular Value

This section presents a short synopsis of Packard and Doyle [PD93]. The system is linear time invariant with complex perturbations. For more information refer to [PD93]. Consider $M \in \mathbb{C}^{n \times n}$. In the definition of $\mu(M)$ there is an underlying structure Δ on which everything in the sequel depends. This structure may be defined differently for each problem depending on the uncertainty and performance objectives of the problem. This structure depends on the type of each block, the number of blocks, and their dimensions. These blocks can be repeated scalar blocks and/or full blocks, where S and F denote the number of repeated scalar blocks and the number of full blocks, respectively (scalar S : r_1, \dots, r_s ; full block F : m_1, \dots, m_F). Therefore, Δ is defined as

$$\Delta = \{\text{diag}[\delta_1 I_{r_1}, \dots, \delta_s I_{r_s}, \Delta_{s+1}, \dots, \Delta_F] : \delta_i \in \mathbb{C}, \\ \Delta_{s+j} \in \mathbb{C}^{m_j \times m_j}, 1 \leq i \leq S, 1 \leq j \leq F\}$$

and $\sum_{i=1}^S r_i + \sum_{j=1}^F m_j = n$ gives consistency among all dimensions. The norm bounded subsets of Δ are defined as

$$B_\Delta = \{\Delta \in \Delta : \bar{\sigma}(\Delta) \leq 1\}$$

For $M \in \mathbb{C}^{n \times n}$, $\mu_\Delta(M)$ is defined

$$\mu_\Delta(M) := \frac{1}{\min\{\bar{\sigma}(\Delta) : \Delta \in \Delta, \det(I - M\Delta) = 0\}}$$

unless no $\Delta \in \Delta$ makes $I - M\Delta$ singular, in which case $\mu_\Delta(M) \equiv 0$. Clearly, $\mu_\Delta(M)$ depends on the block structure as well as the matrix M . In general, $\mu_\Delta(M)$ can't be calculated

exactly, and its value is placed between lower and upper bounds for certain type of Δ block structures (scalar blocks or complex uncertainty blocks; see [PD93]). Two special cases of $\mu_\Delta(M)$ are:

- if $\Delta = \{\delta I: \delta \in \mathbb{C}\}$; ($S = 1, F = 0, r_1 = n$)
then $\mu_\Delta(M) = \rho(M)$, (the spectral radius of M)
- if $\Delta = \mathbb{C}^{nm}$; ($S = 0, F = 1, m_1 = n$)
then $\mu_\Delta(M) = \bar{\sigma}(M)$

For all but the two special cases above, μ is bounded by

$$\rho(M) \leq \mu_\Delta(M) \leq \bar{\sigma}(M)$$

These bounds by themselves may provide little information on the value of μ , because the gap between ρ and $\bar{\sigma}$ can be arbitrarily large. These bounds are refined with transformations on M that do not affect $\mu_\Delta(M)$, but do affect ρ and $\bar{\sigma}$. To do this, define two subsets of \mathbb{C}^{nm}

$$\mathbf{Q} = \{Q \in \Delta: Q^*Q = I_n\}$$

$$\mathbf{D} = [\text{diag}\{D_1, \dots, D_S, d_{s+j}I_{m_j}, \dots, d_{s+p}I_{m_p}\}: D_i \in \mathbb{C}^{r_i \times r_i}, D_i > 0, d_{s+j} \in \mathbb{R}, d_{s+j} > 0]$$

Notice that for any $\Delta \in \Delta$, $Q \in \mathbf{Q}$, and $D \in \mathbf{D}$

$$Q^* \in \mathbf{Q}, Q\Delta \in \Delta, \Delta Q \in \Delta,$$

$$\bar{\sigma}(Q\Delta) = \bar{\sigma}(\Delta Q) = \bar{\sigma}(\Delta),$$

$$D\Delta = \Delta D$$

Theorem 3.8 from [PD93] says: For all $Q \in \mathbf{Q}$ and $D \in \mathbf{D}$

$$\mu_\Delta(MQ) = \mu_\Delta(QM) = \mu_\Delta(M) = \mu_\Delta(DMD^{-1})$$

Therefore, the bounds can be tightened to

$$\max_{Q \in \mathbf{Q}} \rho(QM) \leq \max_{\Delta \in \mathbf{B}\Delta} \rho(\Delta M) = \mu_\Delta(M) \leq \inf_{D \in \mathbf{D}} \bar{\sigma}(DMD^{-1})$$

2.3.1 Structured Singular Value in Control Systems

The structured singular value is a framework based on the small gain theorem, in which the robustness of a system can be quantified [ABSB92]. μ -based methods have been useful for analyzing the performance and robustness properties of linear feedback systems, where the closed loop system and weighting functions are contained in the $M(s)$ matrix, and all uncertainty blocks are put into a block diagonal $\Delta(s)$ matrix. $M(s)$ and $\Delta(s)$ are stable transfer functions; they are arranged as shown in Figure 2-4. This figure is meant to represent the loop equations $e = Md$, $d = \Delta e$. Assuming a fixed $s = j\omega$, as long as $I - M\Delta$ is nonsingular, the only solutions e, d to the loop equations are $e = d = 0$. However, if $I - M\Delta$ is singular, there are infinitely many solutions to the equations, and the norms $\|e\|$ and $\|d\|$ of solutions can be arbitrarily large; therefore, this constant matrix feedback system is "unstable". Likewise, the term "stable" will describe the situation where the only solutions are identically zero. In this context, $\mu_{\Delta}(M)$ provides a measure of the smallest structured Δ that causes instability of the constant matrix feedback loop. The norm of this destabilizing Δ is exactly $1/\mu_{\Delta}(M)$ [PD93]. This interpretation can then be repeated for all frequencies.

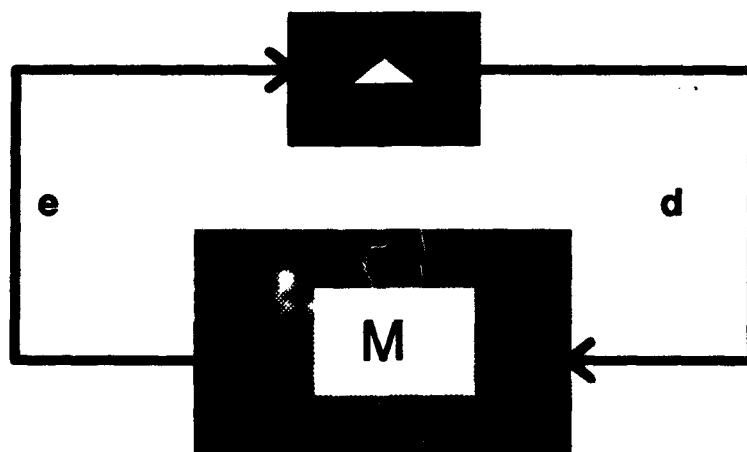


Figure 2-4 M- Δ feedback connection

2.3.2 Structured Singular Value Analysis

The robustness of a closed loop system can be analyzed by forming the block diagram as shown in Figure 2-5, where d_Δ and e_Δ are the inputs and outputs related with uncertainty block Δ_2 . The inputs and outputs related to the performance specification are given by d and e .

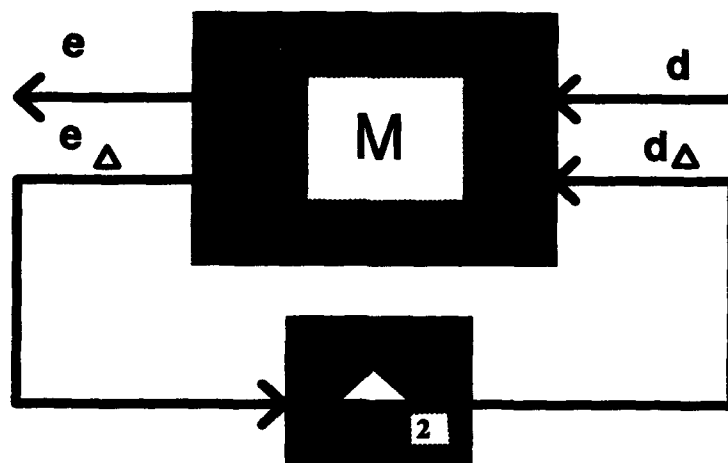


Figure 2-5 Robust Performance Diagram

The transfer functions between inputs and outputs are:

$$\begin{bmatrix} e \\ e_\Delta \end{bmatrix} = \begin{bmatrix} M_{11} & M_{12} \\ M_{21} & M_{22} \end{bmatrix} \begin{bmatrix} d \\ d_\Delta \end{bmatrix}$$

$$d_\Delta = \Delta_2 e_\Delta$$

This set of equations is called well posed if for any vector d there exist unique vectors e_Δ , e , and d_Δ satisfying the loop equations. This implies that the inverse of $I - M_{22}\Delta_2$ exists; otherwise, there is either no solution to the loop equations or there are an infinite number of solutions. When the inverse exists

$$e = L_l(M, \Delta_2)d$$

$$L_l(M, \Delta_2) := M_{11} + M_{12}\Delta_2(I - M_{22}\Delta_2)^{-1}M_{21}$$

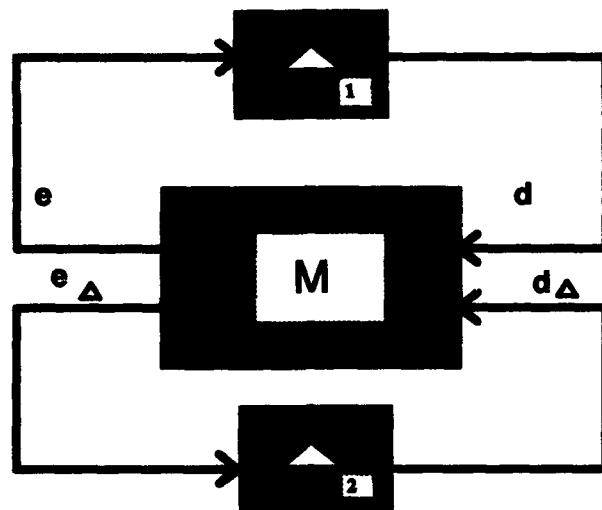


Figure 2-6 Nominal and Robust Performance specifications Diagram

where $L_f(M, \Delta_2)$ is called a lower linear fractional transformation. In order to analyze the performance specifications, a fictitious block is created between the input d and the output e . Figure 2-6 shows the new structure. The set of all allowable blocks is defined as

$$B_i = \{\Delta_i \in \Delta: \bar{\sigma}(\Delta_i) \leq 1\}$$

In this formulation the matrix $M_{11} = L_f(M, 0)$ may be thought of as the nominal map and $\Delta_2 \in B_2$ viewed as a norm bounded perturbation from an allowable perturbation class, Δ_2 . The matrices M_{12} , M_{21} , and M_{22} and the formula $L(M, \cdot)$ reflect prior knowledge on how the unknown perturbation (Δ_2) affects the nominal map, M_{11} . In this case $L(M, \cdot)$ is related to $L_f(M, \Delta_2)$ as defined earlier. This type of uncertainty, called linear fractional, is natural for many control problems, and encompasses many other special cases considered by researchers in robust control and matrix perturbation theory. The constant matrix problem to solve is: determine whether the LFT is well posed for all Δ_2 in B_2 and, if so, determine how "large" $L_f(M, \Delta_2)$ can get for $\Delta_2 \in B_2$. Define a new structure Δ as

$$\Delta := \left\{ \begin{bmatrix} \Delta_1 & 0 \\ 0 & \Delta_2 \end{bmatrix} : \Delta_1 \in \Delta_1, \Delta_2 \in \Delta_2 \right\}$$

Now there are three structures with respect to which μ can be computed. They are as follows: $\mu_1(\cdot)$ is with respect to Δ_1 , $\mu_2(\cdot)$ is with respect to Δ_2 , and $\mu_\Delta(\cdot)$ is with respect to Δ . In view of this, $\mu_1(M_{11})$, $\mu_2(M_{22})$, and $\mu_\Delta(M)$ are all defined. Theorem 4.2 from [PD93] says: The linear fractional transformation $L_f(M, \Delta_2)$ is well posed for all $\Delta_2 \in \mathcal{B}_2$ if and only if $\mu_2(M_{22}) < 1$. As the perturbation Δ_2 deviates from zero, the matrix $L_f(M, \Delta_2)$ deviates from M_{11} . The range of values that $\mu_1(L_f(M, \Delta_2))$ takes on is intimately related to $\mu_\Delta(M)$, as follows:

$$\mu_\Delta(M) < 1 \Leftrightarrow \begin{cases} \mu_2(M_{22}) < 1 \\ \max_{\Delta_2 \in \mathcal{B}_2} \mu_1(L_f(M, \Delta_2)) < 1 \end{cases}$$

This relationship is known as the Main Loop Theorem [PD93].

2.3.3 Structured Singular Value Synthesis

The μ -synthesis problem is described by the attempt to find a controller $K(s)$ that minimizes an upper bound on the structured singular value,

$$\inf_{K \text{ stabilizing}} \inf_{D \in \mathcal{D}} \sup_{\omega} \bar{\sigma}[DM(K)D^{-1}]$$

where $M(K)$ is the closed loop transfer function. One way to solve this problem is called D-K iteration; it calls for alternately minimizing $\sup \bar{\sigma}(DM(K)D^{-1})$ for either K or D while holding the other constant. First the controller synthesis problem is solved using H_∞ design on the nominal design model (nominal plant plus weighting functions); i.e., $D \equiv I$. μ -analysis is then performed on the closed loop transfer function $M(K)$, producing values of the D scaling matrices at each frequency. The resulting frequency response data is fit with an invertible, stable, minimum phase transfer function which becomes part of the nominal synthesis structure. With D fixed, the controller synthesis problem is again solved by performing an H_∞ design on the augmented system. The D-K iterations are continued

until a satisfactory controller is found or a minimum is reached. The resulting controller order is the order of the design plant and weighting matrices, as well as the order of the D-scale transfer function fits [ABSB92]. MatLabTM provides a μ -toolbox that will be used in this thesis which performs this D-K iteration.

2.4 Nominal Performance, Robust Stability and Robust Performance tests

This section presents the tests for Nominal Performance (NP), Robust Stability (RS), and Robust Performance (RP) for the system of Figure 2-6. Depending on the type of perturbation (structured or unstructured), the infinity norm test is conservative and μ -analysis is required as shown in Table 2-2.

Table 2-2 Test for NP, RS, and RP From [Doy85]

Perturbation	Stability Test	Performance Test
$\Delta=0$	No C_+ poles	$\ M_{11}\ _{\infty} \leq 1$ (NP)
$\bar{\sigma}(\Delta) < 1$	$\ M_{22}\ _{\infty} \leq 1$ (RS)	$\mu(M) \leq 1$ (RP)
$\Delta \in B\Delta$	$\mu(M_{11}) \leq 1$ (RS)	$\mu(M) \leq 1$ (RP)

Table 2-2 summarizes the objectives of H_{∞} optimization and μ - synthesis. Notice that this table does not mention any test using the two norm, and the objective in this table is only to minimize $\| \cdot \|_{\infty}$ or $\mu(\cdot)$. This means that performance based on white Gaussian noise inputs is not accounted for. This is the true objective of the mixed H_2/H_{∞} control design problem: to address the tests for $\| \cdot \|_{\infty}$ and provide a low $\| \cdot \|_2$, as will be seen in the next chapters.

2.5 Guaranteed MIMO Gain and Phase Margins Using T and S

One way to measure the robustness of a system is to calculate the Vector Gain Margin (VGM) and Vector Phase Margin (VPM) at the input and output of the plant (MIMO). The VGM and VPM tell us how much the system can tolerate a change in gain and phase before it goes unstable. The VGM and VPM using the complementary sensitivity function is measured by

$$r(\omega) = \frac{1}{\bar{\sigma}(T(j\omega))}$$

where T can be at the input if we are looking at the input margins or at the output of the plant if we are looking at the output margins. Whichever point we are looking at, the general formulas are

$$\text{VGM}_T = [1 - r_{\min}, 1 + r_{\min}] \text{ where } r_{\min} = \inf_{\omega \in \mathbb{R}} r(\omega)$$

and

$$\text{VPM}_T = [-\theta, +\theta] \text{ where } \theta = 2 \sin^{-1} \left(\frac{r_{\min}}{2} \right)$$

The VGM and VPM using the sensitivity function are defined through

$$p(\omega) = \frac{1}{\bar{\sigma}(S(j\omega))}$$

where S can be at the input if we are looking at the input margins or at the output of the plant if we are looking at the output margins. Whichever point we are looking at, the general formulas are

$$\text{VGM}_S = \left[\frac{1}{1 + p_{\min}}, \frac{1}{1 - p_{\min}} \right] \text{ where } p_{\min} = \inf_{\omega \in \mathbb{R}} p(\omega)$$

and

$$\text{VPM}_s = [-\theta, +\theta] \text{ where } \theta = 2 \sin^{-1} \left(\frac{p_{\min}}{2} \right)$$

Since VGM_T , VGM_s , VPM_T , and VPM_s are all important, this thesis will compute all of them in order to evaluate the level of robustness at the input and output of the plant. For more details see [Dai90].

III. Mixed H_2/H_∞ Optimization with a Single H_∞ Constraint

This section presents the mixed H_2/H_∞ optimization developed by [Rid91]. Mixed H_2/H_∞ optimization is a nonconserve tool that trades between H_2 and H_∞ objectives.

The goal of the mixed problem is to find a stabilizing compensator $K(s)$ that achieves

$$\inf_{K \text{ stabilizing}} \|T_{zw}\|_2, \text{ subject to } \|T_{ed}\|_\infty \leq \gamma$$

where T_{zw} and T_{ed} can be defined to be independent of each other. Figure 3-1 shows the block diagram.

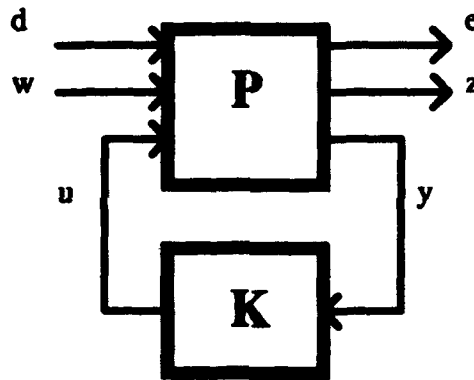


Figure 3-1 Mixed H_2/H_∞ Design Diagram

The state space matrices are:

$$\begin{aligned} \dot{x} &= Ax + B_d d + B_w w + B_u u \\ e &= C_e x + D_{ed} d + D_{ew} w + D_{eu} u \\ z &= C_z x + D_{zd} d + D_{zw} w + D_{zu} u \\ y &= C_y x + D_{yd} d + D_{yw} w + D_{yu} u \end{aligned}$$

3.1 Nonsingular H_∞ Constraint

The following assumptions are made on the state space matrices:

- (i) $D_{ed} = 0$; (ii) $D_{zw} = 0$; (iii) $D_{ya} = 0$
- (iv) (A, B_u) stabilizable and (C_y, A) detectable
- (v) $D_{eu}^T D_{eu}$ full rank; $D_{yd} D_{yd}^T$ full rank
- (vi) $D_{zu}^T D_{zu}$ full rank ; $D_{yw} D_{yw}^T$ full rank
- (vii) $\begin{bmatrix} A - j\omega I & B_u \\ C_z & D_{zu} \end{bmatrix}$ has full column rank for all ω
- (viii) $\begin{bmatrix} A - j\omega I & B_w \\ C_y & D_{yw} \end{bmatrix}$ has full row rank for all ω
- (ix) $\begin{bmatrix} A - j\omega I & B_u \\ C_e & D_{eu} \end{bmatrix}$ has full column rank for all ω
- (x) $\begin{bmatrix} A - j\omega I & B_d \\ C_y & D_{yd} \end{bmatrix}$ has full row rank for all ω

These conditions are the union of the H_2 assumptions and the H_∞ assumptions, except that the controller, $K(s)$, for the mixed problem must be strictly proper in order to guarantee a finite two-norm for T_{zw} . The state space matrices for $K(s)$ are:

$$\begin{aligned}\dot{x}_c &= A_c x_c + B_c y \\ u &= C_c x_c ; D_c = 0\end{aligned}$$

and the closed-loop matrices are:

$$\begin{aligned}\dot{x} &= Ax + B_d d + B_w w \\ e &= C_e x + D_{ed} d + D_{ew} w \\ z &= C_z x + D_{zd} d + D_{zw} w\end{aligned}$$

$$D_{zw} = 0 \text{ and } D_{ed} = 0$$

T_{ed} and T_{zw} can be written as

$$T_{ed} = C_e(sI - A)^{-1}B_d \quad ; \quad T_{zw} = C_z(sI - A)^{-1}B_w$$

The following definitions will be made:

$$\gamma \equiv \inf_{K \text{ stabilizing}} \|T_{ed}\|_{\infty}$$

$$\alpha_0 \equiv \inf_{K \text{ stabilizing}} \|T_{zw}\|_2$$

$$K_{2opt} \equiv \text{the unique } K(s) \text{ that makes } \|T_{zw}\|_2 = \alpha_0$$

$$\bar{\gamma} \equiv \|T_{ed}\|_{\infty} \text{ when } K(s) = K_{2opt}$$

$$K_{mix} \equiv \text{a } K(s) \text{ that solves the mixed } H_2/H_{\infty} \text{ problem for some } \gamma$$

$$\gamma^* \equiv \|T_{ed}\|_{\infty} \text{ when } K(s) = K_{mix}$$

$$\alpha^* \equiv \|T_{zw}\|_2 \text{ when } K(s) = K_{mix}$$

Theorem 4.1.1 from [Rid91] says:

Theorem 3.1 : Let (A_e, B_e, C_e) be given and assume there exists a $Q_{\infty} = Q_{\infty}^T \geq 0$ satisfying

$$AQ_{\infty} + Q_{\infty}A^T + \gamma^{-2}Q_{\infty}C_e^TC_eQ_{\infty} + B_dB_d^T = 0 \quad (**)$$

The following are equivalent:

- i) (A, B_d) is stabilizable
- ii) A is stable

Moreover, if i) - ii) hold, the following are true:

- iii) the transfer function T_{ed} satisfies

$$\|T_{ed}\|_{\infty} \leq \gamma$$

- iv) the two norm of the transfer function T_{zw} is given by

$$\|T_{zw}\|_2^2 = \text{tr}[C_zQ_2C_z^T] = \text{tr}[Q_2C_z^TC_z]$$

where $Q_2 = Q_2^T \geq 0$ is the solution to the Lyapunov equation

$$AQ_2 + Q_2A^T + B_wB_w^T = 0$$

- v) all real symmetric solutions to (**) are positive semidefinite
- vi) there exists a unique minimal solution to (**) in the class of real symmetric solutions
- vii) Q_{∞} is the minimal solution to (**) iff

$$\operatorname{Re}[\lambda_i(A + \gamma^{-2}Q_{\infty}C_e^TC_e)] \leq 0 \quad \forall i$$

- viii) $\|T_{ed}\|_{\infty} < \gamma$ iff $A + \gamma^{-2}Q_{\infty}C_e^TC_e$ is stable, where Q_{∞} is the minimal solution to (**) (**))

Proof: See Theorem 4.1.1, [Rid91].

Using Theorem 3.1, the mixed problem can be restated as:

Find a strictly proper controller $K(s)$ that minimizes the index

$$J(A_c, B_c, C_c) = \operatorname{tr}(Q_2 C_z^T C_z)$$

where Q_2 is the real, symmetric, positive semidefinite solution to

$$AQ_2 + Q_2 A^T + B_w B_w^T = 0$$

and such that

$$AQ_{\infty} + Q_{\infty} A^T + \gamma^{-2}Q_{\infty}C_e^TC_eQ_{\infty} + B_d B_d^T = 0$$

has a real symmetric positive semidefinite solution. To solve this minimization problem with two equality constraints, a Lagrange multiplier approach is used:

$$L = \operatorname{tr}[Q_2 C_z^T C_z] + \operatorname{tr}[(AQ_2 + Q_2 A^T + B_w B_w^T)X] \\ + \operatorname{tr}[(AQ_{\infty} + Q_{\infty} A^T + \gamma^{-2}Q_{\infty}C_e^TC_eQ_{\infty} + B_d B_d^T)Y]$$

where X and Y are the Lagrange multiplier matrices. The necessary conditions for a minimum are given by [Rid91]. Conclusions from these conditions are:

- (i) No mixed solution exists for $\gamma < \underline{\gamma}$
- (ii) The mixed solution comes from seven first order necessary conditions, which are highly coupled and nonlinear.
- (iii) For $\underline{\gamma} < \gamma < \bar{\gamma}$, neutrally stabilizing ARE solutions are required, and $\gamma^* = \gamma$.

(iv) For $\gamma \geq \bar{\gamma}$, K_{2opt} is the unique mixed solution.

3.2 Singular H_∞ Constraint

This section presents the mixed H_2/H_∞ optimization problem with a singular H_∞ constraint, developed by [WR94a].

3.2.1 General Formulation

Here, mixed H_2/H_∞ optimization will be extended to handle a (possibly non-strictly proper) singular H_∞ constraint. Assume the plant P contains the H_2 and the H_∞ designs. The individual H_2 and H_∞ designs can be represented as two independent systems

$$P_2 = \left[\begin{array}{c|cc} A_2 & B_w & B_{u_2} \\ \hline C_z & D_{zw} & D_{zu} \\ \hline C_{y_2} & D_{yw} & D_{yu} \end{array} \right] \quad P_\infty = \left[\begin{array}{c|cc} A_\infty & B_d & B_{u_\infty} \\ \hline C_e & D_{ed} & D_{eu} \\ \hline C_{y_\infty} & D_{yd} & D_{yu} \end{array} \right] \quad (3-1)$$

where

$$B_{u_2} = \begin{bmatrix} B_{\text{plant}} \\ B_{H_2 \text{ design}} \end{bmatrix} ; B_{u_\infty} = \begin{bmatrix} B_{\text{plant}} \\ B_{H_\infty \text{ design}} \end{bmatrix}$$

$$C_{y_2} = \begin{bmatrix} C_{\text{plant}} & C_{H_2 \text{ design}} \end{bmatrix} ; C_{y_\infty} = \begin{bmatrix} C_{\text{plant}} & C_{H_\infty \text{ design}} \end{bmatrix}$$

The objective for the mixed case is to find a stabilizing compensator $K(s)$ that achieves

$$\inf_{K \text{ stabilizing}} \|T_{zw}\|_2, \text{ subject to } \|T_{ed}\|_\infty \leq \gamma \quad (3-2)$$

where

$$T_{ed} = C_e(sI - A)^{-1}B_d + D_{ed} \quad ; \quad T_{zw} = C_z(sI - A)^{-1}B_w + D_{zw} \quad (3-3)$$

are the closed loop transfer functions from w to z and d to e , respectively. The following assumptions are made in the state space matrices:

$$(i) D_{zw} = 0 \quad ; (ii) D_{yu} = 0$$

$$(iii) (A_2, B_{u_1}) \text{ stabilizable and } (C_{y_2}, A_2) \text{ detectable}$$

$$(iv) (A_\infty, B_{u_\infty}) \text{ stabilizable and } (C_{y_\infty}, A_\infty) \text{ detectable}$$

$$(v) D_{zu}^T D_{zu} \text{ full rank ; } D_{yw} D_{yw}^T \text{ full rank}$$

$$(vi) \begin{bmatrix} A_2 - j\omega I & B_{u_1} \\ C_z & D_{zu} \end{bmatrix} \text{ has full column rank for all } \omega$$

$$(vii) \begin{bmatrix} A_2 - j\omega I & B_w \\ C_{y_2} & D_{yw} \end{bmatrix} \text{ has full row rank for all } \omega$$

Notice that D_{ed} is not restricted to zero and no assumptions are made as to the ranks of D_{eu} and D_{yd} ; this means that a singular H_∞ design can be allowed. For the mixed problem, $K(s)$ must be strictly proper in order to guarantee a finite two-norm for T_{zw} . The state space matrices for $K(s)$ are:

$$\dot{x}_c = A_c x_c + B_c u \quad (3-4)$$

$$u = C_c x_c \quad ; D_c = 0$$

and the closed-loop matrices are:

$$\begin{aligned} \dot{x}_2 &= A_2 x_2 + B_w w \\ z &= C_z x_2 \end{aligned} \quad (3-5)$$

$$\begin{aligned} \dot{x}_\infty &= A_\infty x_\infty + B_d d \\ e &= C_e x_\infty + D_{ed} d \end{aligned} \quad (3-6)$$

where

$$A_2 = \begin{bmatrix} A_2 & B_{u_2} C_c \\ B_c C_{y_2} & A_c \end{bmatrix}; \quad A_\infty = \begin{bmatrix} A_\infty & B_{u_\infty} C_c \\ B_c C_{y_\infty} & A_c \end{bmatrix} \quad (3-7)$$

$$B_w = \begin{bmatrix} B_w \\ B_c D_{yw} \end{bmatrix}; \quad B_d = \begin{bmatrix} B_d \\ B_c D_{yd} \end{bmatrix} \quad (3-8)$$

$$C_z = [C_z \quad D_{zw} C_c]; \quad C_e = [C_e \quad D_{ed} C_c] \quad (3-9)$$

$$D_{ed} = D_{ed} \quad (3-10)$$

Using the definitions from Section 3.1, the mixed H_2/H_∞ problem is now to find a controller $K(s)$ such that:

- i. A_z and A_w are stable
- ii. $\|T_{ed}\|_\infty \leq \gamma$ for $\gamma \geq \underline{\gamma}$
- iii. $\|T_{zw}\|_2$ is minimized.

Now Theorem 3.1 can be restated as follows:

Theorem 3.2: Let (A_c, B_c, C_c) be given and assume there exists a solution

$Q_\infty = Q_\infty^T \geq 0$ satisfying

$$A_w Q_\infty + Q_\infty A_w^T + (Q_\infty C_e^T + B_d D_{ed}^T) R^{-1} (Q_\infty C_e^T + B_d D_{ed}^T)^T + B_d B_d^T = 0 \quad (3-11)$$

where $R = (\gamma^2 I - D_{ed} D_{ed}^T) > 0$. Then, the following are equivalent:

- i) (A_w, B_d) is stabilizable
- ii) A_w is stable.

Moreover, if i) - ii) hold, the following are true:

$$\text{iii) } \|T_{ed}\|_\infty \leq \gamma$$

iv) the two norm of the transfer function T_{zw} is given by

$$\|T_{zw}\|_2^2 = \text{tr}[C_z Q_2 C_z^T] = \text{tr}[Q_2 C_z^T C_z]$$

where $Q_2 = Q_2^T \geq 0$ is the solution to the Lyapunov equation

$$A_z Q_2 + Q_2 A_z^T + B_w B_w^T = 0$$

- v) all real symmetric solutions to (3-11) are positive semidefinite
- vi) there exists a unique minimal solution to (3-11) in the class of real symmetric

solutions

vii) Q_{∞} is the minimal solution to (3-11) iff

$$\operatorname{Re}[\lambda_j(A_{\infty} + B_d D_{cd}^T R^{-1} C_e + Q_{\infty} C_e^T R^{-1} C_e)] \leq 0$$

viii) $\|T_{cd}\|_{\infty} < \gamma$ iff $(A_{\infty} + B_d D_{cd}^T R^{-1} C_e + Q_{\infty} C_e^T R^{-1} C_e)$ is stable, where Q_{∞} is the minimal solution to (3-11)

Proof: See Theorem 3 [WR94a].

Using Theorem 3.2, the mixed case can be restated as:

Find a strictly proper controller $K(s)$ that minimizes the index

$$J(A_c, B_c, C_c) = \operatorname{tr}(Q_2 C_z^T C_z) \quad (3-12)$$

where Q_2 is the real, symmetric, positive semidefinite solution to

$$A Q_2 + Q_2 A^T + B_w B_w^T = 0 \quad (3-13)$$

and such that

$$A_{\infty} Q_{\infty} + Q_{\infty} A_{\infty}^T + (Q_{\infty} C_e^T + B_d D_{cd}^T) R^{-1} (Q_{\infty} C_e^T + B_d D_{cd}^T)^T + B_d B_d^T = 0 \quad (3-14)$$

(with $R > 0$) has a real symmetric positive semidefinite solution. The Lagrangian for this problem becomes

$$\begin{aligned} L = & \operatorname{tr}[Q_2 C_z^T C_z] + \operatorname{tr}[(A_2 Q_2 + Q_2 A_2^T + B_w B_w^T) X] \\ & + \operatorname{tr}[(A_{\infty} Q_{\infty} + Q_{\infty} A_{\infty}^T + (Q_{\infty} C_e^T + B_d D_{cd}^T) R^{-1} (Q_{\infty} C_e^T + B_d D_{cd}^T)^T + B_d B_d^T] Y \end{aligned} \quad (3-15)$$

where X and Y are symmetric Lagrange multiplier matrices. The resulting first order necessary conditions have not been solved analytically but do provide some insight into the nature of the solution. In particular, the condition

$$\begin{aligned} \frac{\partial L}{\partial Q_{\infty}} = & (A_{\infty} + B_d D_{cd}^T R^{-1} C_e + Q_{\infty} C_e^T R^{-1} C_e)^T Y \\ & + Y (A_{\infty} + B_d D_{cd}^T R^{-1} C_e + Q_{\infty} C_e^T R^{-1} C_e) = 0 \end{aligned} \quad (3-16)$$

implies that either $Y = 0$ or $(A_{\infty} + B_d D_{\infty}^T R^{-1} C_e + Q_{\infty} C_e^T R^{-1} C_e)$ is neutrally stable. The former condition means the solution is off the boundary of the H_{∞} constraint, and the latter solution implies the solution lies on the boundary of the H_{∞} constraint and Q_{∞} is the neutrally stabilizing solution of the Riccati equation. The necessary conditions for a minimum are given by [WR94a]. However, it is easy to show that

- (i) No mixed solution exists for $\gamma < \underline{\gamma}$
- (ii) For $\underline{\gamma} < \gamma < \bar{\gamma}$, neutrally stabilizing ARE solutions are required, and $\gamma^* = \gamma$.
- (iii) For $\gamma \geq \bar{\gamma}$, $K_{\text{mix}} = K_{2\text{opt}}$.

3.2.2 Numerical Solution

Walker and Ridgely [WR94a] developed a numerical method for synthesizing a family of general mixed H_2/H_{∞} controllers which can handle a proper, singular H_{∞} constraint. In the single constraint mixed problem, for $\underline{\gamma} < \gamma < \bar{\gamma}$, the solution to the mixed problem must lie on the boundary of the constraint. Further, for $\underline{\gamma} < \gamma < \bar{\gamma}$, α^* is a monotonically decreasing function of γ . Finally, for $\gamma < \underline{\gamma}$, no solution exists. This is shown graphically in Figure 3-2. The numerical method for solving the mixed problem was motivated by Figure 3-2. Since the optimal H_2 controller is relatively easy to calculate and it provides a point on the desired curve, it was selected as the initial controller. The optimal H_2/H_{∞} curve is generated by starting at the optimal H_2 controller and stepping along the α versus γ curve by reducing γ from $\bar{\gamma}$ to $\underline{\gamma}$ by increments.

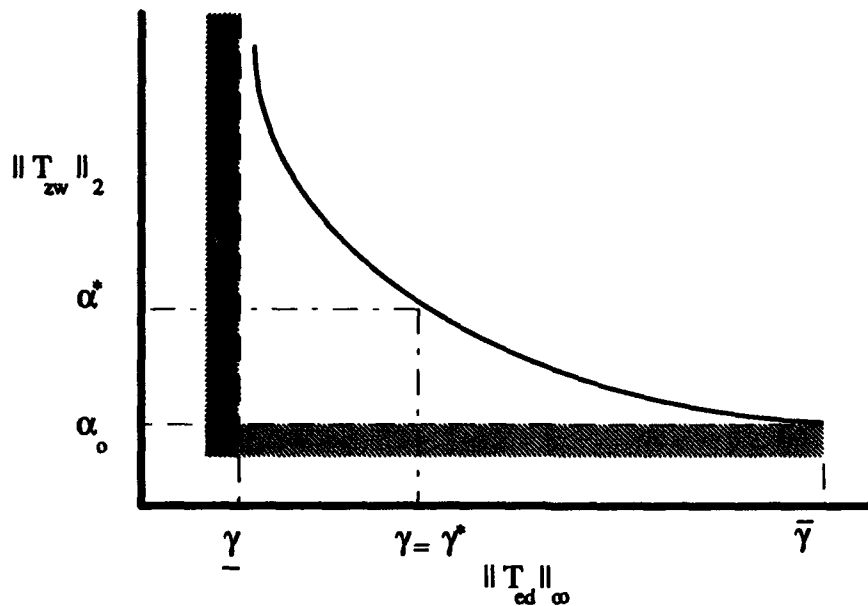


Figure 3-2 H_2/H_∞ Boundary plot

Applying the results from the previous section, it is seen that the optimal mixed H_2/H_∞ controller for a fixed γ will have the property that $\|T_{cd}\|_\infty = \gamma$. This suggested a penalty function approach to the problem. Consider the following performance index

$$J_\gamma = \|T_{zw}\|_2^2 + \lambda (\|T_{cd}\|_\infty - \gamma)^2 \quad (3-17)$$

where λ is a penalty on the error between the desired γ and the infinity-norm of the transfer function T_{cd} . Define the vector X as

$$X = [a_{c_1}^T \dots a_{c_n}^T \ b_{c_1}^T \dots b_{c_r}^T \ c_{c_1}^T \dots c_{c_m}^T]^T \quad (3-18)$$

where a_{c_j} , b_{c_j} and c_{c_j} are the columns of A_c , B_c and C_c , respectively. The first order necessary conditions for J_γ to be a minimum are

$$\frac{\partial J}{\partial x_i} = 0 \text{ for } i=1, \dots, (nxn+nxp+nxm) \quad (3-19)$$

$$= \frac{\partial \|T_{zw}\|_2^2}{\partial x_i} + \frac{\partial \lambda (\|T_{cd}\|_\infty - \gamma)^2}{\partial x_i} \quad (3-20)$$

where x_i are the elements of X [WR94a]. The first term on the right hand side of (3-20) can be solved analytically using the results of the previous section. The second term, however, represents complex matrix relations and is evaluated analytically using the sensitivity of the H_∞ norm developed by [GL93]. Assuming the maximum singular value of T_{ed} has a single peak for $\omega \in \mathbb{R}^+$, then the derivative of the infinity-norm can be written as

$$\frac{\partial \|T_{ed}\|_\infty}{\partial x_j} = \Re \left[u_1^H \left(\frac{dT_{ed}(\omega_0)}{dx} \right) \Big|_{X_{nom}} v_1 \right] \quad (3-21)$$

where u_1 and v_1 are the singular vectors associated with T_{ed} , ω_0 is the frequency where the maximum singular value reaches its peak value, X_{nom} is the nominal X vector, and \Re denotes the real part. The derivative of the transfer function can be determined from

$$\left. \frac{dT_{ed}(\omega_0)}{dx} \right|_{X_{nom}} = \left. \frac{d}{dx} (C_e (j\omega - A_\infty)^{-1} B_d + D_{ed}) \right|_{X_{nom}} \quad (3-22)$$

The second term on the right hand side of equation 3-20 can now be written as

$$\frac{\partial [\lambda (\|T_{ed}\|_\infty - \gamma)^2]}{\partial x_j} = 2\lambda (\|T_{ed}\|_\infty - \gamma) \frac{\partial \|T_{ed}\|_\infty}{\partial x_j} \quad (3-23)$$

A DFP approach similar to the algorithm described in [RMV92] is used to minimize the performance index. The basic algorithm is as follows:

1. Compute the optimal H_2 controller and set up the initial X vector
2. Compute $\bar{\gamma}$ and set $\gamma = \bar{\gamma}$
3. Decrement γ
4. Perform DFP search over X vector space for minimum J_γ
5. Store resulting controller and repeat from step 3.

Initially, the algorithm can be run with loose tolerances on the DFP search to define the desired α versus γ curve, then the convergence tolerances can be tightened and a particular point can be refined to desired accuracy. In addition, this algorithm can be applied from any initial condition, not just the optimal H_2 controller, by substituting the appropriate initial X vector and γ . Finally, the X vector was defined with a fully populated state space form; by using canonical forms, the number of variables can be reduced. However, there are drawbacks to using some canonical forms such as the controllability canonical form due to numerical instability. The modal canonical form has been used successfully to reduce the parameter space. The numerical solution for the mixed problem with a singular H_∞ constraint can be extended to allow multiple H_∞ constraints as will be shown in the next chapter.

IV. Mixed H_2/H_∞ Optimization Problem with Multiple H_∞ Constraints

Two major goals in a control design are to design controllers which yield Nominal Performance (NP) and Robust Stability (RS). These can be represented as

$$\|W_1 S\|_\infty \leq 1 \quad \text{for Nominal Performance (NP) (tracking)}$$

$$\|W_2 T\|_\infty \leq 1 \quad \text{for Robust Stability (RS)}$$

$$(\text{Multiplicative perturbation } (1 + \Delta W_2)G; \|\Delta\|_\infty < 1)$$

Using this perturbation model and the NP condition, [DFT92] defines the Robust Performance (RP) condition for a SISO system as

$$\|W_2 T\|_\infty \leq 1 \quad \text{and} \quad \left\| \frac{W_1 S}{1 - |W_2 T|} \right\|_\infty \leq 1$$

which is also given by

$$\| |W_1 S| + |W_2 T| \|_\infty < 1$$

This formulation is often solved with a mixed-sensitivity approach, which penalizes both Sensitivity (S) and Complementary Sensitivity (T), as

$$T_{ed} = \begin{bmatrix} W_1 S \\ W_2 T \end{bmatrix}$$

This mixed sensitivity cost function is required to satisfy

$$\|T_{ed}\|_\infty < 1/\sqrt{2}$$

in order to have RP. In the author's opinion, this method is conservative, because the designer has no control over the trade-off between RS and NP. This chapter presents a nonconservative method. Recall the conditions for NP and RS at the start of this chapter. Both H_∞ conditions are solved independently using mixed H_2/H_∞ optimization with multiple H_∞ constraints. For a MIMO system, the objective is to achieve RS to certain

perturbations and NP at possibly a different location in the loop. Therefore, this new technique will permit the exploration of these different objectives independently.

4.1 Development of Multiple Constraints

This section presents the mixed H_2/H_∞ optimization problem with multiple H_∞ constraints. Mixed H_2/H_∞ optimization is a nonconservative tool that trades between H_2 optimization and multiple H_∞ constraints. Consider the system in Figure 4-1, where d_i , $i=1,\dots,n_\infty$ are of bounded energy ($\|d_i\|_2 \leq 1$) and w is of bounded spectrum. The transfer function P is the underlying plant with all weights associated with the problem absorbed. It is assumed, in general, that there is no relationship between e_i , $i=1,\dots,n_\infty$ and z or d_i and w . The input w is unit intensity zero-mean, white-Gaussian noise and the inputs d_i are of bounded energy. In general, the state space of P is formed by wrapping the weights from an H_2 problem from w to z and the weights of the H_∞ problems from d_i to e_i around the basic system resulting in the augmented plant

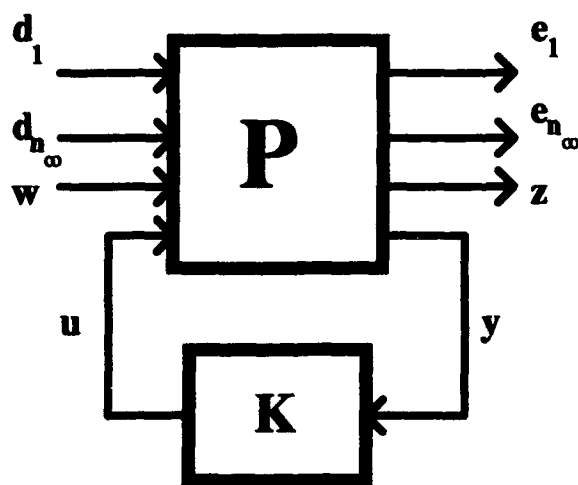


Figure 4-1 Mixed H_2/H_∞ with Multiple H_∞ Constraints Design Diagram

$$P = \left[\begin{array}{c|ccc} \tilde{A} & \tilde{B}_{d_1} & \dots & \tilde{B}_{d_{n_d}} & \tilde{B}_w & \tilde{B}_u \\ \hline \tilde{C}_{e_1} & \tilde{D}_{e_1 d_1} & \dots & \tilde{D}_{e_1 d_{n_d}} & \tilde{D}_{e_1 w} & \tilde{D}_{e_1 u} \\ \vdots & \vdots & \vdots & \vdots & \vdots & \vdots \\ \tilde{C}_{e_{n_e}} & \tilde{D}_{e_{n_e} d_1} & \dots & \tilde{D}_{e_{n_e} d_{n_d}} & \tilde{D}_{e_{n_e} w} & \tilde{D}_{e_{n_e} u} \\ \tilde{C}_z & \tilde{D}_{z d_1} & \dots & \tilde{D}_{z d_{n_d}} & \tilde{D}_{zw} & \tilde{D}_{zu} \\ \tilde{C}_y & \tilde{D}_{y d_1} & \dots & \tilde{D}_{y d_{n_d}} & \tilde{D}_{yw} & \tilde{D}_{yu} \end{array} \right] \quad (4-1)$$

The plant P contains the H_2 design and the H_{∞} designs. The individual H_2 and H_{∞} problems can be represented as different systems, where

$$P_2 = \left[\begin{array}{c|cc} A_2 & B_w & B_{u_2} \\ \hline C_z & D_{zw} & D_{zu} \\ \hline C_{y_2} & D_{yw} & D_{yu} \end{array} \right] \quad P_{\infty_i} = \left[\begin{array}{c|cc} A_{\infty_i} & B_{d_i} & B_{u_{\infty_i}} \\ \hline C_{e_i} & D_{e_i d_i} & D_{e_i u} \\ \hline C_{y_{\infty_i}} & D_{y d_i} & D_{yu} \end{array} \right] \quad i=1, \dots, n_{\infty} \quad (4-2)$$

where

$$B_{u_2} = \begin{bmatrix} B_{\text{plant}} \\ B_{H_2 \text{ design}} \end{bmatrix} ; B_{u_{\infty_i}} = \begin{bmatrix} B_{\text{plant}} \\ B_{H_{\infty_i} \text{ design}} \end{bmatrix}$$

$$C_{y_2} = \begin{bmatrix} C_{\text{plant}} & C_{H_2 \text{ design}} \end{bmatrix} ; C_{y_{\infty_i}} = \begin{bmatrix} C_{\text{plant}} & C_{H_{\infty_i} \text{ design}} \end{bmatrix}$$

The objective for the mixed problem is to find a stabilizing compensator $K(s)$ that achieves

$$\inf_{K \text{ stabilizing}} \|T_{zw}\|_2, \text{ subject to } \|T_{ed_i}\|_{\infty} \leq \gamma_i \quad ; \quad i=1, \dots, n_{\infty} \quad (4-3)$$

where

$$T_{zw} = C_z(sI - A_2)^{-1} B_w + D_{zw}$$

$$T_{ed_i} = C_{e_i}(sI - A_{\infty_i})^{-1} B_{d_i} + D_{ed_i} \quad (4-4)$$

are the closed loop transfer functions from w to z and d_i to e_i , respectively.

The following assumptions are made in the state space matrices:

- (i) $D_{zw} = 0$; (ii) $D_{yu} = 0$
- (iii) (A_2, B_{u_2}) stabilizable and (C_{y_2}, A_2) detectable
- (iv) $(A_{-i}, B_{u_{-i}})$ stabilizable and $(C_{y_{-i}}, A_{-i})$ detectable for all i
- (v) $D_{zu}^T D_{zu}$ full rank ; $D_{yw} D_{yw}^T$ full rank

$$(viii) \begin{bmatrix} A_2 - j\omega I & B_{u_2} \\ C_z & D_{zu} \end{bmatrix} \text{ has full column rank for all } \omega$$

$$(ix) \begin{bmatrix} A_2 - j\omega I & B_w \\ C_{y_2} & D_{yw} \end{bmatrix} \text{ has full row rank for all } \omega$$

Notice that the D_{ed_i} are not restricted to zero and no assumptions are made as to the ranks of $D_{e,u}$ and D_{y_d} . This means that singular H_∞ constraints can be allowed. The controller $K(s)$, for the mixed problem, must be strictly proper in order to guarantee a finite two-norm for T_{zw} . The state space matrices for $K(s)$ are:

$$\begin{aligned} \dot{x}_c &= A_c x_c + B_c y \\ u &= C_c x_c ; D_c = 0 \end{aligned} \tag{4-5}$$

and the closed-loop matrices are:

$$\begin{aligned} \dot{x}_2 &= A_2 x_2 + B_w w \\ z &= C_z x_2 \end{aligned} \tag{4-6}$$

$$\begin{aligned} \dot{x}_{-i} &= A_{-i} x_{-i} + B_{d_i} d_i \\ e_i &= C_{e_i} x_{-i} + D_{ed_i} d_i \end{aligned}$$

where

$$A_2 = \begin{bmatrix} A_2 & B_{u_2} C_c \\ B_c C_{y_2} & A_c \end{bmatrix}; \quad A_{u_i} = \begin{bmatrix} A_{u_i} & B_{u_i} C_c \\ B_c C_{y_{u_i}} & A_c \end{bmatrix} \quad (4-7)$$

$$B_w = \begin{bmatrix} B_w \\ B_c D_{yw} \end{bmatrix}; \quad B_{d_i} = \begin{bmatrix} B_{d_i} \\ B_c D_{y_{d_i}} \end{bmatrix} \quad (4-8)$$

$$C_z = [C_z \quad D_{zu} C_c]; \quad C_{e_i} = [C_{e_i} \quad D_{e_i u} C_c] \quad (4-9)$$

$$D_{ed_i} = D_{e_i d_i} \quad (4-10)$$

The following new definitions are made:

$$\gamma_i = \inf_{K \text{ stabilizing}} \|T_{ed_i}\|_\infty$$

$$\bar{\gamma}_i \equiv \|T_{ed_i}\|_\infty \text{ when } K(s) = K_{2 \text{ opt}}$$

$$\Gamma \equiv \{\gamma_1, \dots, \gamma_n\}$$

$K_{\min} \equiv$ a solution to the H_2/H_∞ problem for some set Γ

$$\gamma_i^* \equiv \|T_{ed_i}\|_\infty \text{ when } K(s) = K_{\min}$$

$$\alpha^* \equiv \|T_{zw}\|_2 \text{ when } K(s) = K_{\min}$$

The mixed H_2/H_∞ problem is now to find a controller $K(s)$ such that:

- i. A_2 and A_{u_i} are stable for all i
- ii. $\|T_{ed_i}\|_\infty \leq \gamma_i$ for some given set of $\gamma_i > \bar{\gamma}_i$
- iii. $\|T_{zw}\|_2$ is minimized.

Now Theorem 3.2 can be extended to multiple H_∞ constraints as follows:

Theorem 4.1: Let (A_c, B_c, C_c) be given and assume there exists a solution

$Q_{u_i} = Q_{u_i}^T \geq 0$ satisfying

$$A_{u_i} Q_{u_i} + Q_{u_i} A_{u_i}^T + (Q_{u_i} C_{e_i}^T + B_{d_i} D_{ed_i}^T) R_i^{-1} (Q_{u_i} C_{e_i}^T + B_{d_i} D_{ed_i}^T)^T + B_{d_i} B_{d_i}^T = 0 \quad (4-11)$$

for all i , where $R_i = (\gamma_i^2 I - D_{ed_i} D_{ed_i}^T) > 0$. Then, for each i the following are equivalent:

- i) $(A_{\infty i}, B_{d_i})$ is stabilizable
- ii) $A_{\infty i}$ is stable.

Moreover, if i) - ii) hold, the following are true:

iii) $\|T_{ed_i}\|_{\infty} \leq \gamma_i$ for all i

iv) the two norm of the transfer function T_{zw} is given by

$$\|T_{zw}\|_2^2 = \text{tr}[C_z Q_2 C_z^T] = \text{tr}[Q_2 C_z^T C_z]$$

where $Q_2 = Q_2^T \geq 0$ is the solution to the Lyapunov equation

$$A_2 Q_2 + Q_2 A_2^T + B_w B_w^T = 0$$

v) all real symmetric solutions to (4-11) are positive semidefinite for all i

vi) there exists a unique minimal solution to (4-11) in the class of real symmetric solutions for each i

vii) $Q_{\infty i}$ are the minimal solutions to (4-11) iff

$$\text{Re}[\lambda_j (A_{\infty i} + B_{d_i} D_{ed_i}^T R_i^{-1} C_{e_i} + Q_{\infty i} C_{e_i}^T R_i^{-1} C_{e_i})] \leq 0 \text{ for all } j$$

viii) $\|T_{ed_i}\|_{\infty} < \gamma_i$ iff $(A_{\infty i} + B_{d_i} D_{ed_i}^T R_i^{-1} C_{e_i} + Q_{\infty i} C_{e_i}^T R_i^{-1} C_{e_i})$ is stable, where $Q_{\infty i}$ are

the minimal solutions to (4-11) for all i

Proof: See Theorem 1, [UWR94].

Using Theorem 4.1, the mixed case can be restated as:

Find a strictly proper controller $K(s)$ that minimizes the index

$$J(A_c, B_c, C_c) = \text{tr}(Q_2 C_z^T C_z) \quad (4-12)$$

where Q_2 is the real, symmetric, positive semidefinite solution to

$$A Q_2 + Q_2 A^T + B_w B_w^T = 0 \quad (4-13)$$

and such that

$$A_{\infty i} Q_{\infty i} + Q_{\infty i} A_{\infty i}^T + (Q_{\infty i} C_{e_i}^T + B_{d_i} D_{ed_i}^T) R_i^{-1} (Q_{\infty i} C_{e_i}^T + B_{d_i} D_{ed_i}^T)^T + B_{d_i} B_{d_i}^T = 0 \quad (4-14)$$

has a real symmetric positive semidefinite solution for all i . To solve this minimization problem with many equality constraints, a Lagrange multiplier approach is used. The Lagrangian is

$$L = \text{tr}[Q_2 C_z^T C_z] + \text{tr}\{[A_2 Q_2 + Q_2 A_2^T + B_w B_w^T]X\} \\ + \sum_{i=1}^{n_s} \text{tr}\{[A_{\infty i} Q_{\infty i} + Q_{\infty i} A_{\infty i}^T + (Q_{\infty i} C_{e_i}^T + B_{d_i} D_{ed_i}^T)R_i^{-1}(Q_{\infty i} C_{e_i}^T + B_{d_i} D_{ed_i}^T)^T + B_{d_i} B_{d_i}^T]Y_i\} \quad (4-15)$$

where X and Y_i are symmetric Lagrange multiplier matrices. The resulting first order necessary conditions have not been solved analytically but do provide some insight into the nature of the solution. In particular, the condition

$$\frac{\partial L}{\partial Q_{\infty i}} = (A_{\infty i} + B_{d_i} D_{ed_i}^T R_i^{-1} C_{e_i} + Q_{\infty i} C_{e_i}^T R_i^{-1} C_{e_i})^T Y_i \\ + Y_i (A_{\infty i} + B_{d_i} D_{ed_i}^T R_i^{-1} C_{e_i} + Q_{\infty i} C_{e_i}^T R_i^{-1} C_{e_i}) = 0 \quad (4-16)$$

implies that either $Y_i = 0$ or $(A_{\infty i} + B_{d_i} D_{ed_i}^T R_i^{-1} C_{e_i} + Q_{\infty i} C_{e_i}^T R_i^{-1} C_{e_i})$ is neutrally stable. The former condition means the solution is off the boundary of the corresponding H_{∞} constraint, and the latter solution implies the solution lies on the boundary of the corresponding H_{∞} constraint and $Q_{\infty i}$ is the neutrally stabilizing solution for that H_{∞} Riccati equation. From this, it is not hard to show that:

- (i) no solution to the mixed problem exists if $\gamma_i < \bar{\gamma}_i$ for any i
- (ii) the solution to the mixed problem is the H_2 optimal compensator, K_{2opt} , if $\gamma_i \geq \bar{\gamma}_i$ for all i
- (iii) if neither (i) nor (ii), the solution to the mixed problem is on at least one of the H_{∞} constraint boundaries, and a neutrally stabilizing ARE solution is required.

Condition (iii), which holds for any "non-trivial" mixed problem, poses severe numerical problems, as addressed in the next section.

4.2 Multiple H_∞ Constraints: Numerical Methods

Two approaches have been developed to compute controllers which solve the mixed H_2/H_∞ problem for multiple constraints. The first method, called the Grid Method, computes the set of controllers which satisfy the H_∞ constraints in the region of interest. This is accomplished by holding all but one constraint constant and varying the remaining constraint. The second method, called the Direct Method, attempts to simultaneously reduce all H_∞ constraints. For the remainder of the discussion it will be assumed that there are only two H_∞ constraints. The results can be extended as necessary to handle larger constraint sets. The methods are based on the performance index

$$J_\gamma = \|T_{zw}\|_2^2 + \lambda_1 \left(\|T_{ed_1}\|_\infty - \gamma_1 \right)^2 + \lambda_2 \left(\|T_{ed_2}\|_\infty - \gamma_2 \right)^2 \quad (4-24)$$

where λ_i are penalties on the error between the desired γ_i and the infinity-norm of the respective transfer function. Note that this requires every H_∞ constraint to be achieved with equality, which is not necessarily the optimal solution. In order to avoid this, the constraints should actually be treated as inequality constraints, which requires a constrained optimization method. This has been accomplished using Sequential Quadratic Programming; see [Wal94]. In this thesis, the constraints will be treated as equality constraints, however. Since a large portion of the "active" region will be mapped out, this poses only a small restriction. Furthermore, as it has been shown that the optimal order problem has all H_∞ constraints satisfied at equality [WR94c], the controllers found here are the closest fixed order controllers in a two-norm sense to the optimal (free order) controllers. The resulting numerical optimization is basically that of Section 3.2.2, except with additional similar H_∞ terms.

4.2.1 Grid Method

The grid method consists of solving a series of mixed problems by holding one H_{∞} constraint constant and reducing the second. Once the optimal curve has been determined, the first constraint is decremented and the process is repeated. The initial conditions for the method are determined by solving the two single constraint mixed H_2/H_{∞} problems to define the region of interest. The process results in a grid defined by α versus γ_1 versus γ_2 . The resulting grid is shown in Figure 4-2.

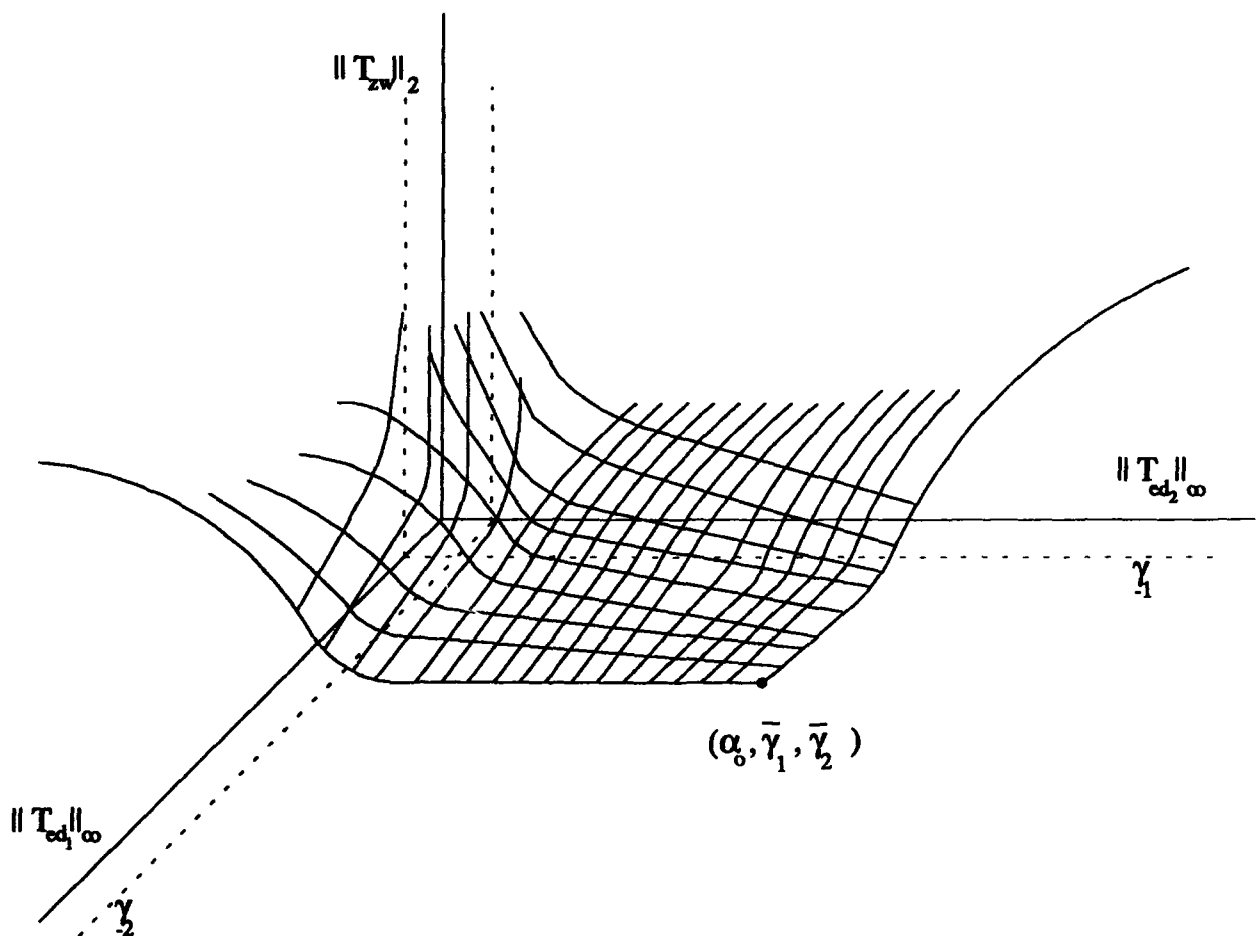


Figure 4-2 Grid Method

4.2.2 Direct Method

The introduction to this chapter suggested this method. Since the design objectives are limited to a specific region, one approach to synthesizing a controller would be to reduce both H_∞ constraints to the desired level without computing the entire grid mentioned in the previous approach. The direct method does this by concurrently reducing the constraints. The process used in this approach is to begin at the optimal H_2 controller and simultaneously reduce γ_1 and γ_2 until the controller is found which meets both objectives. This results in a controller of fixed order which meets both the H_∞ constraints and has the smallest two-norm for the H_2 transfer function. Figure 4-3 shows this method. Notice that by proper selection of the step size of the H_∞ constraints, the designer can select a desired direction. Also note the "hooks" at the end of each curve. These are the result of

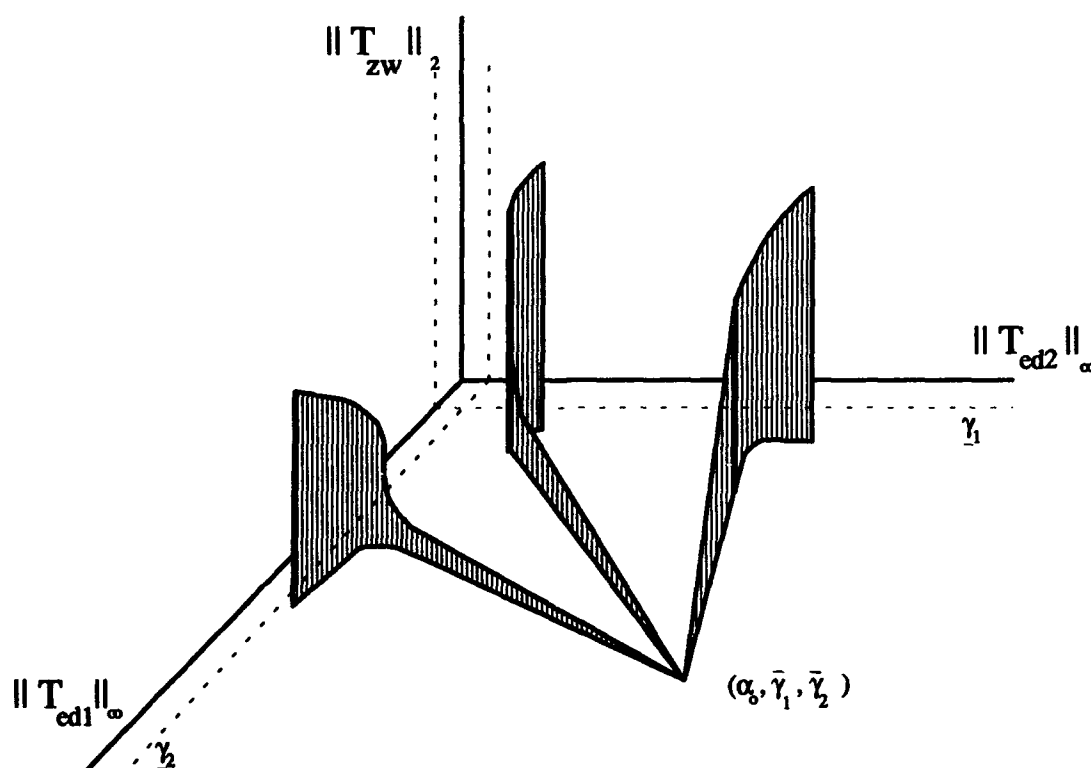


Figure 4-3 Direct Method

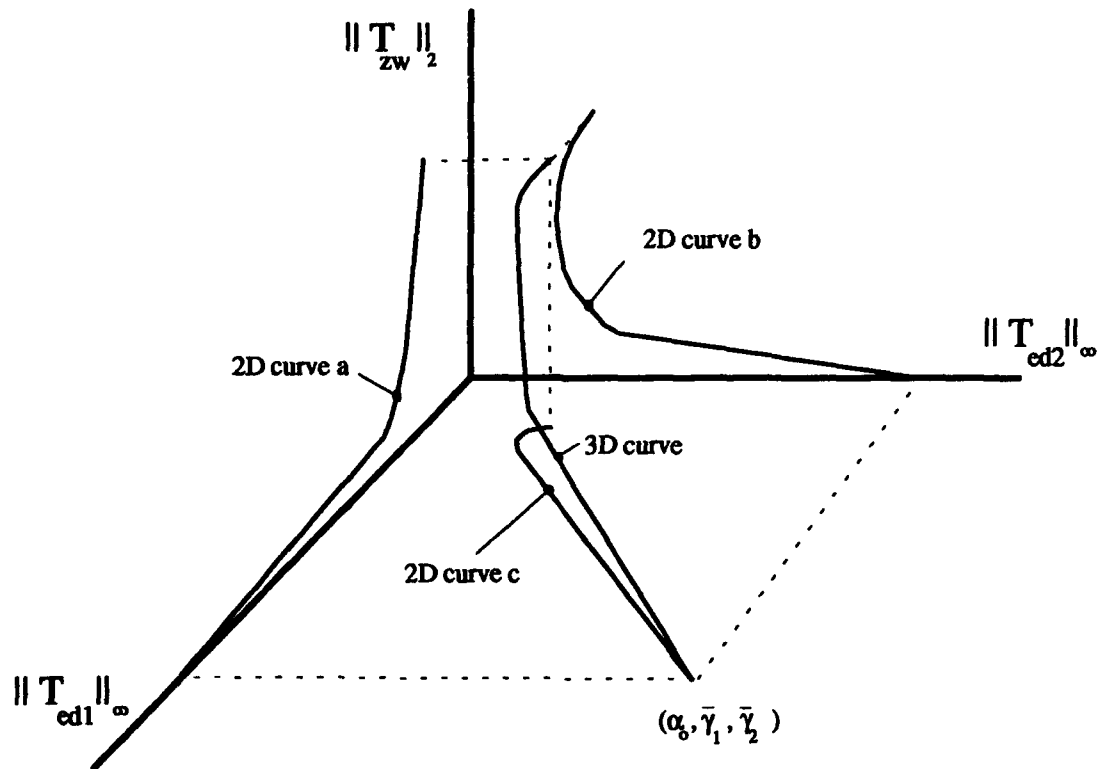


Figure 4-4 Direct Method 3D curve and 2D projections

the trade off between the H_∞ constraints encountered as γ_i approaches $\bar{\gamma}_i$. Figure 4-3 shows that the resulting curve is a 3D curve ($\|T_{zw}\|_2$ vs. $\|T_{ed1}\|_\infty$ vs. $\|T_{ed2}\|_\infty$). Therefore, for any 3D curve there are three projections. These 2D curves are the $\|T_{zw}\|_2$ vs. $\|T_{ed1}\|_\infty$ curve, the $\|T_{zw}\|_2$ vs. $\|T_{ed2}\|_\infty$ curve, and the $\|T_{ed1}\|_\infty$ vs. $\|T_{ed2}\|_\infty$ curve. This is shown in Figure 4-4, and the curves are denoted as curve a, b and c, respectively.

4.3 Feasible Solutions

Assume for this section that numerical problems in computing a solution do not exist. There are boundaries in the mixed problem where feasible solutions do not exist. These boundaries are:

- (i) No controller results in $\alpha < \alpha_0$
- (ii) No mixed solution exists for $\gamma_i < \bar{\gamma}_i$ for either $i=1$ or 2

(iii) For certain values of γ_i , no mixed solution exists which simultaneously satisfies all ∞ -norms constraints, even though $\gamma_i > \underline{\gamma}_i$, $\forall i$

First, define three planes:

Plane α_o : the plane defined by letting $\alpha = \alpha_o$ for all γ_i , $i=1,2$. All α 's above this plane represent a suboptimal solution to the H_2 problem, and solutions below this plane are not feasible.

Plane $\underline{\gamma}_1$: the plane defined by letting $\gamma_1 = \underline{\gamma}_1$, for all α, γ_2 . All γ_1 above this plane are suboptimal solutions to the corresponding $H_{\infty 1}$ design, and solutions below this plane are not feasible.

Plane $\underline{\gamma}_2$: direct analogy of plane $\underline{\gamma}_1$.

Figure 4-5 shows these planes.

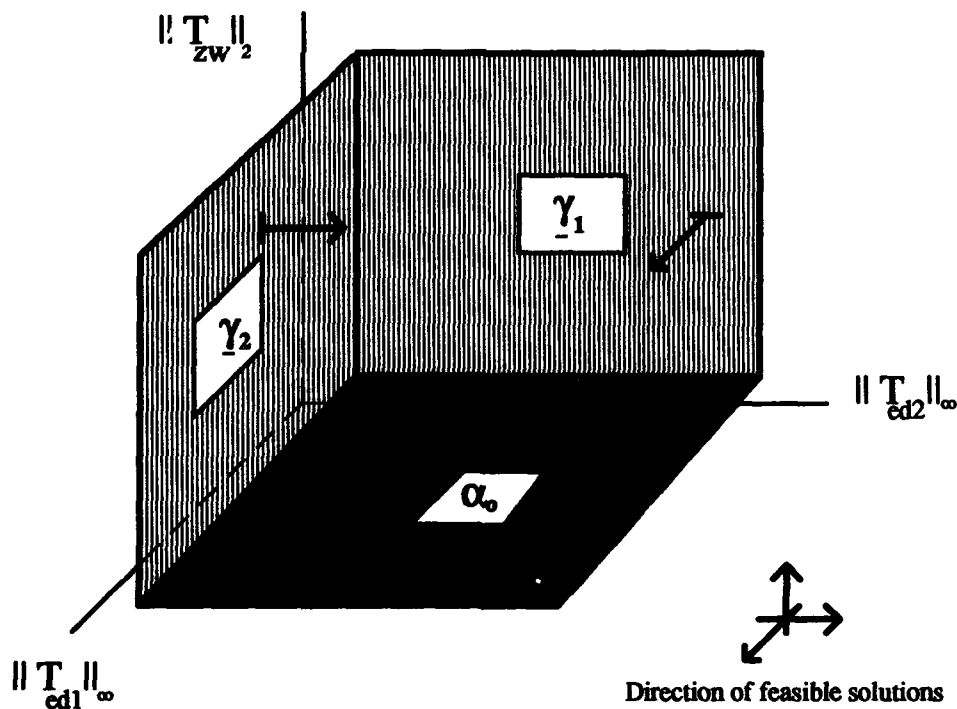


Figure 4-5 $H_2/H_{\infty 1}$ feasible planes

Mixed H_2/H_∞ design is a tool that trades among the H_2 design and the different H_∞ designs. The trade-offs taken two at a time are examined next.

4.3.1 Trade off between H_2 design and the $H_{\infty i}$ design

[Rid91] showed that α^* is a monotonically decreasing function of γ for a single constraint mixed problem. Therefore, α^* is now a monotonically decreasing function of γ_i . If the optimal α versus γ_i curve is computed, then unfeasible solutions lie below this curve, and any solution above this curve is feasible but suboptimal. Graphically, this is shown in Figure 4-6. The numerical method computes a suboptimal curve that is close to the optimal curve. This is due to the requirement of finding a mixed solution numerically.

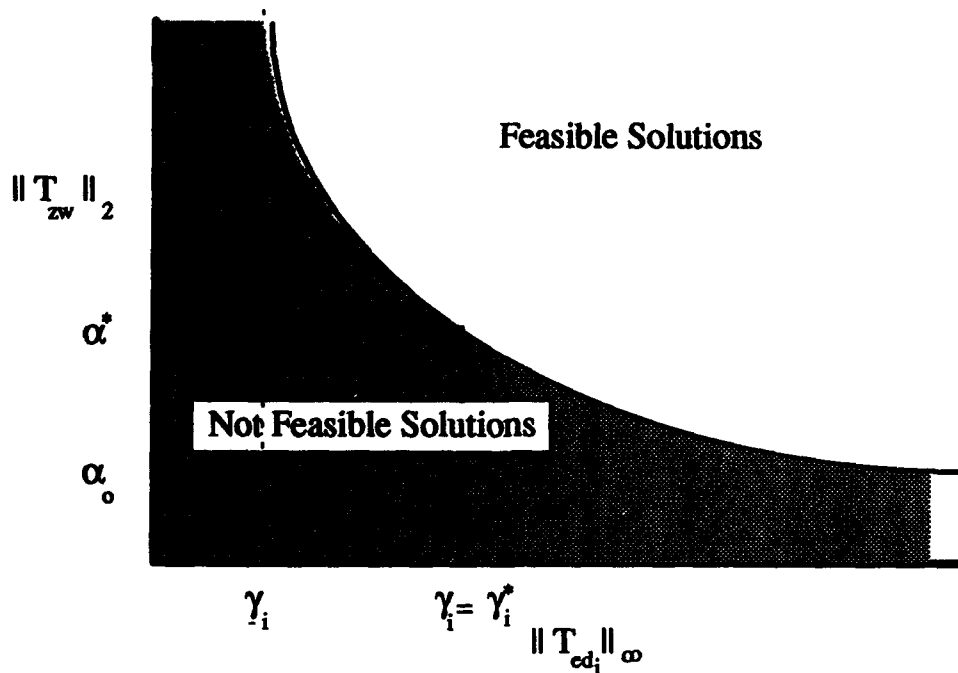


Figure 4-6 Trade-off among H_2/H_∞ (feasible solutions)

4.3.2 Trade off between $H_{\infty i}$ designs ($i=1,2$)

First consider that the mixed problem has only $\|T_{ed1}\|_{\infty}$ as a constraint (a single constraint problem). In this case the mixed problem is just a mixed $H_2/H_{\infty 1}$ design. For each point on $H_2/H_{\infty 1}$ curve, $\|T_{ed2}\|_{\infty}$ can be computed. Next, consider that the mixed problem has only $\|T_{ed2}\|_{\infty}$ as a constraint (a single constraint problem). In this case, the mixed problem is just a mixed $H_2/H_{\infty 2}$ design. For each point on $H_2/H_{\infty 2}$ curve, $\|T_{ed1}\|_{\infty}$ can be computed. The resulting curves from the two different designs are shown in Figure 4-7. Define, the $H_2/H_{\infty 1}$ curve as the optimal curve for mixed $H_2/H_{\infty 1}$ design, and the $H_2/H_{\infty 2}$ curve as the optimal curve for the mixed $H_2/H_{\infty 2}$ design. These two curves define the boundary between the region of sub-optimal solutions and the region of "optimal" solutions as shown in Figure 4-7. From a control point of view, we are interested in the

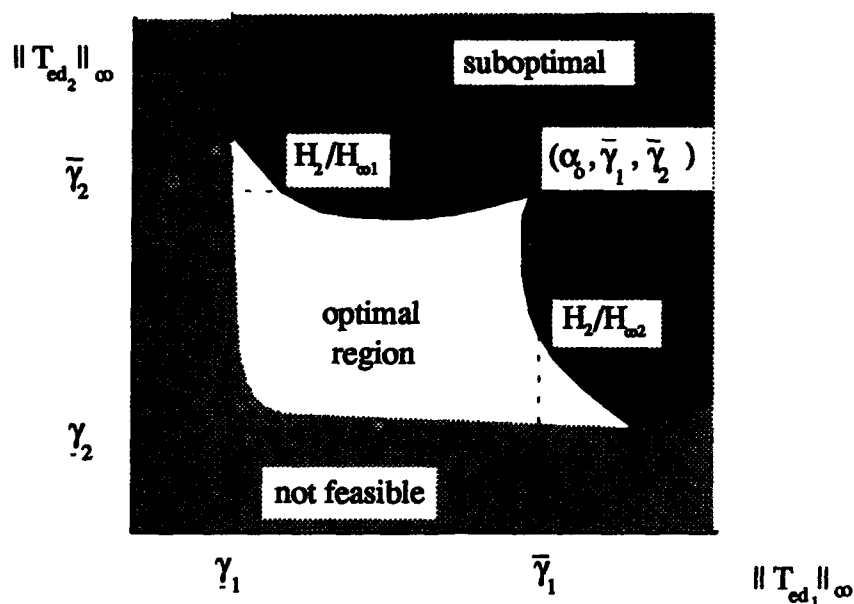


Figure 4-7 Design region in the $\|T_{ed1}\|_{\infty} / \|T_{ed2}\|_{\infty}$ plane

region on or below the optimal mixed $H_2/H_{\infty i}$ design curves; that is, the region of optimal solutions. The region above these curves is not of interest, as shown in [WR94c]. Here, the optimal solution "snaps back" to the optimal single constraint curve, and thus is suboptimal.

Consider now that the mixed problem has both $H_{\infty i}$ designs as constraints. In this case, the mixed problem is a mixed $H_2/H_{\infty 1}/H_{\infty 2}$ design. There exists a boundary close to the γ_i values where, below this boundary, no feasible solutions exist. This is shown graphically in Figure 4-7. This boundary is difficult to find analytically or numerically. This was the region iii) alluded to at the beginning of section 4.3.

Joining the planes and boundaries, a region of feasible solutions can be drawn, as shown in Figure 4-8. Regions of suboptimal solutions are also plotted. Figure 4-9 shows a surface for the mixed $H_2/H_{\infty 1}/H_{\infty 2}$ design. On this surface we are interested in the solid checkered region that corresponds to the optimal region, especially at the "knee" where the γ 's are close to the *optimal values*. Sub-optimal regions (shaded checkered) are also shown in Figure 4-9. These are not optimal mixed solutions, since their values of γ_i are greater than those for the optimal curves corresponding to the mixed $H_2/H_{\infty 1}$ design and the mixed $H_2/H_{\infty 2}$ design, respectively. However, these suboptimal regions help to visually clarify the problem.

The next chapter will present a SISO example as an introduction to this new synthesis method. It will show the boundaries that were discussed in this chapter.

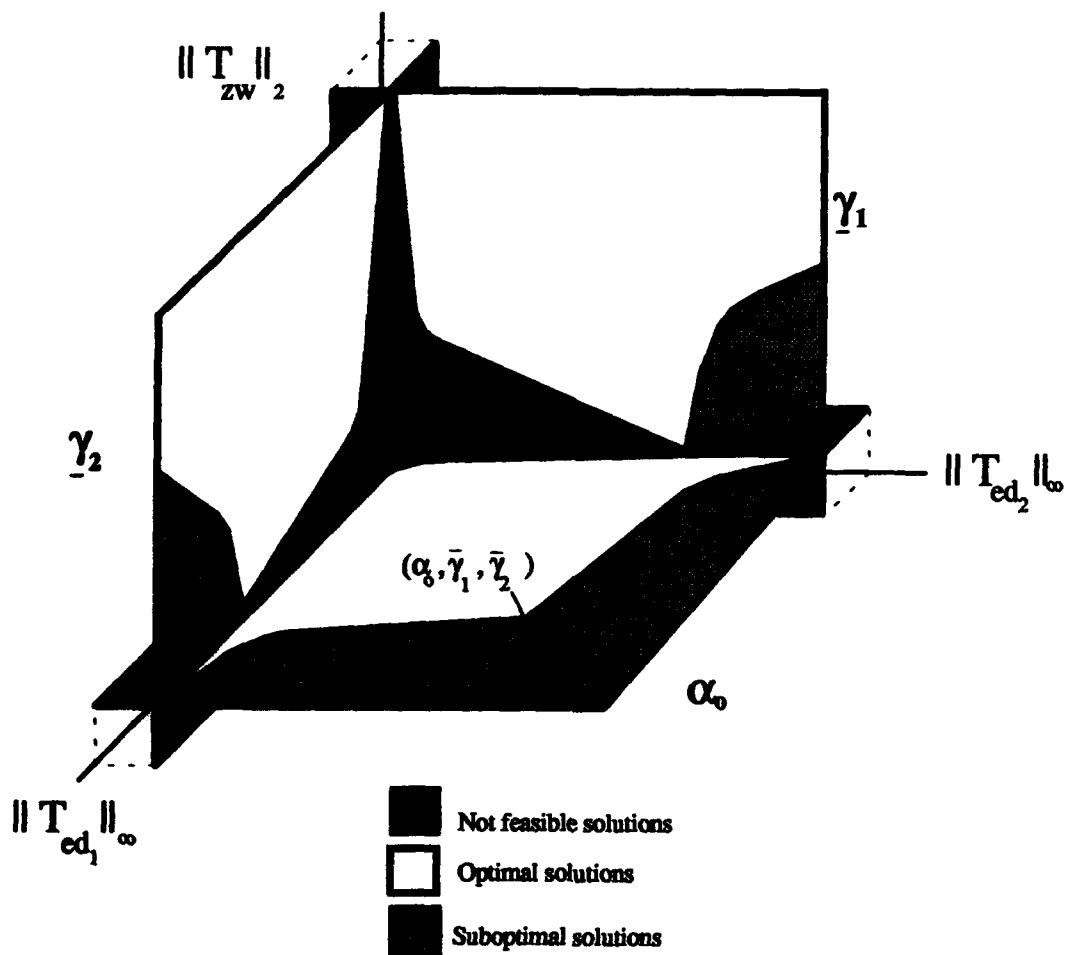


Figure 4-8 H_2/H_{∞} Projection of feasible solution

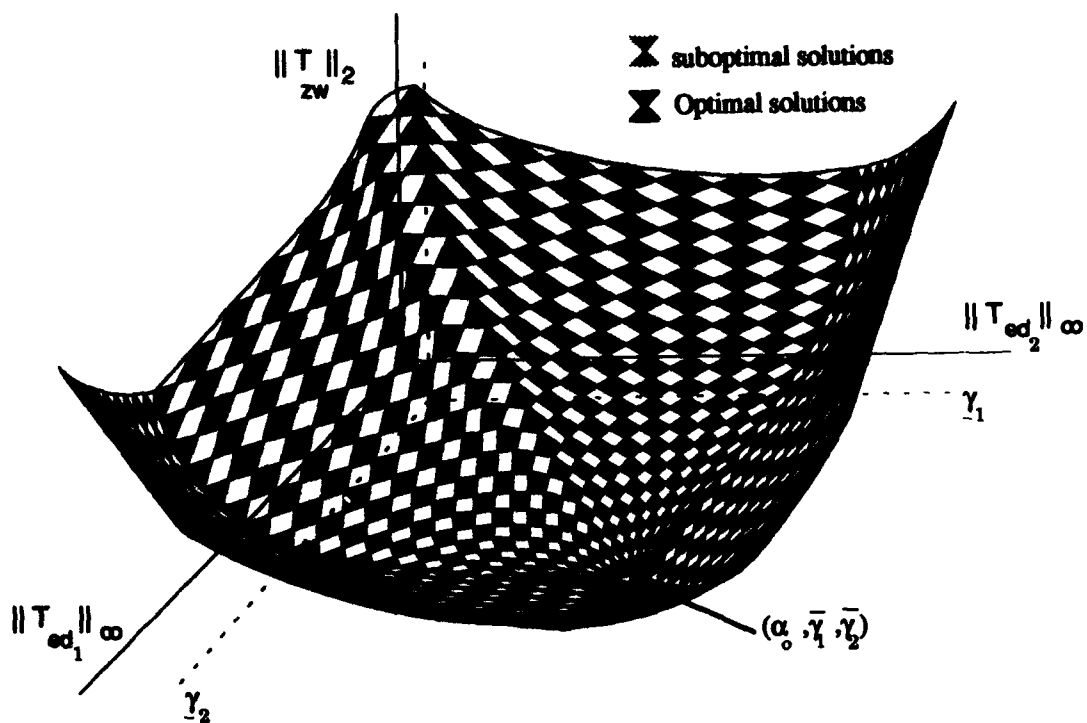


Figure 4-9 H_2/H_∞ Surface of Optimal and Suboptimal solutions

V. Numerical Validation through a SISO example

5.1 Problem Set-Up

This chapter illustrates mixed H_2/H_∞ design with single and multiple H_∞ constraints. The numerical method is that developed by [WR94a], which permits generalization of the H_∞ constraint, (i.e., $D_{en}^T D_{en}$ and / or $D_{yd} D_{yd}^T$ not required to be full rank and $D_{ed} \neq 0$ allowed). For this SISO example, the objective is to show some of the boundaries and methods discussed in the last two chapters. An acceleration command following design for the F-16 is desired. The F-16 plant consists of a short period approximation (α , q), a time delay (δ) [first order Padé approximation], and a first order actuator servo. The state space matrices are:

$$A_g = \begin{bmatrix} -20 & 0 & 0 & 0 \\ -0.188 & -1.491 & 0.996 & 0 \\ -19.04 & 9.753 & -0.096 & 0 \\ -4.367 & 35.264 & -0.334 & -40 \end{bmatrix} \quad (5-1)$$

$$B_g = \begin{bmatrix} 20 \\ 0 \\ 0 \\ 0 \end{bmatrix}; \quad C_g = [4.367 \quad -35.264 \quad 0.334 \quad 80]; \quad D_g = [0] \quad (5-2)$$

The poles and zeros of the plant are:

$$\text{poles } \lambda = [-40.0000; -4.3535; 1.9025; -20.0000]$$

$$\text{zeros} = [-1.2564 + 11.9340i; -1.2564 - 11.9340i; 40.0000]$$

Three designs are produced: an H_2 design, a mixed H_2/H_∞ design with a single constraint, and a mixed H_2/H_∞ design with multiple H_∞ constraints.

5.2 H_2 Design

The H_2 design is set up as a basic LQG problem, as shown in Figure 5-1. In the H_2 design, two exogenous inputs w_1 and w_2 enter the plant; they are zero-mean white Gaussian noise with unit intensity. It is desired to minimize the energy or two norm of the controlled outputs z_1 and z_2 . The weights related with w_1, w_2, z_1 and z_2 are:

Wind disturbance weight: The wind disturbance constitutes an exogenous input (w_1). It passes through a coloring filter W_d and a distribution matrix Ψ , where

$$W_d(s) = \frac{0.0187}{s + 6.7} ; \quad \Psi = \begin{bmatrix} 0 \\ -1.491 \\ 9.753 \\ 35.265 \end{bmatrix}$$

Measurement noise: The measurement noise is represented by an exogenous input (w_2). w_2 is added to the feedback signal. The weight for w_2 is:

$$W_n = 0.025$$

Control Usage: The weight for control usage z_1 is the scalar

$$W_c = 1.0$$

Normal acceleration output weight: It represents the weight on the normal acceleration (z_2); this weight is chosen to be the scalar

$$W_z = 1.0$$

Therefore, the system P_2 is

$$P_2 = \left[\begin{array}{c|cc} A_2 & B_w & B_{u_2} \\ \hline C_z & D_{zw} & D_{zu} \\ \hline C_{y_2} & D_{yw} & D_{yu} \end{array} \right] \quad (5-3)$$

and the corresponding state space matrices are

$$\begin{aligned} \begin{bmatrix} \dot{x}_g \\ \dot{x}_d \end{bmatrix} &= \begin{bmatrix} A_g & \Psi C_d \\ 0 & A_d \end{bmatrix} \begin{bmatrix} x_g \\ x_d \end{bmatrix} + \begin{bmatrix} \Psi D_d & 0 \\ B_d & 0 \end{bmatrix} \begin{bmatrix} w_1 \\ w_2 \end{bmatrix} + \begin{bmatrix} B_g \\ 0 \end{bmatrix} u \\ \begin{bmatrix} z_1 \\ z_2 \end{bmatrix} &= \begin{bmatrix} 0 & 0 \\ W_z C_g & 0 \end{bmatrix} \begin{bmatrix} x_g \\ x_d \end{bmatrix} + \begin{bmatrix} 0 & 0 \\ 0 & 0 \end{bmatrix} \begin{bmatrix} w_1 \\ w_2 \end{bmatrix} + \begin{bmatrix} W_c \\ 0 \end{bmatrix} u \\ y &= \begin{bmatrix} C_g & 0 \end{bmatrix} \begin{bmatrix} x_g \\ x_d \end{bmatrix} + \begin{bmatrix} 0 & W_n \end{bmatrix} \begin{bmatrix} w_1 \\ w_2 \end{bmatrix} + \begin{bmatrix} 0 \\ 0 \end{bmatrix} u \end{aligned} \quad (5-4)$$

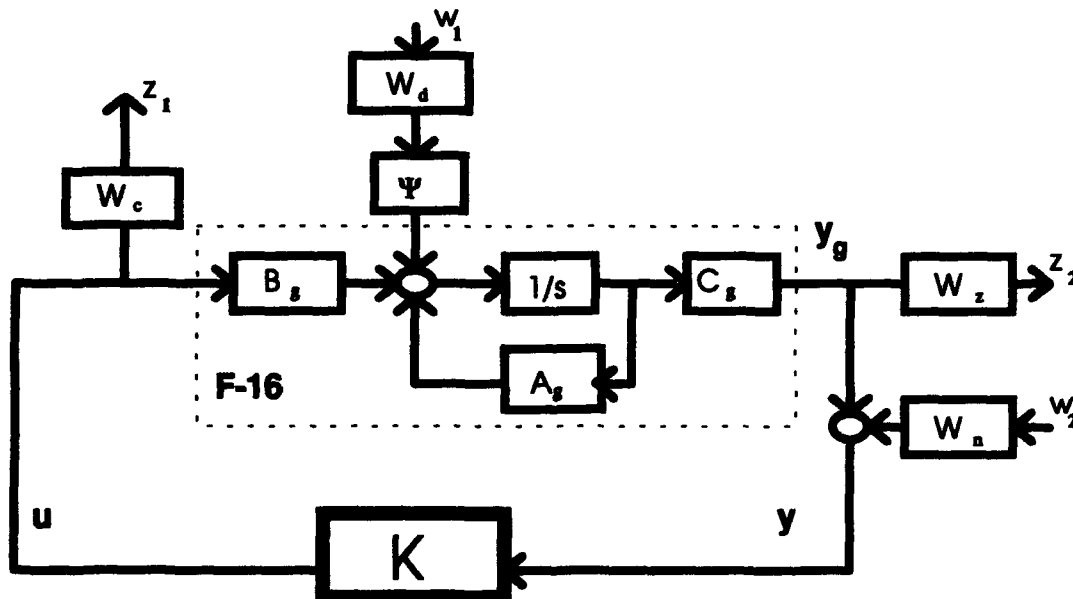


Figure 5-1 H_2 Block diagram (F-16)

The basic conditions that are checked here include $D_{zw} = 0$, $D_{yu} = 0$, $D_{yw}D_{yw}^T$ full rank, and $D_m^T D_m$ full rank; these are met by the design with a non-zero W_n and W_c . Therefore, the design diagram is properly set up. Table 5-1 shows the results.

Table 5-1 H_2 Results

	$\alpha_o = 0.2530$	VPM (deg)
	VGM (dB)	
S	[-5.8609, 28.7686]	± 57.6035
T	[-6.4183, 3.6504]	± 30.2811

Although the objective was to design a pure regulator, from Table 5-1 we see that the H_2 controller provides good margins. The VGM and VPM are based on the magnitude plots of sensitivity and complementary sensitivity as explained in Chapter 2, Section 2.5. Figure 5-2 shows the magnitude plot of sensitivity and complementary sensitivity.

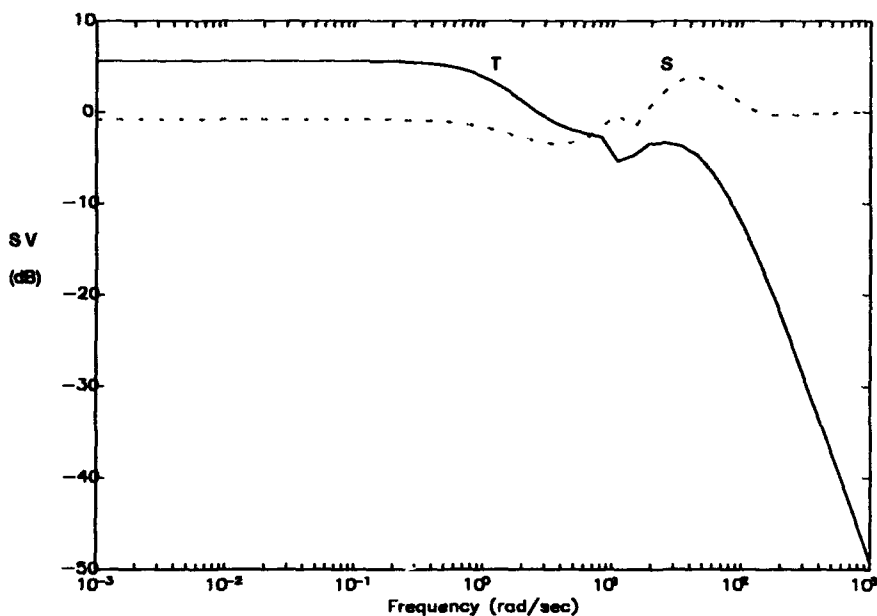


Figure 5-2 Magnitude of Sensitivity and Complementary Sensitivity (dB)

The magnitude of the sensitivity shows that the H_2 controller attenuates the wind disturbance. The magnitude of complementary sensitivity represents the measurement noise feedthrough to the plant output, the inverse of the allowable multiplicative uncertainty, and the closed-loop tracking transfer function. Evidently this design does not provide good tracking since the gain is above 0 dB at low frequencies and rolls off too early.

5.3 Mixed H_2/H_∞ Design with a Single H_∞ Constraint

Two mixed H_2/H_∞ designs with single H_∞ constraints are solved. The first design ($H_2/H_{\infty 1}$) represents a sensitivity constraint ($T_{ed_1} = W_s S$), and the second ($H_2/H_{\infty 2}$) represents a complementary sensitivity constraint ($T_{ed_2} = W_t T$). Two objectives are set up: the first objective is to compute the infinity norm of T_{ed_2} with the controller obtained from the mixed $H_2/H_{\infty 1}$ design, and the second objective is to compute the infinity norm of T_{ed_1} with the controller obtained from the mixed $H_2/H_{\infty 2}$ design.

5.3.1 Sensitivity Constraint Design ($H_2/H_{\infty 1}$)

The block diagram for the sensitivity constraint design is shown in Figure 5-3.

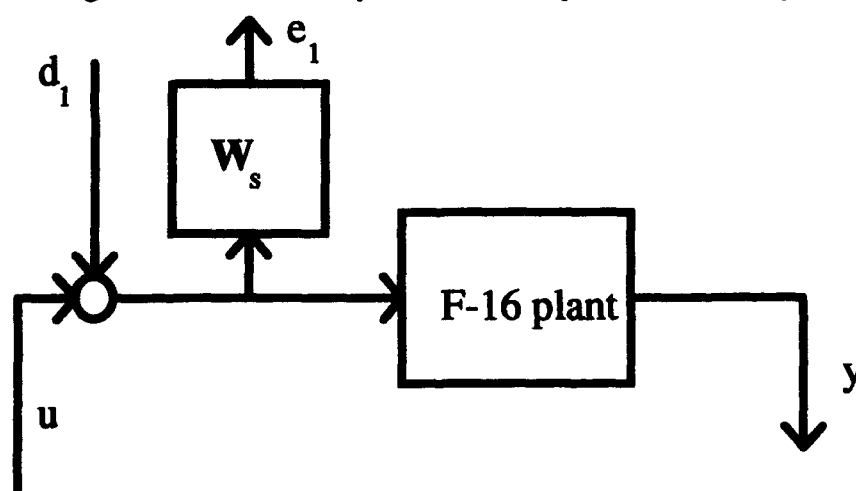


Figure 5-3 Mixed $H_2/H_{\infty 1}$ Block Diagram (Sensitivity Constraint)

The transfer function between the exogenous output e_1 and the exogenous input d_1 is T_{ed_1} , and is given by

$$T_{ed_1} = W_s S \quad (5-5)$$

The weight for sensitivity is a low pass filter W_s , given by

$$W_s(s) = \frac{100}{s + 0.1}$$

The objective for the mixed H_2/H_∞ design is

$$\inf_{K \text{ stabilizing}} \|T_{zw}\|_2 \text{ subject to } \|T_{ed_1}\|_\infty \leq \gamma_1 \quad (5-6)$$

The system $P_{\infty 1}$ is

$$P_{\infty 1} = \left[\begin{array}{c|cc} A_{\infty 1} & B_{d_1} & B_{u_{\infty 1}} \\ \hline C_{e_1} & D_{e_1 d_1} & D_{e_1 u} \\ \hline C_{y_{\infty 1}} & D_{y d_1} & D_{y u} \end{array} \right] \quad (5-7)$$

with the state space matrices given by

$$\begin{aligned} A_{\infty 1} &= \begin{bmatrix} A_g & 0 \\ 0 & A_s \end{bmatrix}; & B_{d_1} &= \begin{bmatrix} B_g \\ B_s \end{bmatrix}; & B_{u_{\infty 1}} &= \begin{bmatrix} B_g \\ B_s \end{bmatrix} \\ C_{e_1} &= [0 \quad C_s]; & D_{e_1 d_1} &= [D_s]; & D_{e_1 u} &= [D_s] \\ C_{y_{\infty 1}} &= [C_g \quad 0]; & D_{y d_1} &= [0]; & D_{y u} &= [0] \end{aligned} \quad (5-8)$$

Since W_s is a strictly proper transfer function, $D_s = 0$, and therefore $D_{e_1 u}^T D_{e_1 u}$ and $D_{y d_1} D_{y d_1}^T$ are not full rank matrices. Thus, we have a mixed H_2/H_∞ optimization problem with a singular H_∞ constraint. The performance index for the numerical solution is

$$J_{\gamma_1} = \|T_{zw}\|_2^2 + \lambda_1 \left(\|T_{ed_1}\|_\infty - \gamma_1 \right)^2 \quad (5-9)$$

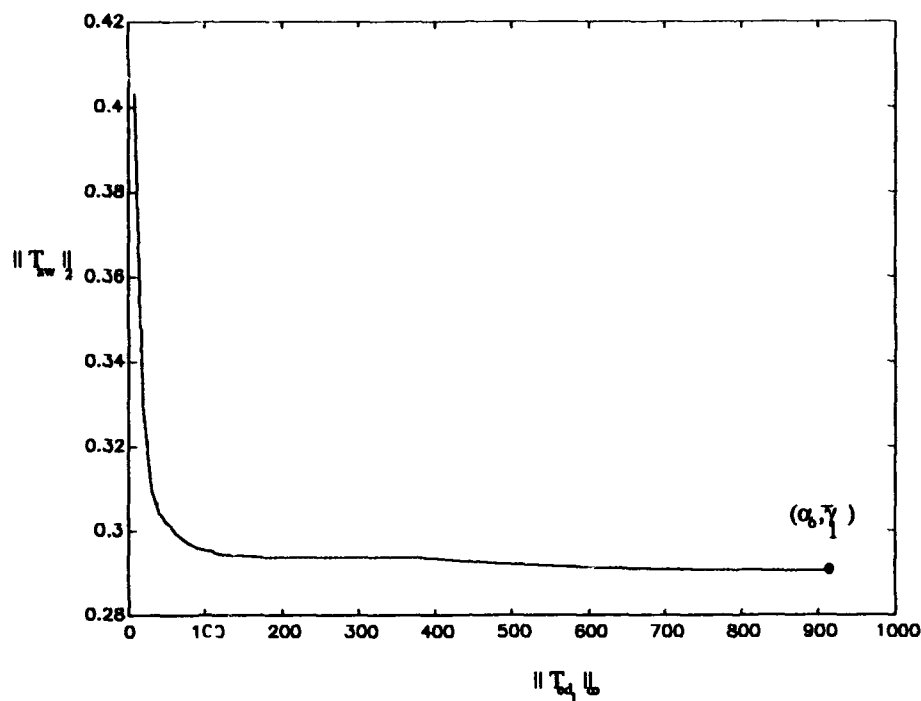


Figure 5-4 $\|T_w\|_2$ vs. $\|T_{ed,1}\|_\infty$ curve

Starting from the optimal H_2 controller and stepping along the α vs. γ_1 curve by reducing from $\bar{\gamma}_1$ to $\underline{\gamma}_1$ by increments produces Figure 5-4.

5.3.2 Complementary Sensitivity Constraint (H_2/H_∞)

$T_{ed,2}$ is the transfer function between the exogenous output e_2 and the exogenous input d_2 as shown in Figure 5-5. Here

$$T_{ed,2} = W_t T \quad (5-10)$$

with the weight for complementary sensitivity denoted by W_t , and given by

$$W_t(s) = \frac{1000 * (s + 0.01)}{(s + 1000)}$$

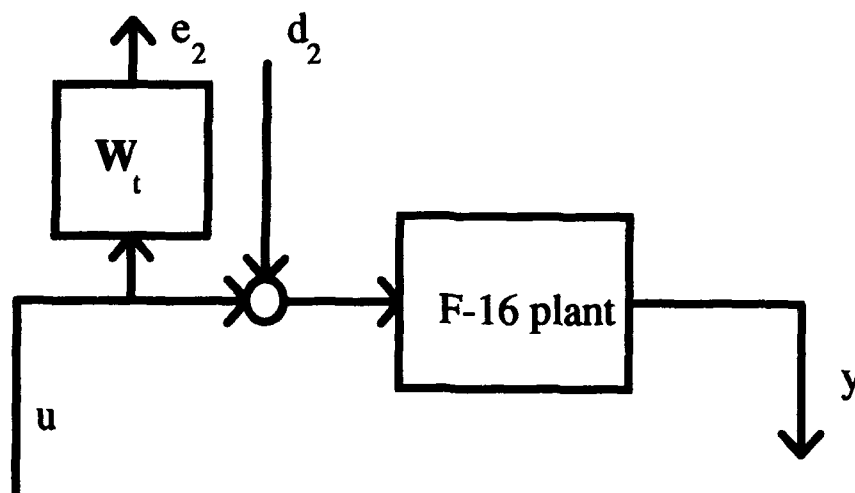


Figure 5-5 Mixed H_2/H_∞ Block Diagram (Complementary Sensitivity Constraint)

The objective for the H_2/H_∞ design is

$$\inf_{K \text{ stabilizing}} \|T_{zw}\|_2 \text{ subject to } \|T_{ed_2}\|_\infty \leq \gamma_2 \quad (5-11)$$

The system $P_{\infty 2}$ is

$$P_{\infty 2} = \left[\begin{array}{c|cc} A_{\infty 2} & B_{d_2} & B_{u_{\infty 2}} \\ \hline C_{e_2} & D_{e_2 d_2} & D_{e_2 u} \\ \hline C_{y_{\infty 2}} & D_{y d_2} & D_{y u} \end{array} \right] \quad (5-12)$$

where the state space matrices are given by

$$\begin{aligned} A_{\infty 2} &= \begin{bmatrix} A_g & 0 \\ 0 & A_t \end{bmatrix}; & B_{d_2} &= \begin{bmatrix} B_g \\ 0 \end{bmatrix}; & B_{u_{\infty 2}} &= \begin{bmatrix} B_g \\ B_t \end{bmatrix} \\ C_{e_2} &= [0 \quad C_t]; & D_{e_2 d_2} &= [0]; & D_{e_2 u} &= [D_t] \\ C_{y_{\infty 2}} &= [C_g \quad 0]; & D_{y d_2} &= [0]; & D_{y u} &= [0] \end{aligned} \quad (5-13)$$

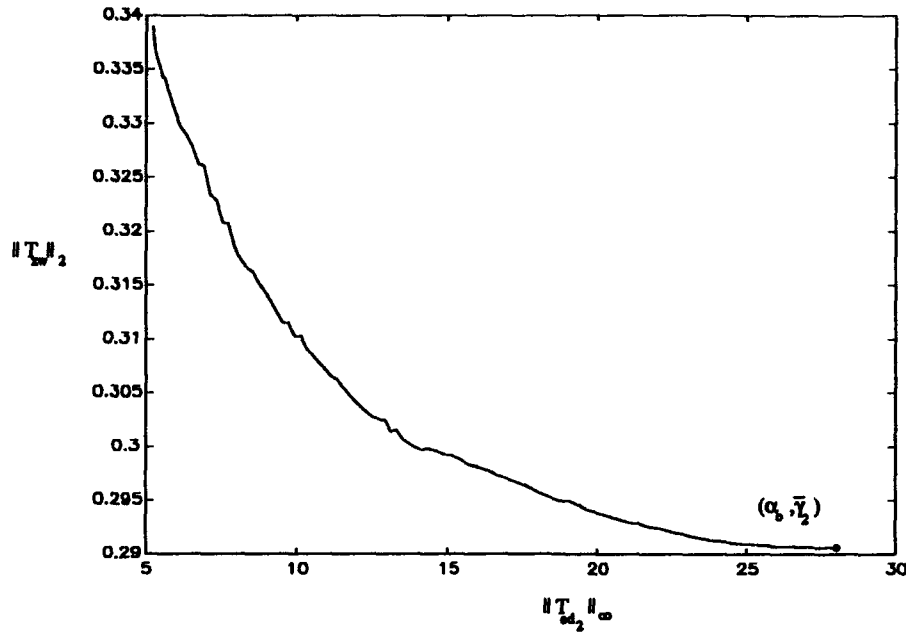


Figure 5-6 $\|T_{zw}\|_2$ vs. $\|T_{cd_2}\|_\infty$ curve

Note that $D_{yd_2} D_{yd_2}^T$ is zero, which implies we have a mixed H_2/H_∞ optimization problem with a singular H_∞ constraint. The performance index for the numerical solution is

$$J_{\gamma_2} = \|T_{zw}\|_2^2 + \lambda_2 \left(\|T_{cd_2}\|_\infty - \gamma_2 \right)^2 \quad (5-14)$$

Starting from the optimal H_2 controller and stepping along the α vs. γ_2 curve by reducing from $\bar{\gamma}_2$ to $\underline{\gamma}_2$ by increments produces Figure 5-6. The "ripples" are due to numerical inaccuracies, and due to the monotonic property, could be "smoothed".

5.3.3 Boundaries on the mixed H_2/H_∞ surface

Using the controllers $K(s)$ from the $H_2/H_{\infty 1}$ design, the infinity norm of T_{cd_2} can be computed, which represents the Complementary Sensitivity constraint. Figure 5-7 shows the trade off between T_{cd_2} (weighted Complementary Sensitivity constraint) and T_{cd_1} (weighted Sensitivity constraint). Figure 5-7 shows that although $\|T_{cd_1}\|_\infty$ is being

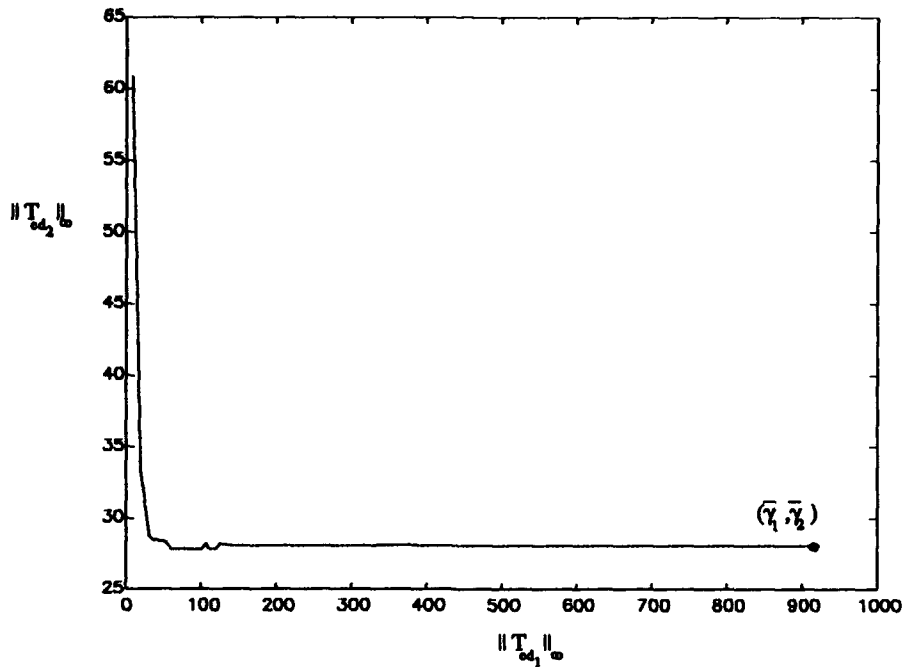


Figure 5-7 $\|T_{ed_2}\|_{\infty}$ vs. $\|T_{ed_1}\|_{\infty}$ curve (H_2/H_{∞} design)

minimized, there isn't a big change in $\|T_{ed_2}\|_{\infty}$ until $\|T_{ed_1}\|_{\infty}$ reaches the knee in the α vs. γ_1 curve. Now with the controllers $K(s)$ from the H_2/H_{∞} design, the infinity norm of T_{ed_1} is computed, which represents the Sensitivity constraint. Figure 5-8 shows the trade off between T_{ed_2} (weighted Complementary Sensitivity constraint) and T_{ed_1} (weighted Sensitivity constraint). Figure 5-8 shows a slightly different type of behavior than Figure 5-7; in Figure 5-8 the trade-off in $\|T_{ed_2}\|_{\infty}$ occurs almost immediately. A graphical interpretation showing the relationship between the two norm and the infinity norms is shown in Figure 5-9. The two 3D curves (solid lines) are the curve for the H_2/H_{∞} design and the curve for the H_2/H_{∞} design. The dotted lines represent the projection of the 3D curve for the H_2/H_{∞} design on the $\|T_{ed_2}\|_{\infty}$ vs. $\|T_{ed_1}\|_{\infty}$, $\|T_{zw}\|_2$ vs. $\|T_{ed_1}\|_{\infty}$, and $\|T_{zw}\|_2$ vs. $\|T_{ed_2}\|_{\infty}$ planes and the dashed lines represent the projection of the 3D curve for the H_2/H_{∞} design on the same set of planes.

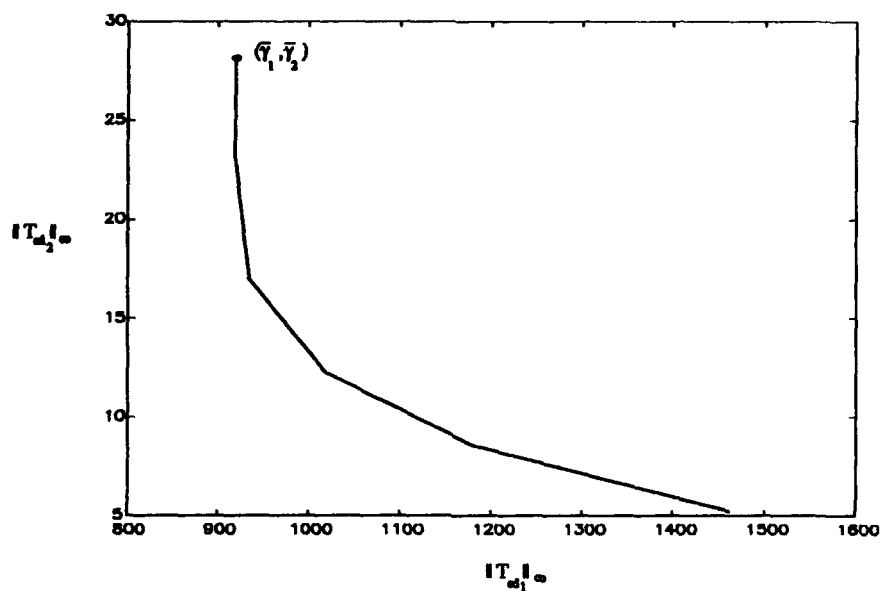


Figure 5-8 $\|T_{ed_2}\|_{\infty}$ vs. $\|T_{ed_1}\|_{\infty}$ curve (H_2/H_{∞} design)

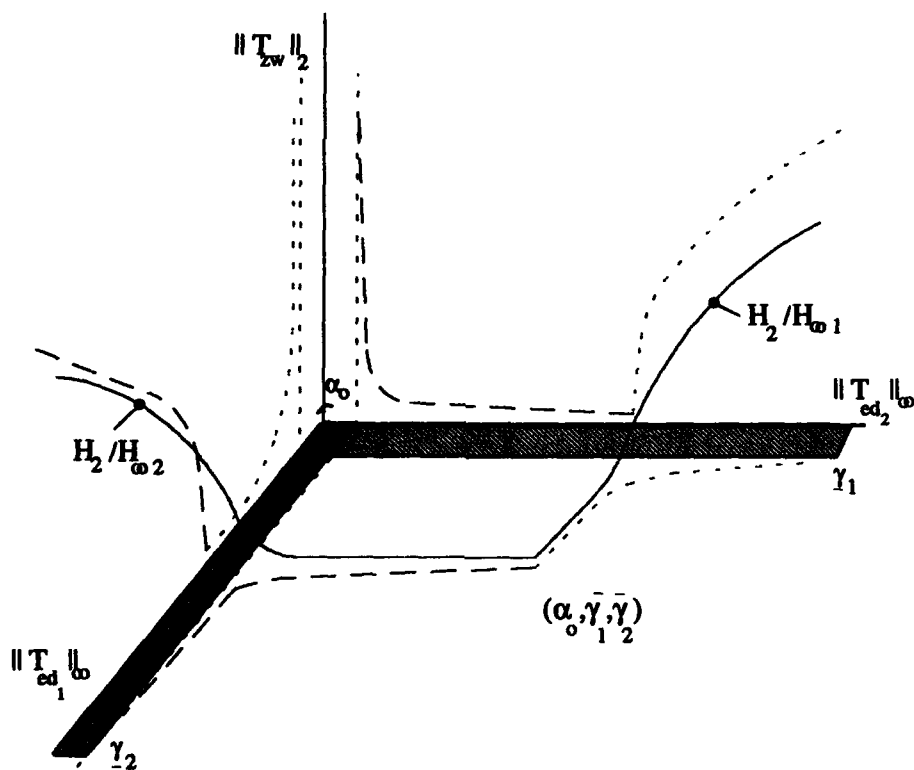


Figure 5-9 3D $\|T_{zw}\|_2$ vs. $\|T_{ed_1}\|_{\infty}$ vs. $\|T_{ed_2}\|_{\infty}$ curve for $H_2/H_{\infty 1}$ design and $H_2/H_{\infty 2}$ design

These two 3D curves represent the boundaries of the mixed $H_2/H_{\infty 1}$ and $H_2/H_{\infty 2}$ design as mentioned in Chapter 4, Section 4-3. Unfortunately, the mixed H_2/H_{∞} with a single H_{∞} constraint problem does not permit both H_{∞} constraints to be made small at the same time, unless they are wrapped in one transfer function. The next section presents the multiple H_{∞} constraint results.

5.4 Mixed H_2/H_{∞} Optimization with Multiple H_{∞} Constraints

Now, the mixed problem is a mixed $H_2/H_{\infty 1}/H_{\infty 2}$ design, and the objective is to find a stabilizing controller $K(s)$ that achieves

$$\inf_{K \text{ stabilizing}} \|T_{zw}\|_2 \text{ subject to } \begin{cases} \|T_{ed_1}\|_{\infty} \leq \gamma_1 \\ \|T_{ed_2}\|_{\infty} \leq \gamma_2 \end{cases} \quad (5-15)$$

Again, recall that both inequality constraints will be treated as equality constraints. Thus, the performance index for the numerical method is

$$J_{\gamma} = \|T_{zw}\|_2^2 + \lambda_1 (\|T_{ed_1}\|_{\infty} - \gamma_1)^2 + \lambda_2 (\|T_{ed_2}\|_{\infty} - \gamma_2)^2 \quad (5-16)$$

Two approaches are used: the first one will be the grid method and the second one the direct method, as mentioned in Chapter 4.

5.4.1 Grid Method

The results of applying the direct method (explained in Chapter 4, Section 4.2.1) are shown in Figures 5-10 and 5-11. Figure 5-10 shows the $\|T_{ed_2}\|_{\infty}$ vs. $\|T_{ed_1}\|_{\infty}$ curves. The lower dotted curve represents the boundaries for both H_{∞} constraints. Also, notice that when smaller values of infinity norms are reached, the trade-off between the infinity norm of the constraints starts to have the effect discussed in Chapter 4, Section 4.3. Figure 5-11

shows the 3D surface. This surface has an almost flat bottom; therefore, the increase in the two norm starts when the knee of the individual curves is reached.

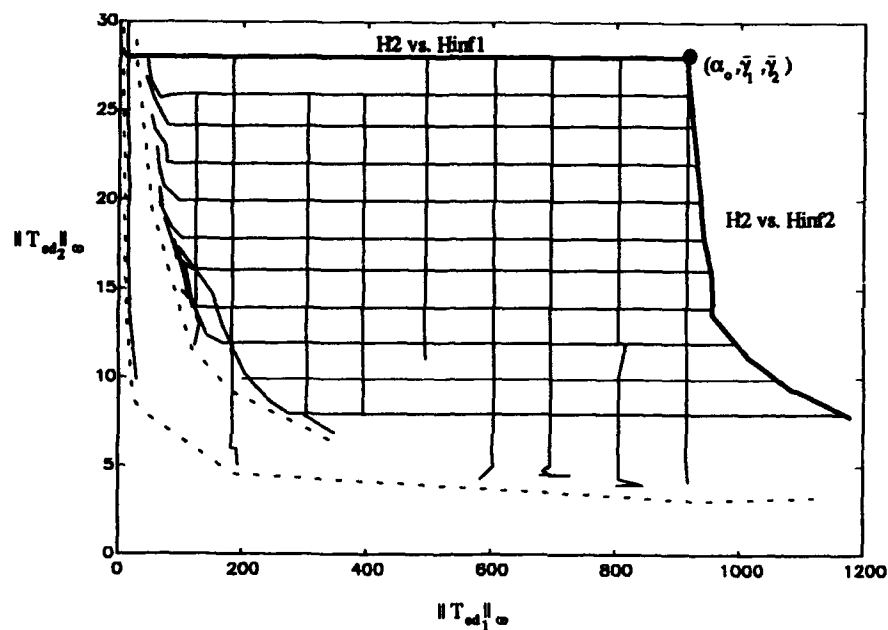


Figure 5-10 $\|T_{ed,2}\|_{\infty}$ vs. $\|T_{ed,1}\|_{\infty}$ Grid Method

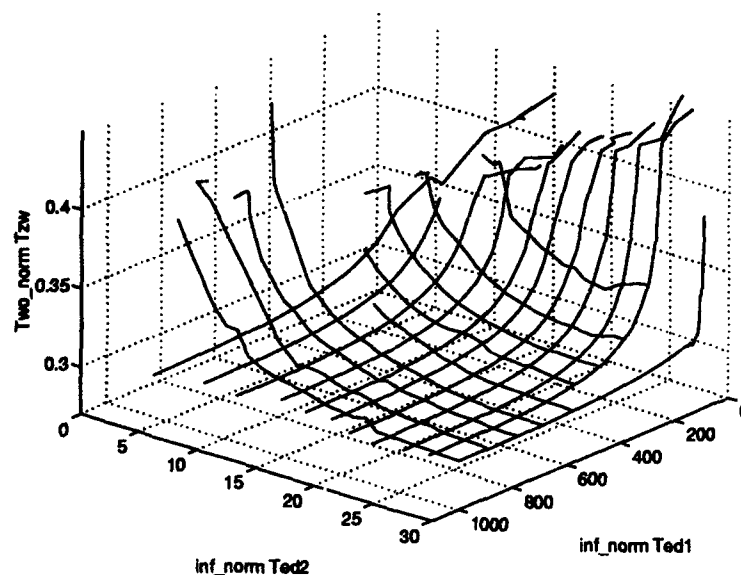


Figure 5-11 3D plot Grid Method $\|T_{zw}\|_2$ vs. $\|T_{ed,1}\|_{\infty}$ vs. $\|T_{ed,2}\|_{\infty}$

5.4.2 Direct method

The direct method, explained in Chapter 4, Section 4.2.2, minimizes both H_∞ constraints at the same time. By proper selection of the steps $\Delta\gamma_1$ and $\Delta\gamma_2$, where $\Delta\gamma_i = \gamma_{i,j} - \gamma_{i,j-1}$ (for $i=1, \dots, n_\infty$ and $j=1, \dots$, number of steps), the designer can guide the direction of minimization to the desired infinity norms $\|T_{ed,1}\|_\infty$ and $\|T_{ed,2}\|_\infty$. Figure 5-12 shows $\|T_{ed,2}\|_\infty$ vs. $\|T_{ed,1}\|_\infty$ for four different directions. The starting controller was K_{2opt} for three of them and a K_{mix} (taken from the grid method) for the last one.

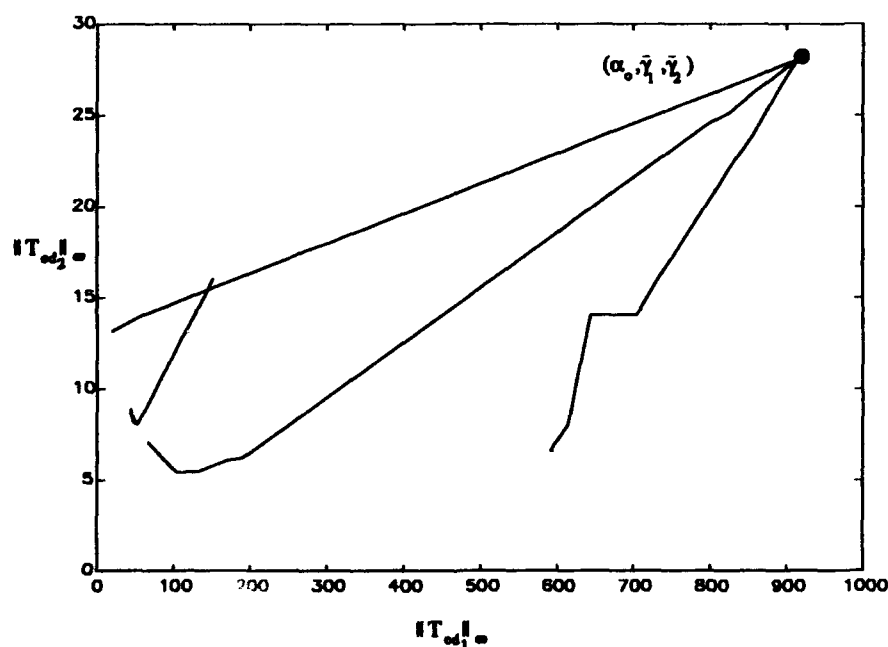


Figure 5-12 $\|T_{ed,2}\|_\infty$ vs. $\|T_{ed,1}\|_\infty$ Direct Method

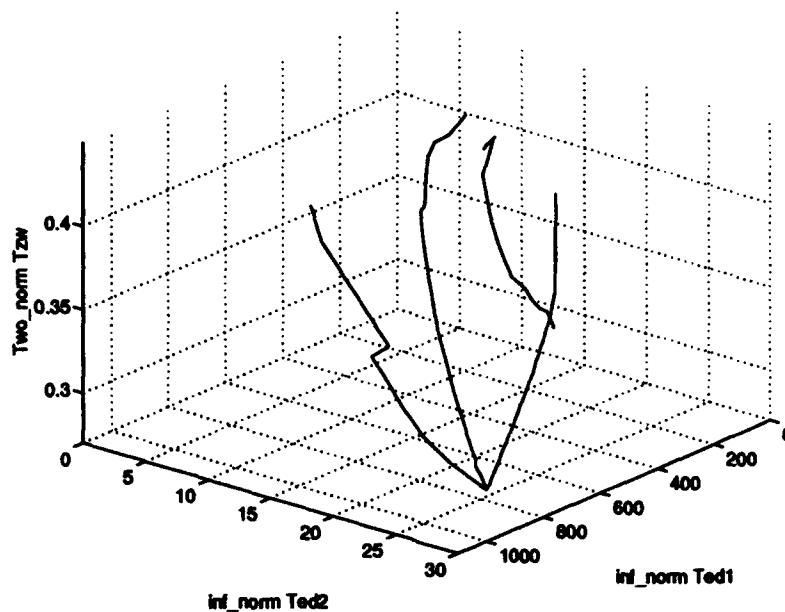


Figure 5-13 3D plot Direct Method

$$\|T_{zw}\|_2 \text{ vs. } \|T_{ed_1}\|_\infty \text{ vs. } \|T_{ed_2}\|_\infty$$

Notice that this numerical method permits the user to start at any point; this means the routine can start with any stabilizing controller. Figure 5-13 shows the different curves in 3D. Finally, Figure 5-14 and 5-15 show the final results of both the grid and the direct methods combined.

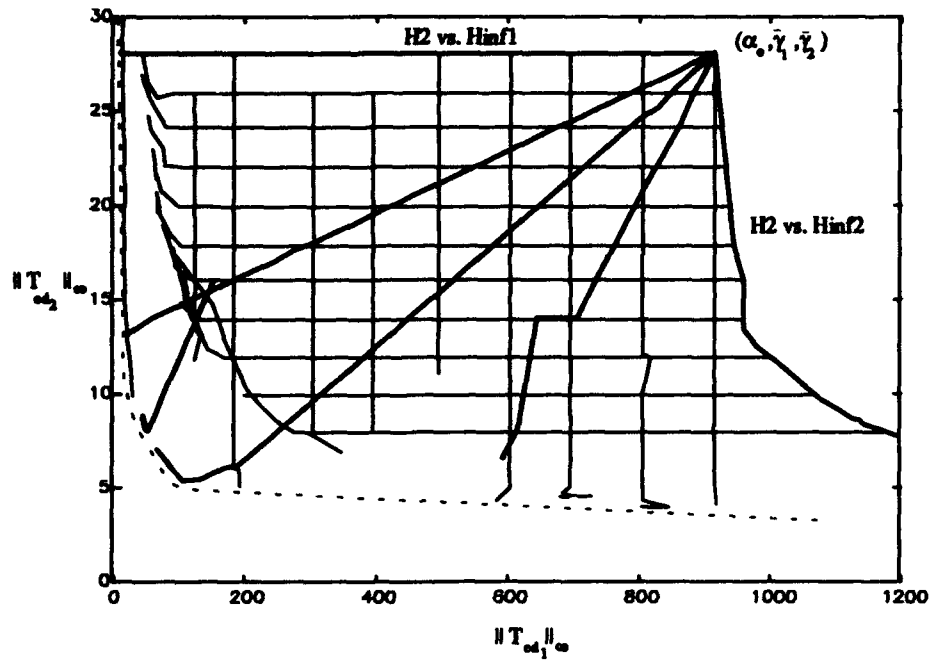


Figure 5-14 $\|T_{ed2}\|_{\infty}$ vs. $\|T_{ed1}\|_{\infty}$ for both methods

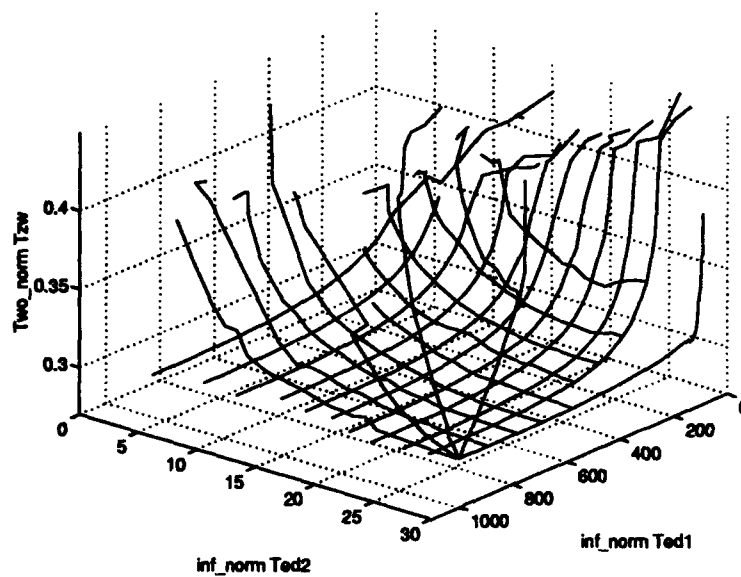


Figure 5-15 $\|T_{zw}\|_2$ vs. $\|T_{ed1}\|_{\infty}$ vs. $\|T_{ed2}\|_{\infty}$ for both methods

5.5 Conclusions for the Multiple H_∞ Constraints SISO case

This new optimization technique permits minimization of the two norm of one transfer function subject to multiple H_∞ constraints. It controls the trade off between the different H_∞ constraints and the H_2 performance.

Suppose a SISO plant has a multiplicative perturbation and a performance requirement on sensitivity; a controller $K(s)$ provides Robust Performance for that plant if and only if

$$\| |W_1 S| + |W_2 T| \|_\infty < 1 \text{ (SISO)}$$

In the mixed H_2/H_∞ optimization problem with multiple H_∞ constraints, the two H_∞ constraints are adjusted; therefore, it does not have frequency specific information. However, if we define the following requirements:

$$\|W_1 S\|_\infty = \beta_S < 1 \text{ and occurs at any } \omega = \omega_S \text{ (Nominal Performance)}$$

and

$$\|W_2 T\|_\infty = \beta_T < 1 \text{ and occurs at any } \omega = \omega_T \text{ (Robust Stability)}$$

where

$$\gamma_S \leq \beta_S \text{ and } \gamma_T \leq \beta_T$$

then two cases for Robust Performance could exist:

Case 1.- The Robust Performance test is passed iff

$$\beta_S + \beta_T < 1$$

This means that the worst case for a Robust Performance test is that $\|W_1 S\|_\infty$ and $\|W_2 T\|_\infty$ occur at the same frequency ($\omega_S = \omega_T$).

Case 2.- If

$$\beta_S + \beta_T > 1$$

the Robust Performance test must be applied. This means that it is necessary to check frequency information.

These two cases relax the requirement for the mixed sensitivity cost function ($\|T_{cd}\|_{\infty} < 1/\sqrt{2}$), where

$$\|T_{cd}\|_{\infty} = \left\| \begin{bmatrix} W_1 S \\ W_2 T \end{bmatrix} \right\|_{\infty}$$

because now the designer has control over the different infinity norms. A graphical interpretation is shown in Figure 5-16.

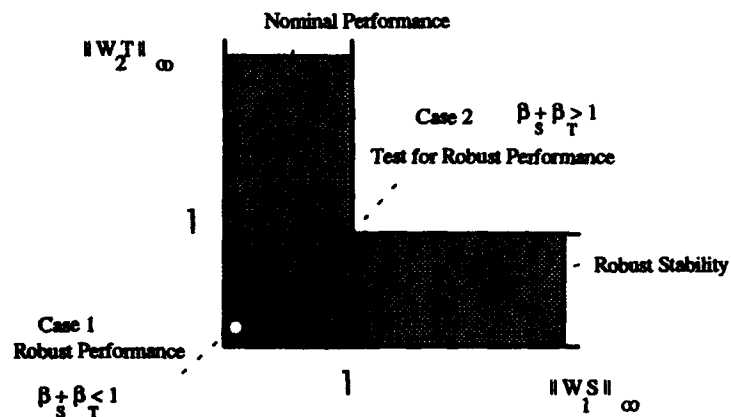


Figure 5-16 Application of the mixed problem with multiple H_{∞} constraints

VI. THE HIMAT PROBLEM: A MIMO EXAMPLE

For a MIMO example, the HIMAT problem from the μ -Tools Manual [Mat] was selected. The HIMAT vehicle is a scaled-down, remotely piloted vehicle (RPV). The design example will consider longitudinal dynamics only. For more information about this problem refer to the μ -Tools Manual [BDGPS91] and [SLH81]. The HIMAT problem will be designed for single and multiple H_∞ constraints.

6.1 Problem Set Up

The states variables of the plant (HIMAT) are:

v - forward speed

α - angle of attack (not to be confused with α from the H_2 design)

q - rate of pitch

θ - pitch angle

Control inputs (u):

δ_e - elevon command

δ_c - canard command

The variables to be measured:

α and θ

The state space matrices are:

$$A_s = \begin{bmatrix} -0.0226 & -36.6 & -18.90 & -32.1 \\ 0 & -1.90 & 0.983 & 0 \\ 0.0123 & -11.7 & -2.63 & 0 \\ 0 & 0 & 1.0 & 0 \end{bmatrix} \quad B_s = \begin{bmatrix} 0 & 0 \\ -0.414 & 0 \\ -77.80 & 22.40 \\ 0 & 0 \end{bmatrix}$$

$$C_s = \begin{bmatrix} 0 & 57.3000 & 0 & 0 \\ 0 & 0 & 0 & 57.3000 \end{bmatrix} \quad D_s = \begin{bmatrix} 0 & 0 \\ 0 & 0 \end{bmatrix}$$

Short period roots = $-2.2321 \pm 3.3779i$; Phugoid roots = $-0.0442 \pm 0.2093i$

6.2 H_2 Design requirement

The objective of the H_2 design is to develop a regulator that limits the white noise feedthrough to the angle of attack and pitch angle plant outputs (y_g) and the control usage (u). Figure 6-1 shows the H_2 regulator design plant with the weights W_c and W_z on the control usage and states, respectively. Energy from the white noise inputs, w_1 and w_2 , will be minimized with respect to the chosen outputs, z_1 and z_2 , by the compensator design.

6.2.1 Weight Selection

Wind disturbance weight: The wind disturbance constitutes an exogenous input (w_1).

It passes through Ψ as an angle of attack perturbation

$$\Psi = [-36.6 \quad -1.90 \quad -11.70 \quad 0]^T$$

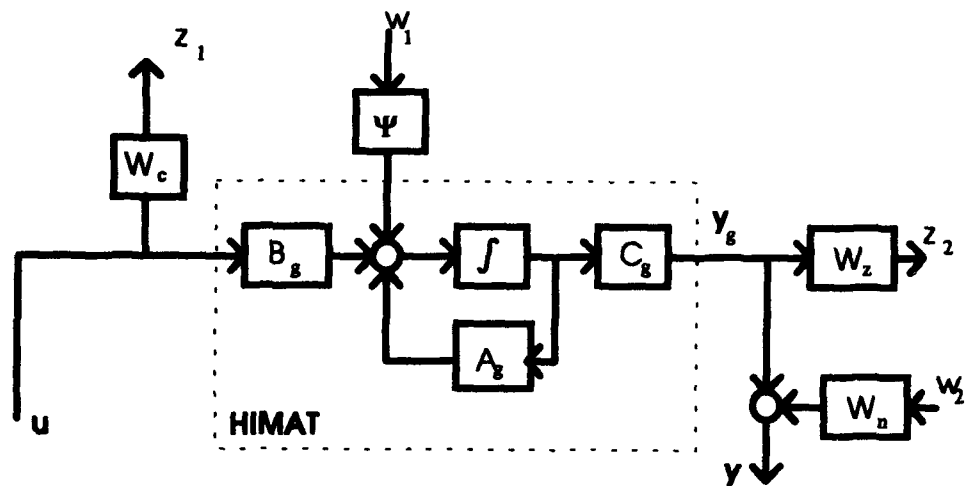


Figure 6-1 H_2 Regulator Diagram (HIMAT)

Measurement noise: The measurement noise is represented by an exogenous input (w_2). w_2 is added to the feedback signal. The weight for w_2 is:

$$W_n = 0.1 * I_{(2)}$$

Control Usage: The weight for control usage W_c is chosen as the identity matrix

$$W_c = I_{(2)}$$

Weighted output: This is the weighted angle of attack and pitch angle; here, this weight is chosen to be the identity matrix

$$W_z = I_{(2)}$$

The state space for the H_2 design plant is

$$P_2 = \left[\begin{array}{c|cc} A_2 & B_w & B_{u_2} \\ \hline C_z & D_{zw} & D_{zu} \\ C_{y_2} & D_{yw} & D_{yu} \end{array} \right] \quad (6-1)$$

and the state space matrices are

$$\begin{aligned}
 \begin{bmatrix} \dot{x}_g \\ x_g \end{bmatrix} &= \begin{bmatrix} A_g \end{bmatrix} \begin{bmatrix} x_g \end{bmatrix} + \begin{bmatrix} \Psi & 0 \end{bmatrix} \begin{bmatrix} w_1 \\ w_2 \end{bmatrix} + \begin{bmatrix} B_g \end{bmatrix} \begin{bmatrix} u \end{bmatrix} \\
 \begin{bmatrix} z_1 \\ z_2 \end{bmatrix} &= \begin{bmatrix} 0 \\ W_z C_g \end{bmatrix} \begin{bmatrix} x_g \end{bmatrix} + \begin{bmatrix} 0 & 0 \\ 0 & 0 \end{bmatrix} \begin{bmatrix} w_1 \\ w_2 \end{bmatrix} + \begin{bmatrix} W_c \\ 0 \end{bmatrix} \begin{bmatrix} u \end{bmatrix} \\
 \begin{bmatrix} y \end{bmatrix} &= \begin{bmatrix} C_g \end{bmatrix} \begin{bmatrix} x_g \end{bmatrix} + \begin{bmatrix} 0 & W_n \end{bmatrix} \begin{bmatrix} w_1 \\ w_2 \end{bmatrix} + \begin{bmatrix} 0 \end{bmatrix} \begin{bmatrix} u \end{bmatrix}
 \end{aligned} \tag{6-2}$$

Notice that the " 0 " represents a zero matrix with the corresponding dimensions in the different state space matrices. The basic conditions that are checked here include $D_{zw} = 0$, $D_{yu} = 0$, $D_{zu}^T D_{zu}$ and $D_{yw} D_{yw}^T$ full rank; these are met by the design with a non-zero W_n and W_c .

6.2.2 H_2 Results

Table 6-1 shows the results.

Table 6-1 H_2 Results (HIMAT)

$\ T_{zw} \ _2$ 4.6970

	VGM input (dB)	VPMi (deg)	VGM output (dB)	VPMo (deg)
T	[-0.1198, 0.1181]	±0.7847	[-11.7255, 4.8147]	± 43.4773
S	[-0.1181, 0.1198]	±0.7847	[-5.1530, 14.4199]	± 47.7754

Although the objective was only to design a pure regulator, from Table 6-1 we see that the H_2 controller provides robustness at the output of the plant, but poor margins at the input

of the plant. The VGM and VPM are based on the magnitude plots of sensitivity and complementary sensitivity. Figure 6-2 shows the maximum singular values of the complementary sensitivity at the input (T_i) and output (T_o) of the plant. This represents the measurement noise feedthrough to the plant input/output and the inverse of the allowable multiplicative uncertainty at the input/output of the plant.

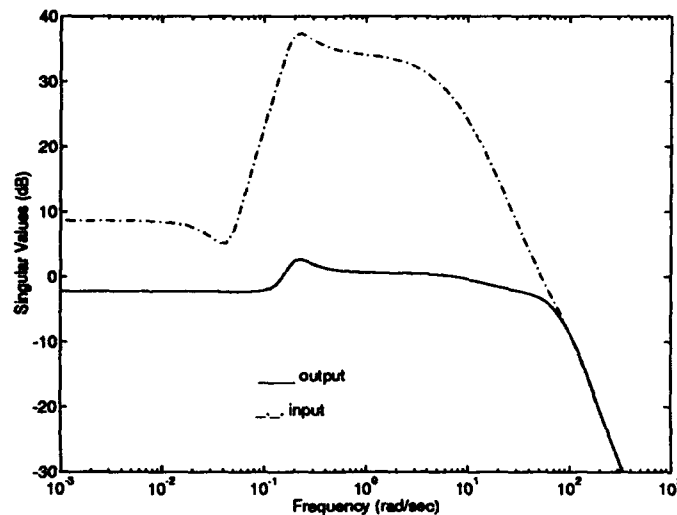


Figure 6-2 Maximum Singular Values of Complementary Sensitivity

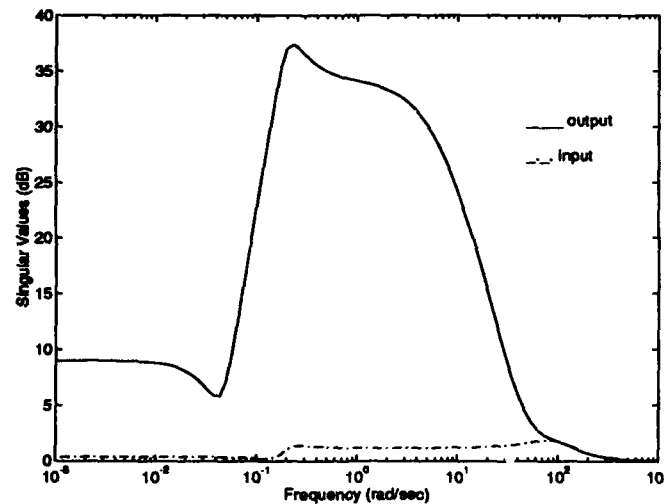


Figure 6-3 Maximum Singular Values of Sensitivity

Therefore, K_{2opt} provides a good level of robustness at the output of the plant, but the system is susceptible to a multiplicative uncertainty at the input of the plant. Figure 6-3 shows the singular values of input sensitivity (S_i) and output sensitivity (S_o). Notice from Figure 6-3 that the input sensitivity is minimized for good wind disturbance rejection, as seen in the low gain in S_i . The problem with this design is poor performance at the output of the plant, as seen by S_o . K_{2opt} therefore produces a system that is weak to a multiplicative perturbation at the input of the plant and has bad tracking properties, as shown in Figure 6-4.

The H_∞ designs to be addressed are: recover the margins at the input of the plant through a weighted input complementary sensitivity, and recover tracking performance through weighted output sensitivity. These must be done while keeping the robustness at the output of the plant.

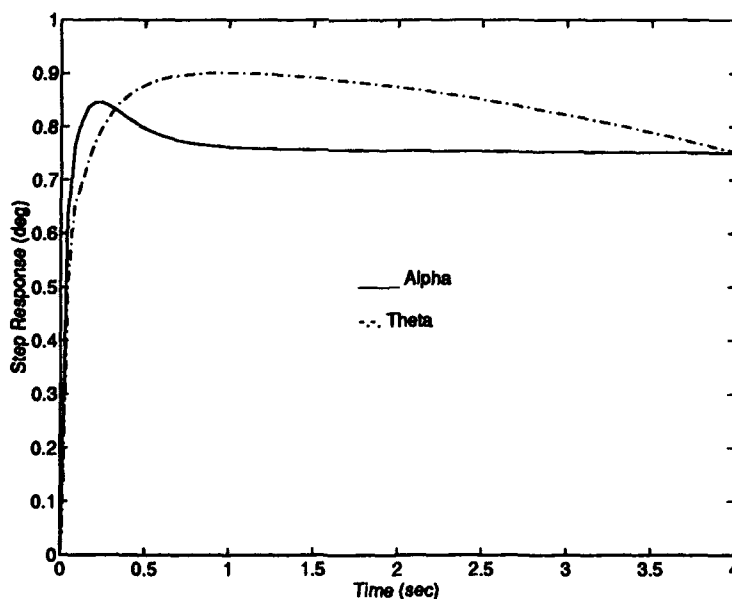


Figure 6-4 Time Responses due to a step α_c and θ_c

6.3 Mixed H_2/H_{∞} problem: H_{∞} Design to a multiplicative uncertainty at the input of the plant

Now a multiplicative uncertainty block at the input of the plant is assumed. The multiplicative uncertainty represents:

1. Uncertainty in the canard and the elevon actuators
2. Uncertainty in the force and moments generated on the aircraft, due to specific deflection of the canard and elevon
3. Uncertainty in the linear and angular accelerations produced by the aerodynamically generated forces and moments
4. Others forms of uncertainty that are less well understood. [BDGPS91]

Figure 6-5 shows the block diagram. The dotted block represents the true plant. The transfer function $\Delta(s)$ is assumed to be stable, unknown, and with an infinity norm less than one ($\|\Delta(s)\|_{\infty} < 1$). The objective for this design is to meet Robust Stability at the input of the plant.

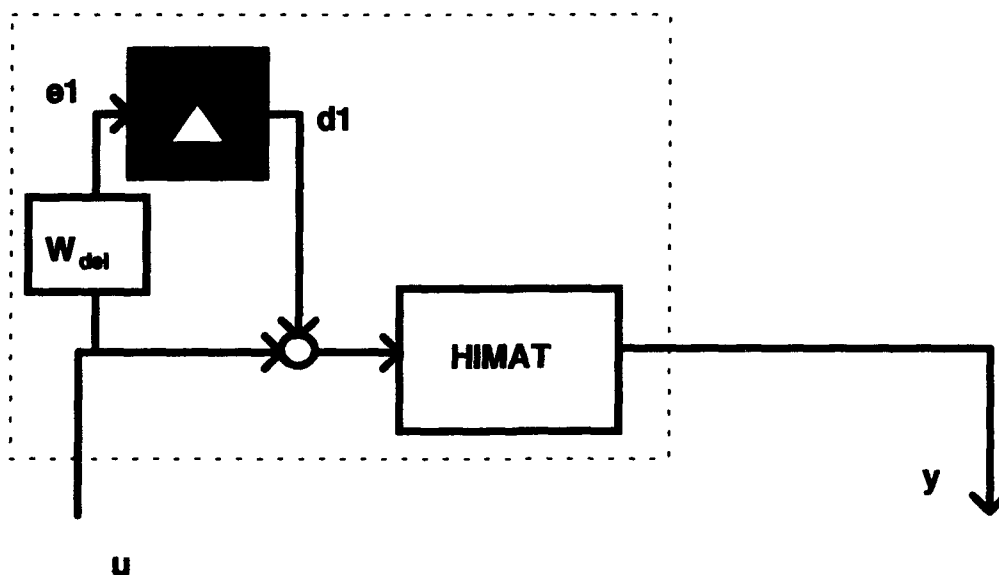


Figure 6-5 Block Diagram of multiplicative uncertainty at the plant input

Robust Stability at the input of the plant is met if

$$\|\Delta(s)T_{ed_1}(s)\|_{\infty} < 1$$

by the small gain theorem. Thus, if we satisfy

$$\|T_{ed_1}\|_{\infty} < 1/\|\Delta(s)\|_{\infty}$$

we have Robust Stability at the input of the plant, or since $\|\Delta(s)\|_{\infty} < 1$,

$$\|T_{ed_1}\|_{\infty} < 1 \quad (6-3)$$

where T_{ed_1} is the weighted closed-loop transfer function from d_1 to e_1 . Now we have

$$T_{ed_1} = W_{del}(s)T_i(s) \quad (6-4)$$

$W_{del}(s)$, called the uncertainty weight, represents a stable transfer function of the form

$$W_{del}(s) = w_{del}(s) * I_{(2)}$$

$$w_{del}(s) = \frac{50 * (s + 100)}{(s + 10000)} \quad (6-5)$$

The weighting function is used to normalize the size of the unknown perturbation Δ . At any frequency ω , the value of $|w_{del}(j\omega)|$ can be interpreted as the percentage of uncertainty in the model at that frequency. The particular uncertainty weight chosen for this problem indicates that at low frequencies, there is potentially a 50% modeling error, and at a frequency of 173 rad/sec, the uncertainty in the model is up to 100% [BDGPS91]. Figure 6-6 shows the Bode magnitude plot of $w_{del}(s)$. The H_{∞} design plant is

$$P_{\infty_1} = \left[\begin{array}{c|cc} A_{\infty_1} & B_{d_1} & B_{u_{\infty_1}} \\ \hline C_{e_1} & D_{e_1 d_1} & D_{e_1 u} \\ \hline C_{y_{\infty_1}} & D_{y d_1} & D_{y u} \end{array} \right] \quad (6-6)$$

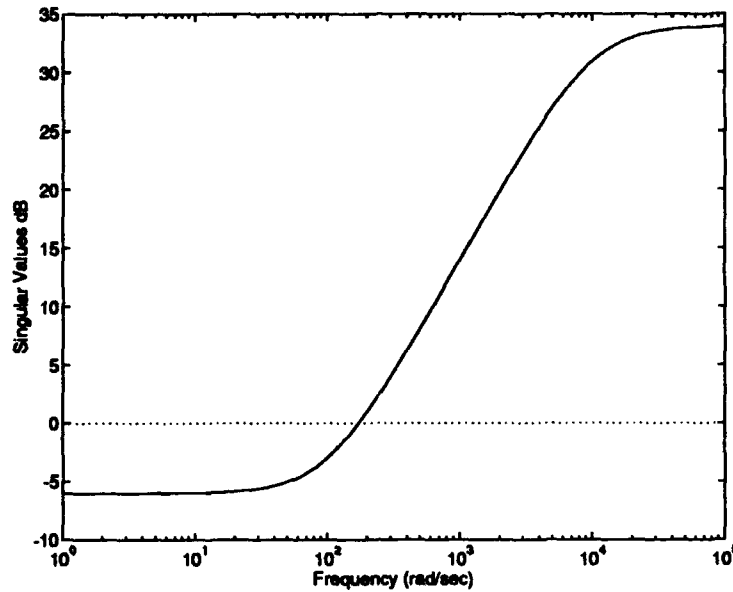


Figure 6-6 Magnitude of Multiplicative Uncertainty Weighting Function (dB)

and the state space matrices are

$$\begin{bmatrix} \dot{x}_g \\ \dot{x}_{del} \end{bmatrix} = \begin{bmatrix} A_g & 0 \\ 0 & A_{del} \end{bmatrix} \begin{bmatrix} x_g \\ x_{del} \end{bmatrix} + \begin{bmatrix} B_g \\ 0 \end{bmatrix} d_1 + \begin{bmatrix} B_g \\ B_{del} \end{bmatrix} u$$

$$[e_1] = \begin{bmatrix} 0 & C_{del} \end{bmatrix} \begin{bmatrix} x_g \\ x_{del} \end{bmatrix} + \begin{bmatrix} 0 \end{bmatrix} d_1 + \begin{bmatrix} D_{del} \end{bmatrix} u \quad (6-7)$$

$$[y] = \begin{bmatrix} C_g & 0 \end{bmatrix} \begin{bmatrix} x_g \\ x_{del} \end{bmatrix} + \begin{bmatrix} 0 \end{bmatrix} d_1 + \begin{bmatrix} 0 \end{bmatrix} u$$

Since $D_{yd_1} D_{yd_1}^T$ is not full rank, this is a singular H_∞ design. The setup for the mixed H_2/H_∞ problem is: Find a stabilizing compensator that achieves

$$\inf_{K \text{ stabilizing}} \|T_{zw}\|_2 \quad \text{subject to} \quad \|T_{ed_1}\|_\infty \leq \gamma_1 \quad (6-8)$$

The performance index in the numerical method is

$$J_{\gamma_1} = \|T_{zw}\|_2^2 + \lambda_1 (\|T_{del}\|_\infty - \gamma_1)^2 \quad (6-9)$$

Two controller orders are presented. The first one is a fourth order controller; it represents the order of the H_2 design. The second one is a sixth order controller and represents the order of the full information H_2/H_∞ plant. Therefore, the 6th order K_{2opt} was found by wrapping the weights of the H_2 design and the weights of the H_∞ design into one system. The starting controller is K_{2opt} (4th or 6th order). Table 6-2 shows the results.

Table 6-2 Input Complementary Sensitivity Design $\|T_{zw}\|_2$ and $\|W_{del}T_i\|_\infty$

4th order Controller		6th order Controller	
$\ T_{zw}\ _2$	$\ W_{del}T_i\ _\infty$	$\ T_{zw}\ _2$	$\ W_{del}T_i\ _\infty$
4.6970	37.0491	4.6970	37.0491
4.6970	34.1981	4.6970	34.1981
6.3685	2.1831	6.5190	2.0029
6.4369	1.8485	6.3395	1.4366
6.5611	1.4709	6.3674	1.2844
6.7332	1.0585	6.6457	0.8946
6.9970	0.6413	6.8571	0.7113
* 7.0968	0.5497	* 7.0705	0.5151
** 7.7440	0.5099	** 7.6167	0.5095

Notice from Table 6-2 that Robust Stability is met for both controllers, but there is a degradation in the H_2 performance. Figure 6-7 shows the α vs. γ_1 curve for the 4th order controller, which is virtually identical to that of the 6th order controller. The vector gain and phase margins at the input and output of the plant are shown in Table 6-3 for the last two controllers in both cases. As expected, the system is very robust at the input of the plant; also notice that good margins at the output were preserved.

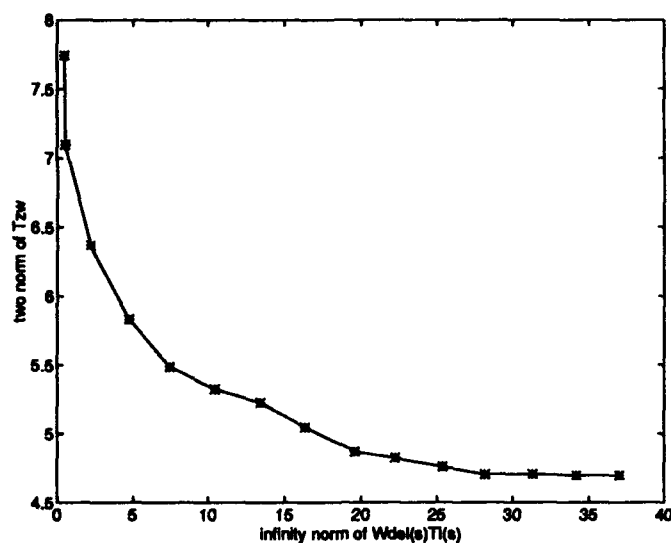


Figure 6-7 $\|T_{zw}\|_2$ vs. $\|W_{del} T_1\|_\infty$ (4th order controller)

Table 6-3 Input Complementary Sensitivity Design VGM_{l_o} and VPM_{l_o}

K_{mixed} controller (4th order)

	VGM_l (dB)	VPM_l (deg)	VGM_o (dB)	VPM_o (deg)
* S	[-5.3269, 16.2768]	± 50.0787	[-4.5991, 10.4018]	± 40.8564
* T	[-20.3299, 5.5921]	± 53.7266	[-11.5388, 4.7866]	± 43.1300
**S	[-5.4318, 17.6493]	± 51.5019	[-4.0590, 7.8659]	± 34.6569
**T	[-40.8853, 6.0000]	± 60.0000	[-8.7230, 4.2634]	± 36.9444

K_{mixed} controller (6th order)

	VGM_l (dB)	VPM_l (deg)	VGM_o (dB)	VPM_o (deg)
* S	[-5.3644, 16.7411]	± 50.5846	[-4.6992, 10.9871]	± 42.0618
* T	[-30.0620, 5.8832]	± 57.9334	[-13.2685, 5.0228]	± 46.0922
**S	[-5.3386, 16.4192]	± 50.2367	[-4.1372, 8.1814]	± 35.5235
**T	[-34.6236, 5.9396]	± 58.7752	[-8.3343, 4.1738]	± 35.9332

6.4 Mixed H_2/H_∞ problem: H_∞ Design for Nominal Performance

The H_2 design showed that the system does not perform tracking at all. Therefore, good performance will be characterized in terms of the H_∞ norm of the output sensitivity. The output sensitivity will be a weighted sensitivity function as shown in Figure 6-8. The exogenous input and output of the plant are denoted as d_2 and e_2 , respectively. The weighted sensitivity is our Nominal Performance requirement. The weight for sensitivity represents an output perturbation. The transfer function e_2/d_2 is

$$e_2/d_2 = W_p S_o ; W_p(s) = w_p(s) * I_{(2)}$$

$$w_p(s) = \frac{.5 * (s + 3)}{(s + 0.03)} \quad (6-10)$$

As in the uncertainty modeling, the weighting function W_p is used to normalize specifications; in this case, to define performance by whether a particular norm is less than 1. Nominal Performance is assured when

$$\|T_{ed_2}\|_\infty < 1$$

or

$$\|W_p S_o\|_\infty < 1 \quad (6-11)$$

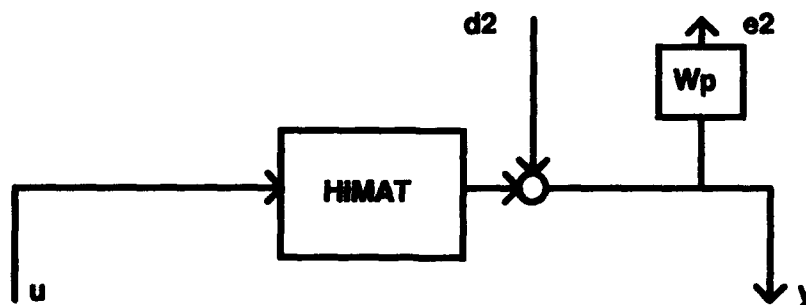


Figure 6-8 H_∞ design for Nominal Performance

and since w_p is a SISO transfer function, the maximum singular value plot of the output

sensitivity transfer function must lie below the plot of $\left| \frac{1}{w_p} \right|$ at every frequency. That is, if

$\|w_p(I + GK)^{-1}\|_{\infty} < 1$, then at all frequencies, $\|(I + GK)^{-1}(j\omega)\|_{\infty} < |1/w_p(j\omega)|$. The

inverse of the weight w_p is shown in Figure 6-9. This sensitivity weight indicates that, at low frequencies, the closed-loop system should reject output disturbances by a factor of 50-1 [BDGPS91]. The closed-loop system should perform better than the open-loop for frequencies up to 1.73 (rad/sec), and for higher frequencies, the closed-loop performance should degrade gracefully, always lying underneath the inverse of the weight w_p as shown in Figure 6-9 [BDGPS91].

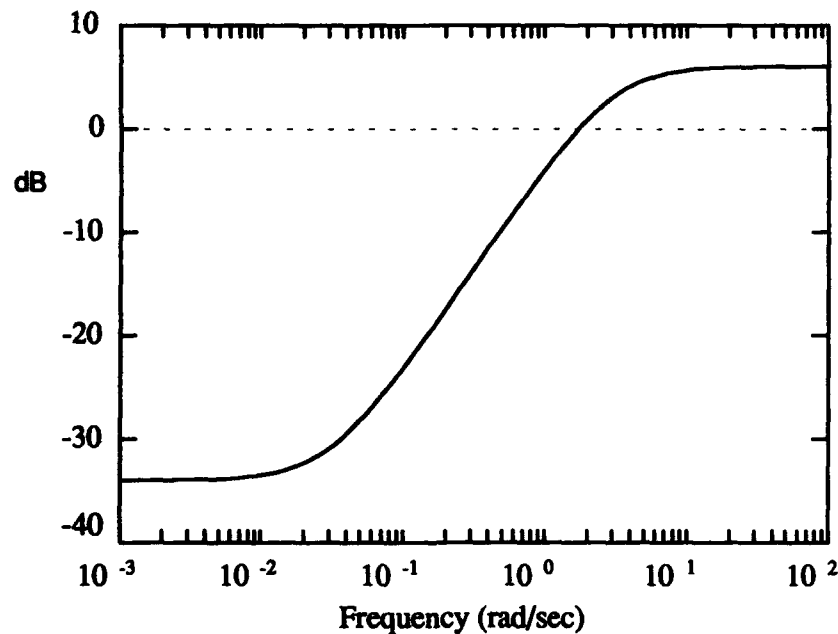


Figure 6-9 Inverse of Performance Weighting Function, w_p

The H_∞ design plant is $P_{\infty 2}$, given by

$$P_{\infty 2} = \left[\begin{array}{c|cc} A_{\infty 2} & B_{d_2} & B_{u_{\infty 2}} \\ \hline C_{e_2} & D_{e_2 d_2} & D_{e_2 u} \\ \hline C_{y_{\infty 2}} & D_{y d_2} & D_{y u} \end{array} \right] \quad (6-12)$$

and the state space matrices are

$$\begin{aligned} \begin{bmatrix} \dot{x}_g \\ \dot{x}_p \end{bmatrix} &= \begin{bmatrix} A_g & 0 \\ B_p C_g & A_p \end{bmatrix} \begin{bmatrix} x_g \\ x_p \end{bmatrix} + \begin{bmatrix} 0 \\ B_p \end{bmatrix} d_2 + \begin{bmatrix} B_g \\ 0 \end{bmatrix} u \\ [e_2] &= [D_p C_g \quad C_p] \begin{bmatrix} x_g \\ x_p \end{bmatrix} + [D_p] d_2 + [0] u \\ [y] &= [C_g \quad 0] \begin{bmatrix} x_g \\ x_p \end{bmatrix} + [I] d_2 + [0] u \end{aligned} \quad (6-13)$$

Since $D_{e,u}^T D_{e,u}$ is not full rank, this is a singular H_∞ design. The mixed H_2/H_∞ problem is now the solution to a regular H_2 problem subject to a singular H_∞ design. The setup for the mixed $H_2/H_{\infty 2}$ problem is: Find a stabilizing compensator that achieves

$$\inf_{K \text{ stabilizing}} \|T_{zw}\|_2 \quad \text{subject to} \quad \|T_{ed_2}\|_\infty \leq \gamma_2 \quad (6-14)$$

The performance index in the numerical method is

$$J_{\gamma_2} = \|T_{zw}\|_2^2 + \lambda_1 \left(\|T_{ed_2}\|_\infty - \gamma_2 \right)^2 \quad (6-15)$$

Two controller orders are presented, 4th and 6th order. The starting controller is K_{2opt} (4th or 6th order). These are the same as generated in the previous section. Table 6-4 shows the results.

Table 6-4 Output Sensitivity Design $\|T_{zw}\|_2$ and $\|W_p S_o\|_\infty$

4th order Controller		6th order Controller	
$\ T_{zw}\ _2$	$\ W_p S_o\ _\infty$	$\ T_{zw}\ _2$	$\ W_p S_o\ _\infty$
4.697	52.1574	4.697	52.1574
4.6994	44.1814	4.6999	40.2441
4.7007	36.186	4.701	36.1963
4.7027	28.2262	4.7012	28.1995
4.7062	20.2295	4.7063	20.2322
4.7129	12.2376	4.7134	12.1711
4.7498	4.2903	5.1424	5.3273
5.1901	1.0049	5.1647	1.4016
5.2453	0.9647	5.2568	1.2114
* 5.2584	0.9467	* 5.3035	1.1291
		* * 5.6429	0.8311

Notice from Table 6-4 that Nominal Performance is met for both controller orders. The degradation in the H_2 performance is not too large. Figure 6-10 shows the α vs. γ_2 curve. The vector gain and phase margins at the input and output of the plant are shown in Table 6-5 for the last controllers in both cases. As expected, the system is not robust at the input of the plant. Also, notice that the margins at the output were reduced. This represents the trade off between performance and robustness.

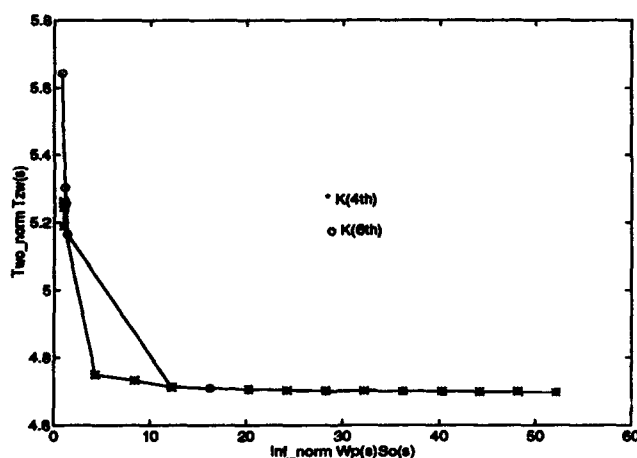


Figure 6-10 $\|T_{zw}\|_2$ vs. $\|W_p S_o\|_\infty$

Table 6-5 Output Sensitivity Design VGM_{l_o} and VPM_{l_o}

K_{mix} controller (4th order)

	VGM_l (dB)	VPM_l (deg)	VGM_o (dB)	VPM_o (deg)
* S	[-0.9002, 1.0044]	± 6.2597	[-3.6380, 6.3789]	± 30.1522
* T	[-1.0015, 0.8979]	± 6.2430	[-5.5480, 3.3584]	± 27.3035

K_{mix} controller (6th order)

	VGM_l (dB)	VPM_l (deg)	VGM_o (dB)	VPM_o (deg)
* S	[-0.9438, 1.0590]	± 6.5802	[-3.7318, 6.6827]	± 31.1321
* T	[-1.0560, 0.9415]	± 6.5629	[-5.7776, 3.4393]	± 28.1164
**S	[0.9341, 1.0468]	± 6.5089	[-4.1272, 8.1405]	± 35.4130
**T	[-1.0437, 0.9316]	± 6.4904	[-7.4109, 3.9398]	± 33.3542

Figures 6-11 and 6-12 show the time responses due to a step angle of attack command and a step pitch angle command (noise included in simulation) respectively, for the H_2 design and the mixed $H_2/H_{\infty 2}$ designs. Notice that the H_2 design does not provide performance at all, which is more evident in the pitch angle. The mixed controller shows an improvement in the tracking performance, and the degradation in the noise rejection is not considerable. The 6th order controller did not significantly improve the infinity norm of the robustness and performance objectives nor the two norm of T_{zw} ; therefore, a fourth order controller seems to be the best solution of the two for this mixed $H_2/H_{\infty 2}$ design problem.

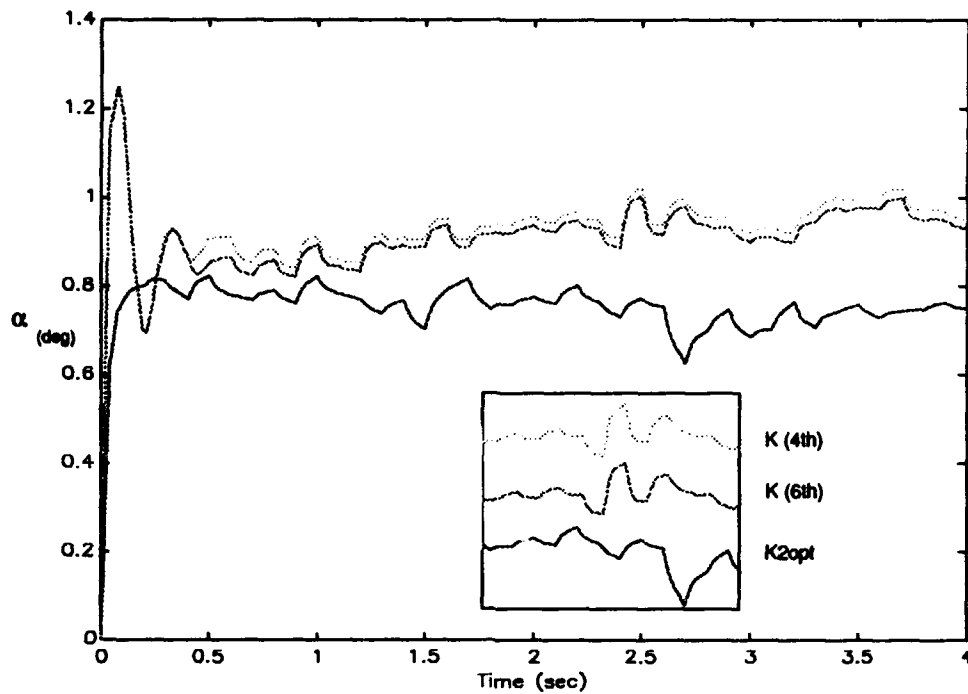


**Figure 6-11 Time Response due to a step angle of attack command
(* controller from Table 6-4)**

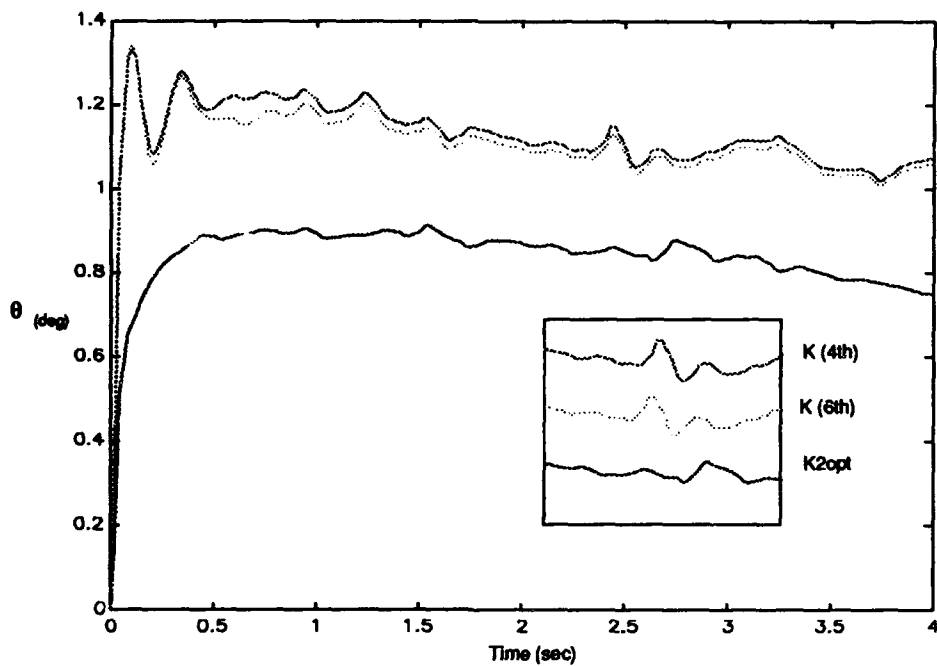


**Figure 6-12 Time Response due to a step pitch angle command
(* controller from Table 6-4)**

6.5 Trade off between Weighted Output Sensitivity and Weighted Input Complementary Sensitivity

This section will examine the trade off between weighted output sensitivity (T_{ed2}) and weighted input complementary sensitivity (T_{ed1}). Since the H_2 design was shown to have good margins at the output of the plant, let's examine the weighted output complementary sensitivity. In other words, the objective is to observe how the robustness at the output of the plant is affected by T_{ed1} and T_{ed2} . The weight for the output complementary sensitivity is chosen to be the same as the weight for input complementary sensitivity, but in this case it is assumed to be a fictitious uncertainty block at the output of the plant $[G(I + W_{del}\Delta_{fictitious})]$. This means that the true plant is represented by an input multiplicative perturbation $[(I + W_{del}\Delta)G]$ and the performance objective is weighted output sensitivity. The block diagram for output complementary sensitivity is shown in Figure 6-13.

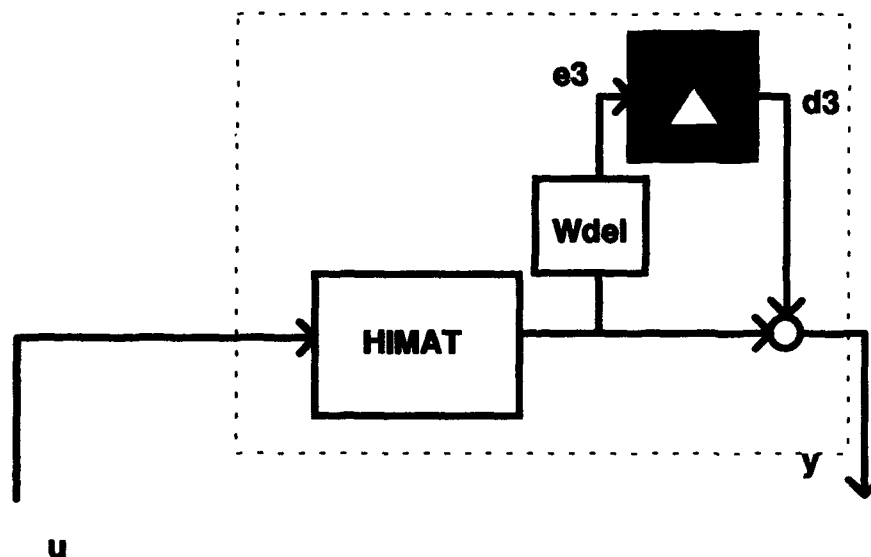


**Figure 6-13 Weighted Output Complementary Sensitivity
Block Diagram**

Thus,

$$T_{ed,1} = W_{del}(s) T_o(s) \quad (6-16)$$

Figure 6-14 shows how the minimization of weighted input complementary sensitivity (Mixed $H_2/H_{\infty,1}$) affects the infinity norm of weighted output sensitivity (Mixed $H_2/H_{\infty,2}$) and how the minimization of weighted output sensitivity affects the infinity norm of weighted input complementary sensitivity. The curve $H_2/H_{\infty,2}$ shows that the minimization of weighted output sensitivity drives the infinity norm of weighted input complementary sensitivity to smaller values. The curve $H_2/H_{\infty,1}$ shows that the minimization of the weighted input complementary sensitivity starts to minimize the infinity norm of weighted output sensitivity also, but when $\|W_{del} T_i\|_{\infty}$ reaches small values, it causes an increase in $\|W_p S_o\|_{\infty}$. Figure 6-15 shows how the minimization of weighted input complementary sensitivity does not affect the weighted output complementary sensitivity. This means that this design does not affect the robustness at the output. The values of the infinity norms for the different transfer functions are in Appendix A, Sections A.1 and A.2.

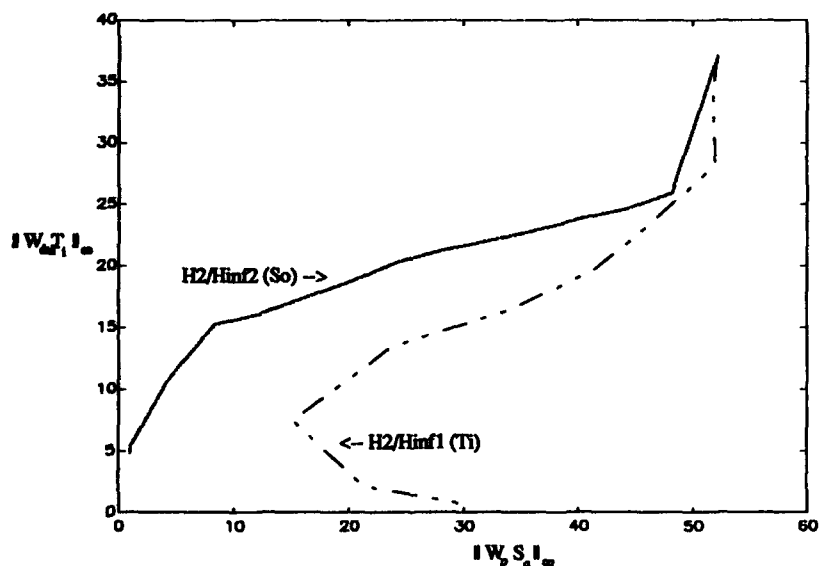


Figure 6-14 $\|W_{del} T_i\|_{\infty}$ vs. $\|W_p S_o\|_{\infty}$ for $H_2/H_{\infty,1}$ design and $H_2/H_{\infty,2}$ design (K 4th)

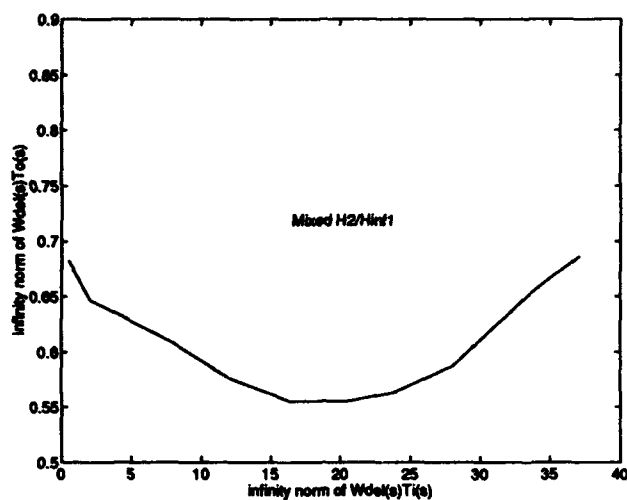


Figure 6-15 $\|W_{del} T_o\|_{\infty}$ vs. $\|W_{del} T_i\|_{\infty}$ for $H_2/H_{\infty 1}$ design (K 4th)

Figure 6-16 shows how the minimization of weighted output sensitivity affects the weighted output complementary sensitivity. Notice how the robustness at the output of the plant starts to decrease as the system gets more performance. The conclusion is that when the weighted output sensitivity is reduced, it drives the weighted complementary sensitivity to higher values.

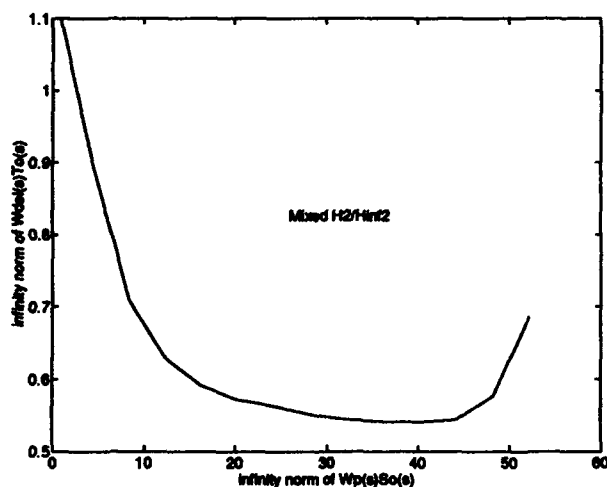


Figure 6-16 $\|W_{del} T_i\|_{\infty}$ vs. $\|W_p S_o\|_{\infty}$ for $H_2/H_{\infty 2}$ design (K 4th)

6.6 Multiple H_∞ Constraints : H_∞ Design for Nominal Performance and Robust Stability (Weighted Input Complementary Sensitivity and Weighted Output Sensitivity).

The setup for this mixed H_2/H_∞ problem is: Find an stabilizing compensator that achieves

$$\inf_{K \text{ stabilizing}} \|T_{zw}\|_2 \text{ subject to } \begin{cases} \|W_{del} T_i\|_\infty \leq \gamma_1 \\ \|W_p S_o\|_\infty \leq \gamma_2 \end{cases} \quad (6-17)$$

where both constraints will be treated as equality constraints. The performance index for the numerical method is

$$J_\gamma = \|T_{zw}\|_2^2 + \lambda_1 (\|W_{del} T_i\|_\infty - \gamma_1)^2 + \lambda_2 (\|W_p S_o\|_\infty - \gamma_2)^2 \quad (6-18)$$

The state space matrices are equation (6-2) for the H_2 part, equation (6-7) for the weighted input complementary sensitivity, and equation (6-13) for the weighted output sensitivity. This design will map the boundary between $\|W_{del} T_i\|_\infty$ and $\|W_p S_o\|_\infty$ when both infinity norms are close to the optimal values, respectively. This will be done by minimizing both constraints using the direct method in different directions as shown in Figure 6-17. Two cases are defined. Case 1 tries to reduce as much as possible the infinity norm of the weighted output sensitivity while holding the infinity norm of the weighted input complementary sensitivity less than one. In other words, the first case tries to get the best level of performance that meets the robustness requirement. Case 2 tries to reduce both infinity norms as much as possible, which means that it is desired to get the best performance and the best robustness. The infinity norm of the weighted output complementary sensitivity will also be calculated in order to observe the trade off between this design and the robustness at the output of the plant.

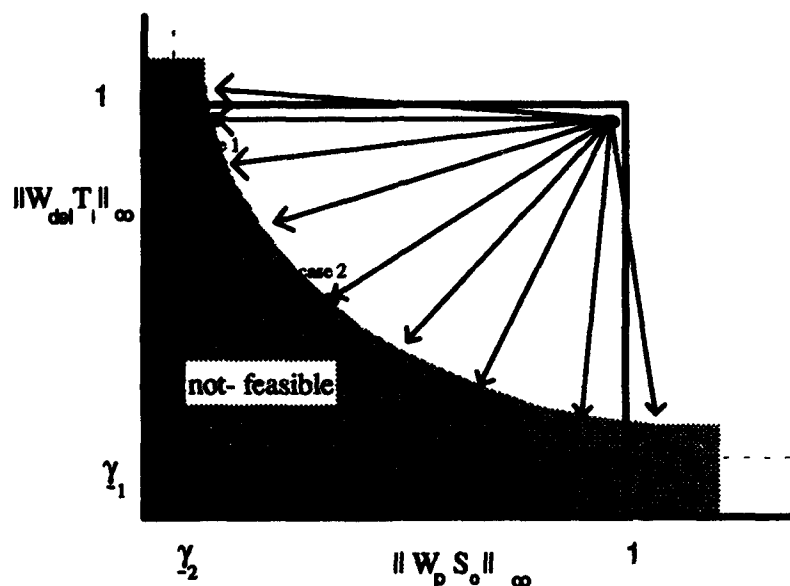


Figure 6-17 Objectives of the mixed problem with two H_∞ constraints

Again the starting controller is the optimal H_2 controller, which is the order of the H_2 part only (fourth order); then the controller order is increased to 6th (explained before) and 8th order (computed by wrapping P_2 , P_{-1} , and P_{-2} into one system, P). Therefore, fourth, sixth, and eight order mixed controllers will be generated. The method used in the numerical technique is the direct method. Table 6-6 shows part of the results (see Appendix A, Section A.3 for more).

Table 6-6 Mixed H_2/H_∞ with two H_∞ Constraints: $\|T_{zw}\|_2$, $\|W_{del}T_i\|_\infty$, and $\|W_pS_o\|_\infty$

	$\ T_{zw}\ _2$	$\ W_{del}T_i\ _\infty$	$\ W_pS_o\ _\infty$	$\ W_{del}T_o\ _\infty$
K_{2opt}	4.6970	37.0491	52.1574	0.6853

Fourth order controller

Case 1	5.6883	0.9938	0.9234	1.0159
Case 2	6.1322	0.8172	0.9110	0.9971

Sixth order controller

Case 1	5.7311	0.9978	0.9574	0.9826
Case 2	6.0274	0.8519	0.9579	0.9828

Eight order controller

Case 1	5.9228	0.9220	0.6845	0.7560
**	5.8145	0.7438	0.7644	0.7030
Case 2	5.6926	0.6109	0.7270	0.6707

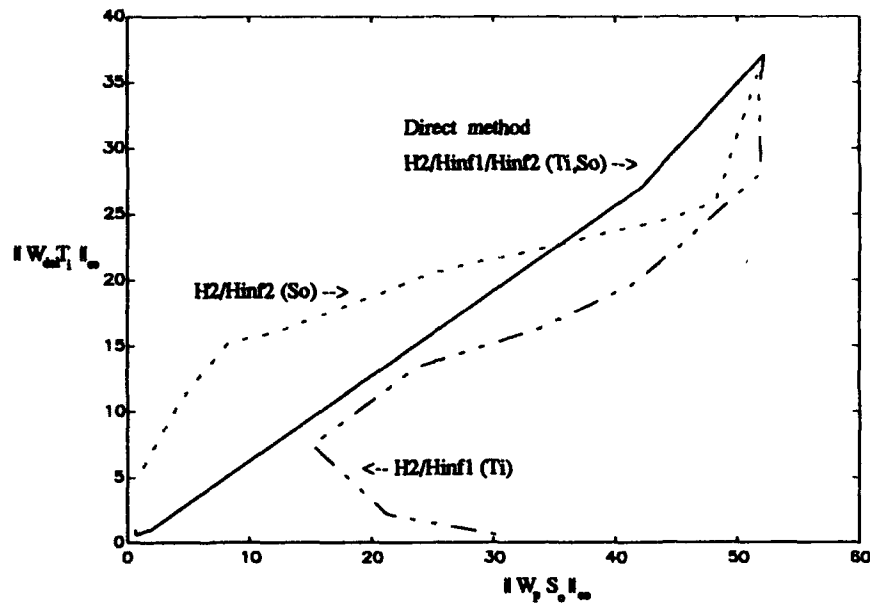


Figure 6-18 Direct Method versus Single H_∞ constraint designs (HIMAT)

Notice that the 6th order controller achieves similar results to the 4th order, and the robustness at the output of the plant is maintained for both. The big difference is the 8th order controller, which achieves smaller infinity norms than the 4th and 6th order controller, and also keeps the level of robustness at the output (the ** 8th order controller will be explained in Section 6.7). Figure 6-18 shows how the direct method with multiple constraints goes directly to the minimum values of the H_∞ constraints. This figure is similar for the 4th, 6th and 8th order controllers using the direct method. Notice that from a control point of view, we are not interested in values of the H_∞ constraints above one, since they do not meet our requirements. The following figures will show the area of interest (below one) for the H_∞ constraints. Figure 6-19 shows the trade off between $W_{del} T_i$ and $W_p S_o$ using a 4th order controller. The constraint boundary between weighted input complementary sensitivity and weighted output sensitivity is defined. This boundary shows that Case 2 is better than Case 1, since it obtains better values of performance and robustness. The 6th order controller shows similar results to the 4th order controller. Figure 6-20 shows the trade off between $W_{del} T_i$ and $W_p S_o$ using an 8th order controller.

Notice that this order of controller improves the values of the infinity norms, and the non-feasible region is also "smaller". Appendix A, Section A.3 shows the complete table of results.

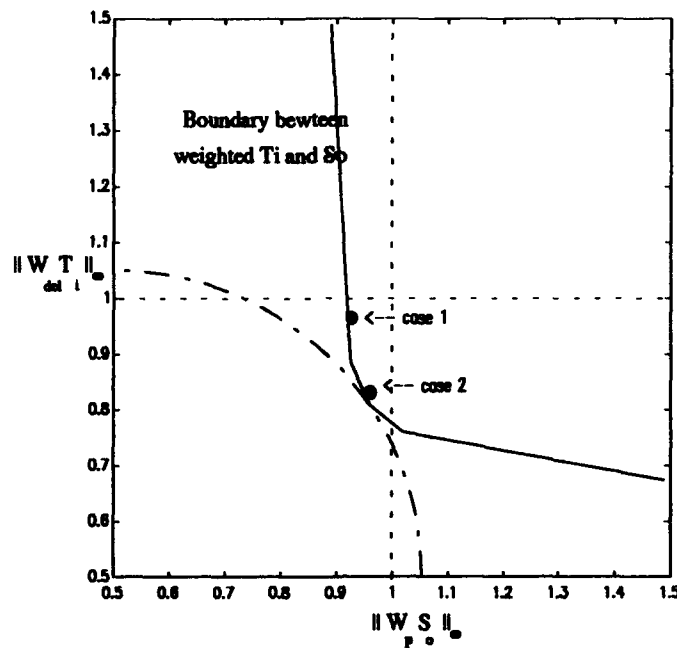


Figure 6-19 Trade off between weighted T_1 and S_0 (4th order controller)

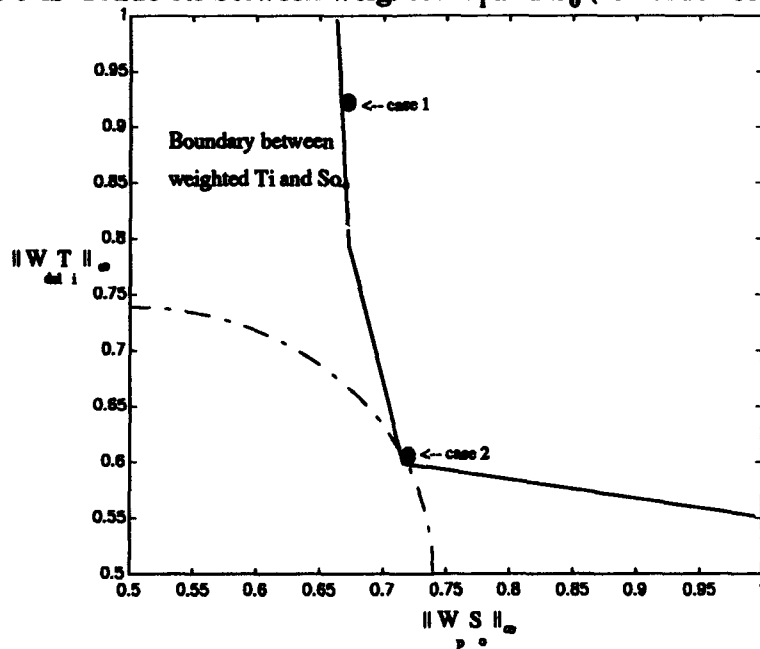


Figure 6-20 Trade off between weighted T_1 and S_0 (8th order controller)

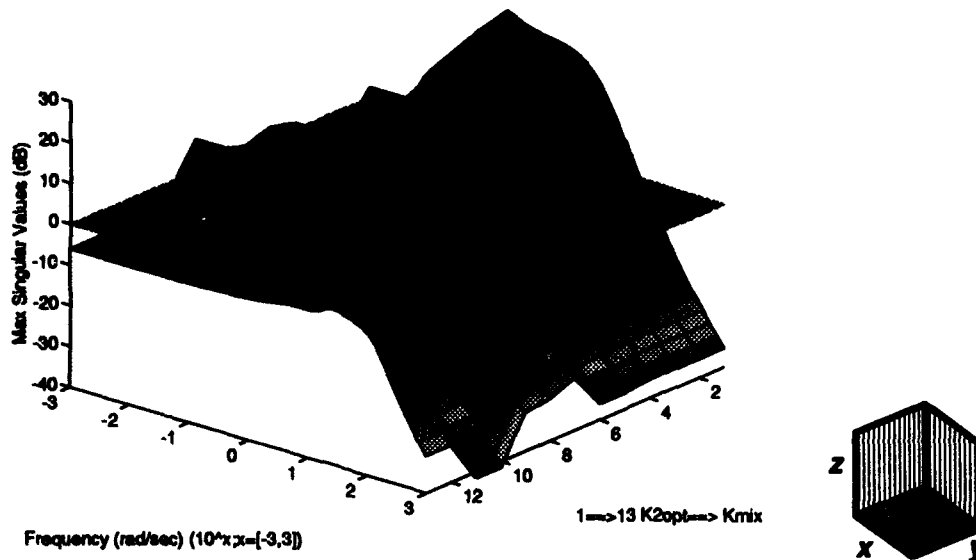


Figure 6-21 $W_{del}(s)T_i(s)$ Maximum Singular values (K_{mix} 8th order)

The maximum singular values of $W_{del}(s)T_i(s)$ are shown in Figure 6-21. The y axis represents some of the different 8th order controllers; it starts at K_{2opt} which corresponds to $y = 1$, and moves into the mixed controllers (from $y = 2$ through $y = 13$). Notice how the maximum singular values are minimized until Robust Stability is met. Figure 6-22 shows the maximum singular values of $W_p(s)S_o(s)$. The same axis orientation is kept. This new technique drives both infinity constraints to the required level of Nominal Performance and Robust Stability, with the two norm also being minimized. It is important to mention again that both H_∞ designs are singular problems. Table 6-7 shows the VGM and VPM for each controller using the final controller. Notice that each controller tries to recover the VGM and VPM at the input of the plant. Now the trade off between input and output margins is more evident, since a weighted output sensitivity output is the driver for margins at the output of the plant.

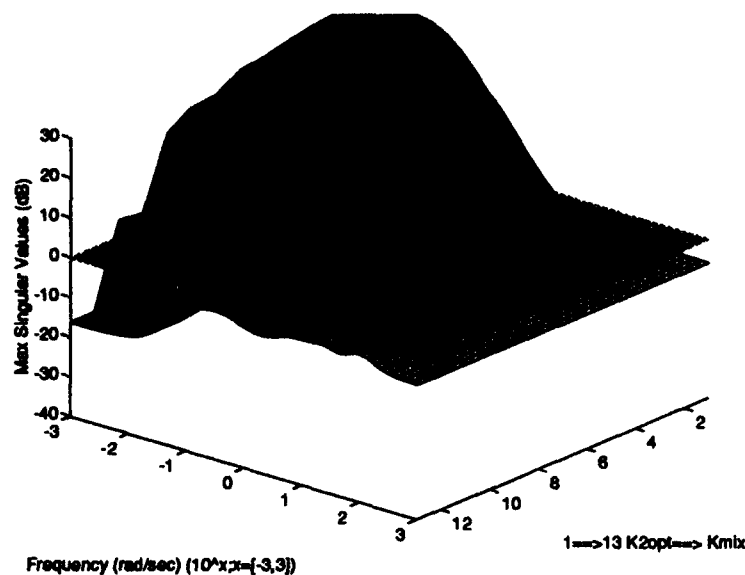


Figure 6-22 $W_p(s)S_o(s)$ Maximum Singular values (K_{mix} 8th order)

Table 6-7 Mixed H_2/H_∞ with two H_∞ Constraints VGM and VPM

K_{mix} controller (4th order)

	VGM ₁ (dB)	VPM ₁ (deg)	VGM ₂ (dB)	VPM ₂ (deg)
S1	[-3.9103, 7.3025]	± 33.0344	[-3.7631, 6.7876]	± 31.4629
T1	[-6.3912, 3.6419]	± 30.1926	[-6.4753, 3.6682]	± 30.4666
S2	[-4.3418, 9.0814]	± 37.8401	[-3.8033, 6.9242]	± 31.8883
T2	[-8.7051, 4.2594]	± 36.8988	[-6.4633, 3.6645]	± 30.4278

K_{mix} controller (6th order)

S1	[-3.6202, 6.3225]	± 29.9668	[-3.6540, 6.4297]	± 30.3183
T1	[-6.2052, 3.5825]	± 29.5776	[-7.2142, 3.8858]	± 32.7709
S2	[-4.1892, 8.3994]	± 36.1056	[-3.6533, 6.4275]	± 30.3112
T2	[-8.1393, 4.1269]	± 35.4095	[-7.1817, 3.8768]	± 32.6735

K_{mix} controller (8th order)

S1	[-3.6560, 6.4359]	± 30.3386	[-4.7985, 11.6176]	± 43.2774
T1	[-6.8178, 3.7721]	± 31.5575	[-9.8992, 4.5066]	± 39.7588
S**	[-4.5405, 10.0795]	± 40.1593	[-4.4862, 9.7928]	± 39.5186
T**	[-8.7010, 4.2584]	± 36.8883	[-7.3548, 3.9246]	± 33.1891
S2	[-4.7691, 11.4256]	± 42.9160	[-4.7003, 10.9939]	± 42.0753
T2	[-14.9428, 5.2062]	± 48.4723	[-12.1456, 4.8756]	± 44.2334

(1= case 1, 2= case 2)

This table suggests the use of a higher order controller in order to avoid a degradation of margins at the output of the plant. The next section will compare the (**) eight order mixed controller with the controller obtained using μ -synthesis, as well as an H_∞ optimal controller.

6.7 Mixed H_2/H_∞ with Multiple Singular H_∞ Constraints

and Robust Performance

μ -Synthesis versus Mixed H_2/H_∞ -Synthesis

This section presents a comparison between the μ controller obtained from running the HIMAT demo in MATLAB, the H_∞ optimal controller for the mixed sensitivity problem, and the mixed H_2/H_∞ controller. In this section, the value of the upper bound on $\mu(\bar{\sigma}(DMD^{-1}))$ will simply be called μ for convenience. A fictitious block Δ_p is created to include the performance requirement, as shown in Figure 6-23.

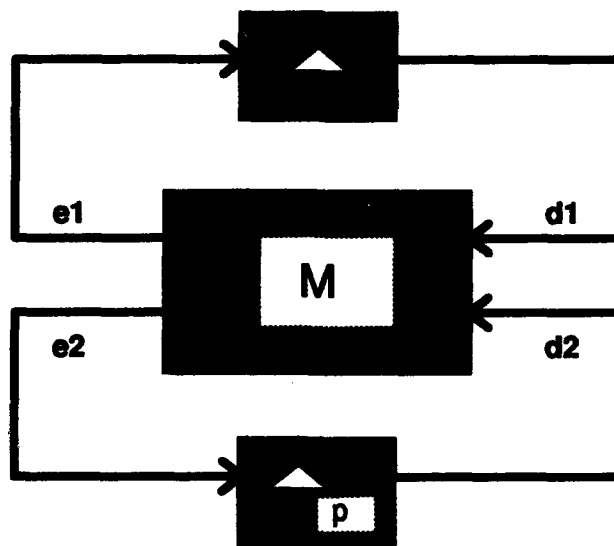


Figure 6-23 Block diagram for Robust Performance

Although the mixed problem does not directly address Robust Performance, the trade off among the infinity norms of the diagonal and cross terms of M will shape the maximum singular values of M , and therefore could affect μ . This is shown when a μ analysis is done for twenty-six 8th order mixed controllers from Section 6.6 (these 26 controllers are only a subset of all 8th mixed controllers; see Appendix A, Section A.3), as shown in Figure 6-24. $\|M\|_\mu$ is defined as the upper bound on $\mu(M)$. The x axis corresponds the different controllers, starting with K_{2opt} and moving along the mixed controllers as the infinity norms are minimized. Notice that the upper bound of μ is minimized. Now, looking at the three 8th order mixed controllers from Table 6-6, we see that the case 1 and case 2 controllers have a $\|M\|_\mu$ value around 1.7, while the controller (**) has $\|M\|_\mu = 1.3404$, as shown in Figure 6-25. This shows that different combinations of infinity norms of the cross and diagonal terms will result in a differing values of $\|M\|_\mu$. This is the reason for using the D scaling (see Chapter 2), since it shapes the maximum singular values of M in order to reduce $\|M\|_\mu$. The mixed problem improves $\|M\|_\mu$, but it does not directly address Robust Performance, since it does not exploit the frequency information. Consider the controller (**) as the best controller in terms of Robust Performance. Figure 6-26 shows the μ bounds for the μ -synthesis design, H_∞ optimal control, and the (**) mixed controller. The mixed controller reduces $\|M\|_\mu$ more than the H_∞ optimal controller does, because it directly addresses Robust Stability and Nominal Performance.

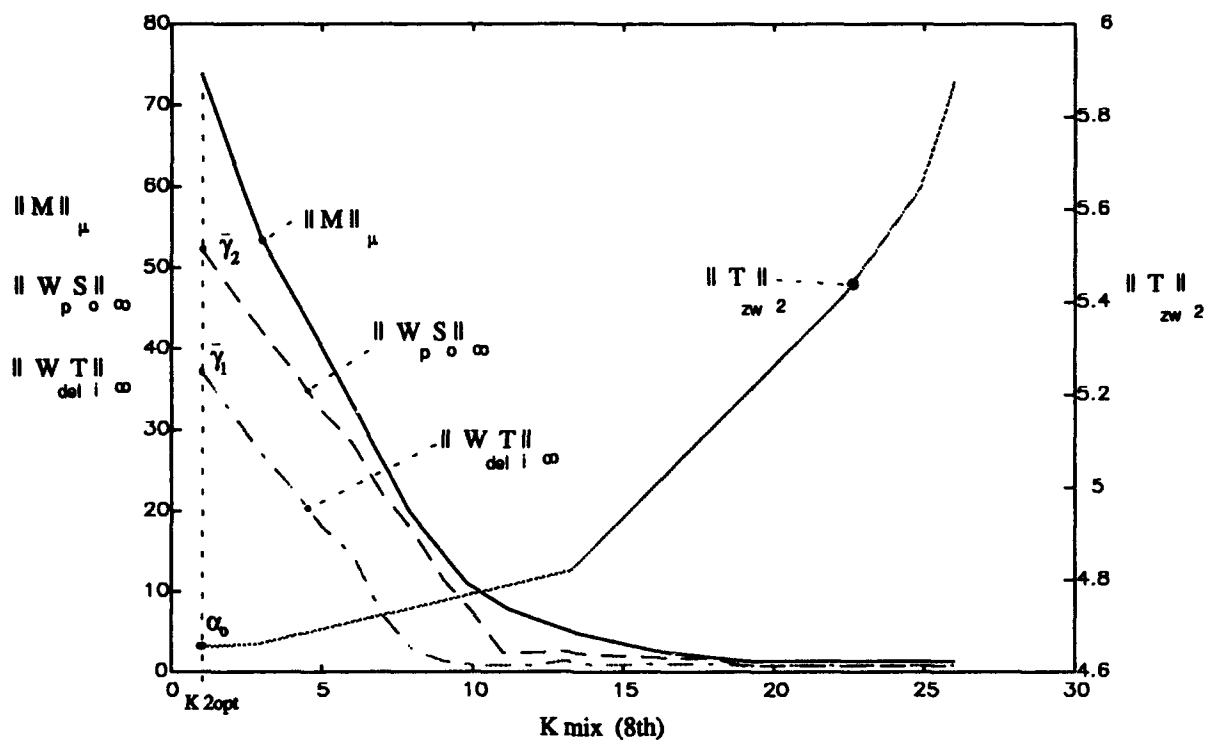


Figure 6-24 Mixed H_2/H_∞ controllers and the effect on $\|M\|_\mu$

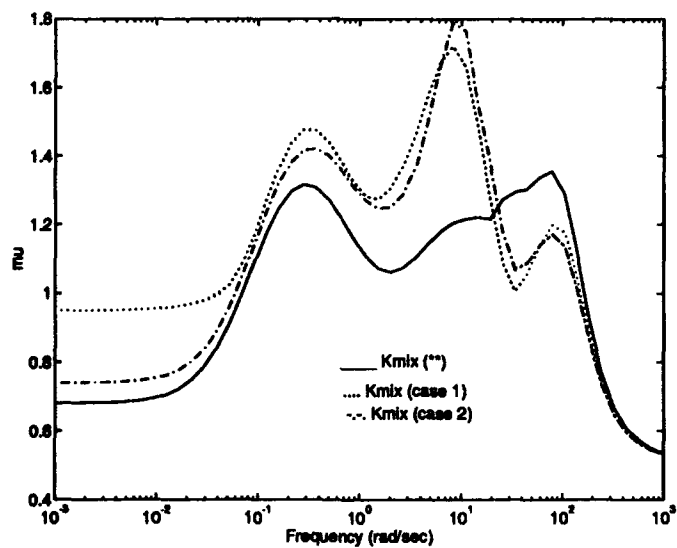


Figure 6-25 $\mu(M)$ of the 8th order Mixed controllers from Table 6-6

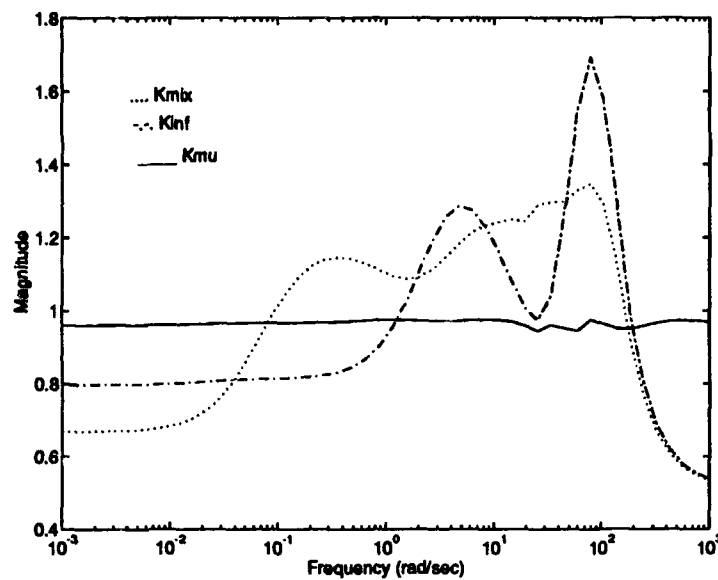


Figure 6-26 $\mu(M)$ of the μ -synthesis, H_∞ opt, and mixed H_2/H_∞ Controller control design

Although the mixed H_2/H_∞ controller does not pass the test for Robust Performance, the order of this controller is much smaller than the $K(s)$ obtained from μ -synthesis. Also, noise rejection is better with the mixed controller than the other two. Table 6-8 summarizes the results, including a 4th order mixed controller as well.

Table 6-8 μ Analysis for the HIMAT example

	Robust Stability	Nominal Performance	Robust Performance	$\ T_{zw}\ _2$	order of controller
μ -synthesis	pass	pass	0.9803	18.51034	20
Mixed H_2/H_∞	pass	pass	1.3404	5.81450	8
* H_∞ optimal controller	pass	pass	1.6230	∞	7
Mixed H_2/H_∞	pass	pass	5.4040	6.1320	4

* the optimal H_∞ controller is for mixed sensitivity and complementary sensitivity

Figures 6-27 and 6-28 show the magnitude of the weighted sensitivity function and weighted complementary sensitivity function for the different control designs, respectively. Notice how the infinity norm for both functions are improved for the mixed problem compared to the H_∞ problem. Figures 6-29 and 6-30 represent the magnitude plot versus frequency for the actual (unweighted) sensitivity and complementary sensitivity functions. Figure 6-29 shows that the mixed H_2/H_∞ controller tries to decrease the magnitude of the sensitivity function at low frequencies, compared to the μ controller. This is probably due to the fact that the mixed controller is trying to reject the low frequency wind disturbance which μ does not account for. In Figure 6-30, the mixed H_2/H_∞ rolls off faster than μ does, and peaks earlier than H_∞ .

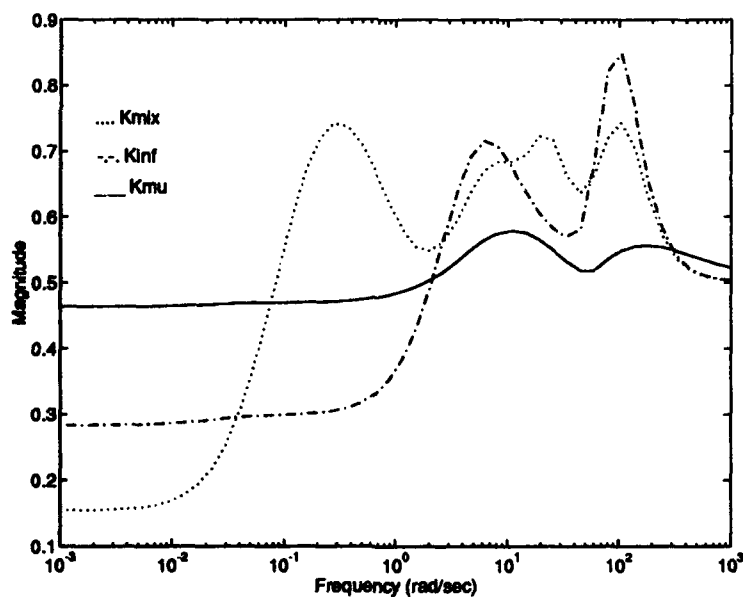


Figure 6-27 Magnitude of $W_p(s)S_o(s)$ for μ -Synthesis, H_∞ , and the Mixed H_2/H_∞

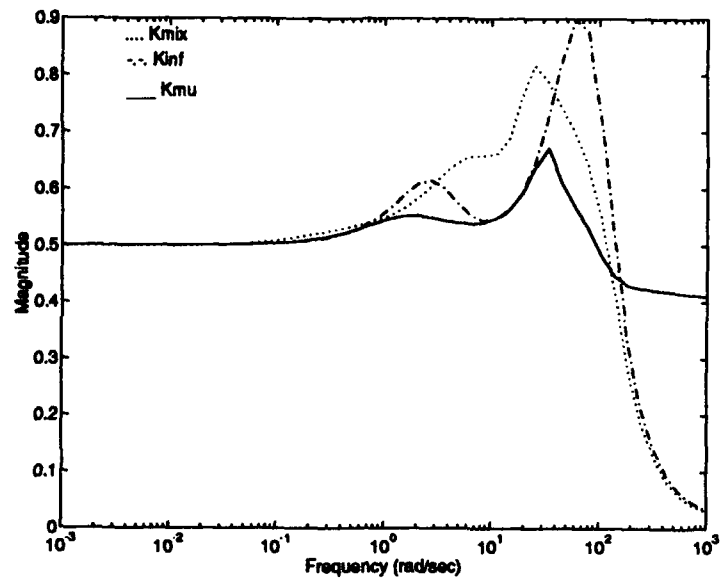


Figure 6-28 Magnitude of $W_{del}(s)T_i(s)$ for μ -Synthesis, H_∞ , and Mixed H_2/H_∞

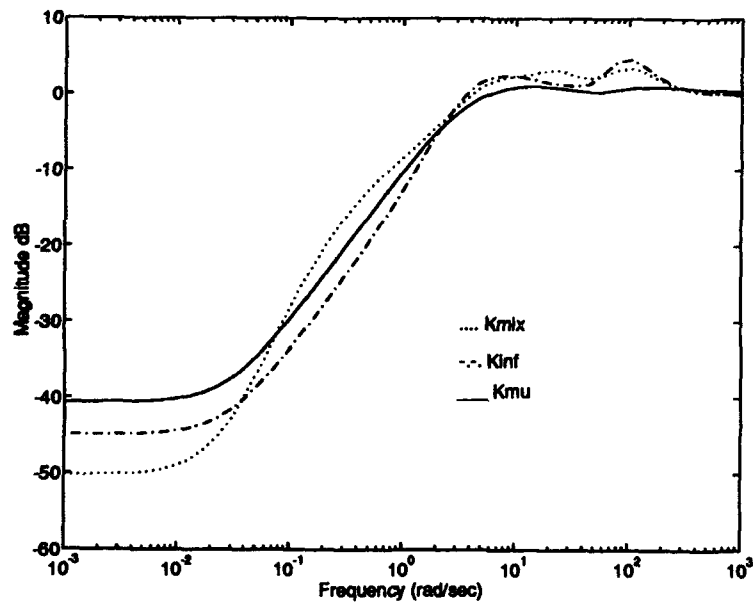


Figure 6-29 Magnitude of Sensitivity Function for μ -Synthesis, H_∞ , and Mixed H_2/H_∞

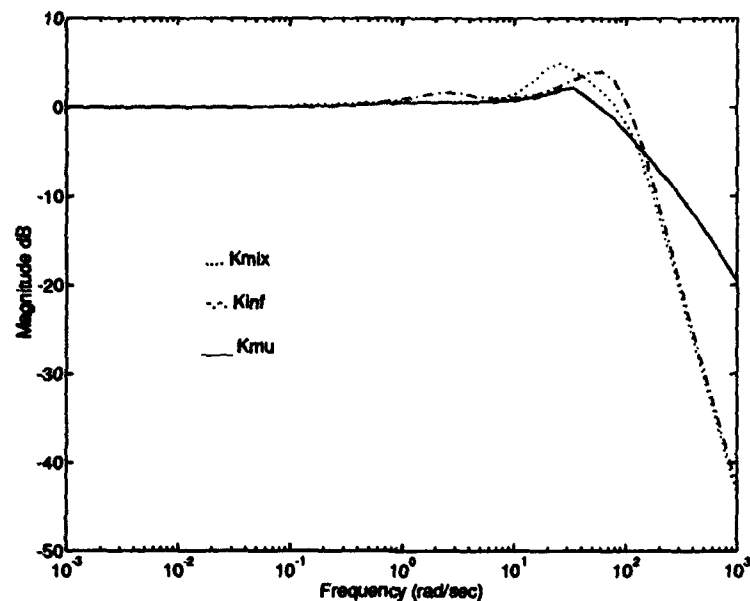


Figure 6-30 Magnitude of Complementary Sensitivity for μ -Synthesis, H_∞ , and Mixed H_2/H_∞

The time responses for a step angle of attack and pitch angle are shown in Figures 6-31 and 6-32. Notice how the wind disturbance and noises affect the μ -synthesis controller and the H_∞ controller. The mixed H_2/H_∞ controller has good noise rejection and good tracking as well. The mixed controller fails the robust performance test with its upper bound of 1.3404; however, this means that in order to pass this test, the robustness and nominal performance requirements must be relaxed by only a factor of 1/1.3404.

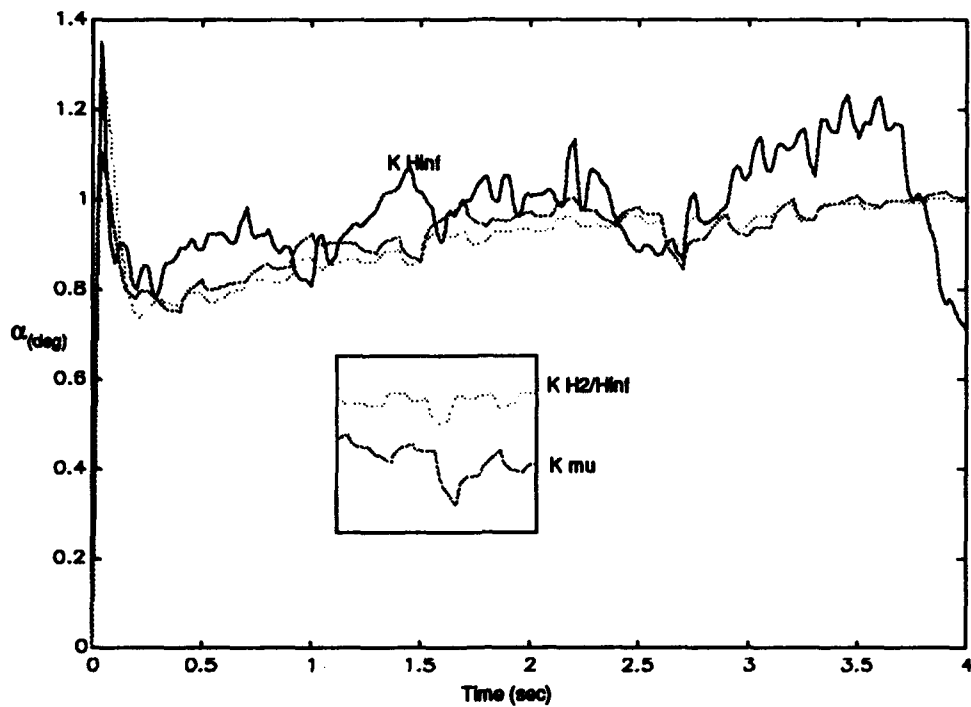


Figure 6-31 Time response for a step angle of attack command

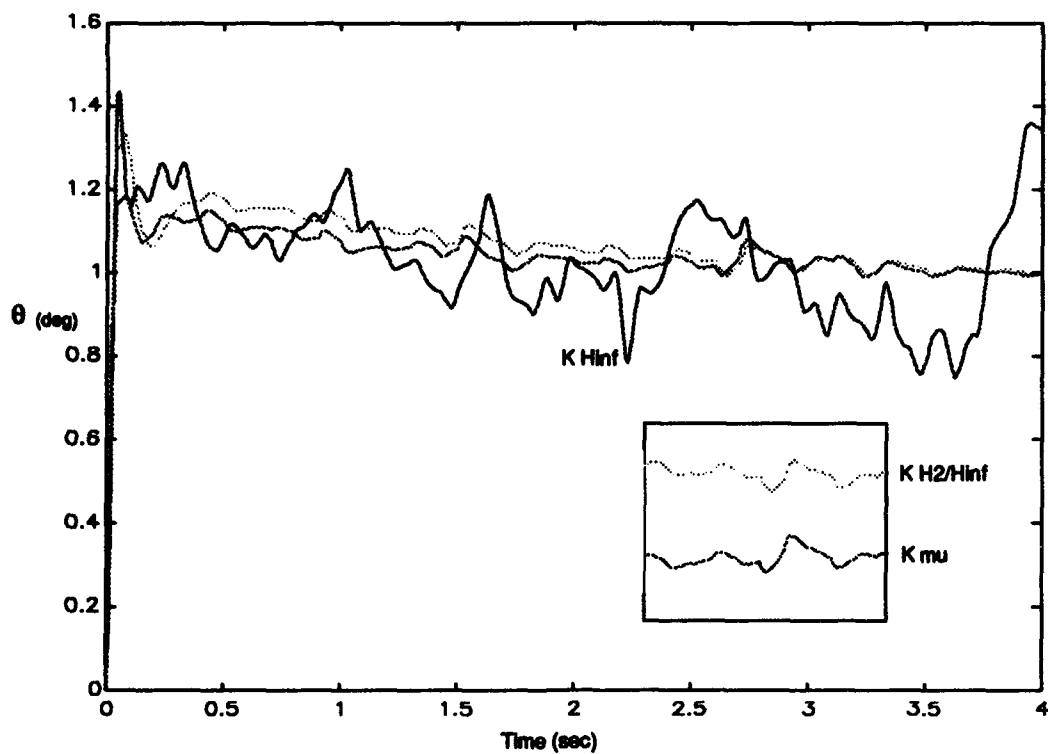


Figure 6-32 Time response for a step pitch angle command

6.8 Mixed H_2/H_∞ design with three H_∞ constraints

The objective of this design is to minimize three H_∞ constraints. The first and second constraints are the previous Robust Stability and Nominal Performance requirements. These H_∞ constraints were examined individually and simultaneously in the previous sections. Now a weighted output complementary sensitivity constraint is introduced, as a third H_∞ constraint. The desire is to drive its infinity norm to less than one. The exogenous input is d_3 and the exogenous output is e_3 for this new H_∞ constraint, as shown in Figure 6-33. The dotted block represents our true plant. The transfer function $\Delta_f(s)$ is a fictitious unstructured block and is assumed to be stable, unknown, and such that its infinity norm is less than one ($\|\Delta_f(s)\|_\infty < 1$). The objective for this design is to meet

$$\|T_{ed1}\|_\infty < 1; \text{ Robust Stability at input}$$

$$\|T_{ed2}\|_\infty < 1; \text{ Nominal Performance at output} \quad (6-19)$$

$$\|T_{ed3}\|_\infty < 1; \text{ Robust Stability at output}$$

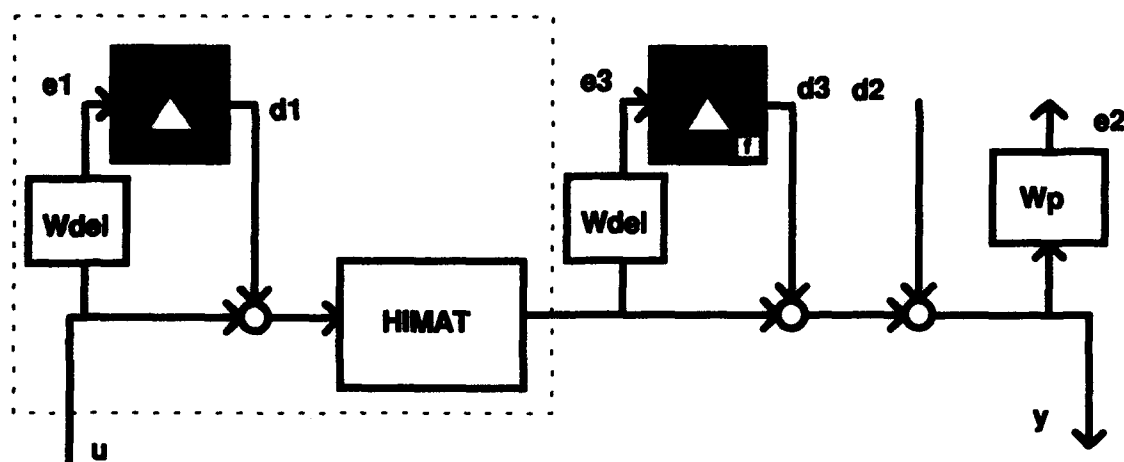


Figure 6-33 Mixed H_2/H_∞ design with three H_∞ constraints Block Diagram

The state space for the H_{∞} design plant is

$$P_{\infty} = \left[\begin{array}{c|cc} A_{\infty} & B_{d_3} & B_{u_{\infty}} \\ \hline C_{e_3} & D_{e_3 d_3} & D_{e_3 u} \\ \hline C_{y_{\infty}} & D_{y d_3} & D_{y u} \end{array} \right] \quad (6-20)$$

where the state space matrices are

$$\begin{aligned} \begin{bmatrix} \dot{x}_g \\ \dot{x}_{del} \end{bmatrix} &= \begin{bmatrix} A_g & 0 \\ B_{del} C_g & A_{del} \end{bmatrix} \begin{bmatrix} x_g \\ x_{del} \end{bmatrix} + \begin{bmatrix} 0 \\ 0 \end{bmatrix} d_3 + \begin{bmatrix} B_g \\ 0 \end{bmatrix} u \\ [e_3] &= [D_{del} C_g \quad C_{del}] \begin{bmatrix} x_g \\ x_{del} \end{bmatrix} + [0] d_3 + [0] u \\ [y] &= [C_g \quad 0] \begin{bmatrix} x_g \\ x_{del} \end{bmatrix} + [I] d_3 + [0] u \end{aligned} \quad (6-21)$$

$D_{e_3 u}^T D_{e_3 u}$ is not full rank; therefore, this is a singular H_{∞} problem. The setup for this mixed H_2/H_{∞} problem is: Find a stabilizing compensator that achieves

$$\inf_{K \text{ stabilizing}} \|T_{zw}\|_2 \text{ subject to } \begin{cases} \|W_{del} T_i\|_{\infty} \leq \gamma_1 \\ \|W_p S_o\|_{\infty} \leq \gamma_2 \\ \|W_{del} T_o\|_{\infty} \leq \gamma_3 \end{cases} \quad (6-22)$$

Again, the three H_{∞} constraints will be treated as equality constraints. Thus, the performance index for the numerical method is

$$J_{\gamma} = \|T_{zw}\|_2^2 + \lambda_1 (\|W_{del} T_i\|_{\infty} - \gamma_1)^2 + \lambda_2 (\|W_p S_o\|_{\infty} - \gamma_2)^2 + \lambda_3 (\|W_{del} T_o\|_{\infty} - \gamma_3)^2 \quad (6-23)$$

The state space matrices are equation (6-2) for the H_2 part, equation (6-7) for weighted input complementary sensitivity, equation (6-13) for the weighted output sensitivity

output and equation (6-21) for weighted output complementary sensitivity for the H_∞ parts.

Again, the starting controller is the optimal H_2 controller. The design is performed to obtain fourth, sixth, and eight order controllers. The method used in the numerical technique is the direct method. Table 6-9 shows part of the results (see Appendix A, Section A.4 for full results). Comparing Table 6-9 with Table 6-6 (two H_∞ constraints), we can see that there is no improvement for the 4th and 6th order controllers. It seems that the third constraint is not dominant, and the trade off among the H_∞ constraints is only related to the weighted input complementary sensitivity and weighted output sensitivity. The 8th order controller does show some improvement in performance, while keeping a good level of robustness at the input and output of the plant. Notice that if an H_∞ controller is found for an unmixed problem, the order would be 10. A tenth order mixed controller was not computed due to time constraints.

Table 6-9 Mixed H_2/H_∞ with three H_∞ Constraints: $\|T_{zw}\|_2$, $\|W_{del}T_i\|_\infty$, $\|W_pS_o\|_\infty$, and $\|W_{del}T_o\|_\infty$

$\ T_{zw}\ _2$	$\ W_{del}T_i\ _\infty$	$\ W_pS_o\ _\infty$	$\ W_{del}T_o\ _\infty$
K_{opt} Controller			
4.6970	37.0491	52.1574	0.6853
Fourth order controller			
6.5415	0.7584	0.9283	0.9975
Sixth order controller			
6.5775	0.8029	0.9416	0.9894
Eight order controller			
5.2653	0.9189	0.6865	0.5956

Table 6-10 shows the VGM and VPM at the input and output of the plant. The time responses for a step angle of attack (α) and pitch angle (θ) command are shown in Figures 6-34 and 6-35 for the controllers from Table 6-9. Notice that the 4th and 6th order

controllers have a considerable overshoot. Although the settling time is almost the same for all three, the 8th order controller has a better response.

Table 6-10 Mixed H_2/H_∞ with three H_∞ Constraints: VGM and VPM

K_{opt} controller (4th order)

	VGM ₁ (dB)	VPM ₁ (deg)	VGM ₂ (dB)	VPM ₂ (deg)
S	[-4.2084, 8.4821]	± 36.3227	[-3.7627, 6.7862]	± 31.4586
T	[-9.9643, 4.5189]	± 39.9042	[-6.3492, 3.6287]	± 30.0548

K_{opt} controller (6th order)

S	[-4.2646, 8.7285]	± 36.9585	[-3.7126, 6.6194]	± 30.9307
T	[-8.8461, 4.2907]	± 37.2559	[-6.4819, 3.6703]	± 30.4881

K_{opt} controller (8th order)

S	[-3.7919, 6.8851]	± 31.7673	[-4.9276, 12.5242]	± 44.8856
T	[-6.8231, 3.7736]	± 31.5740	[-16.1158, 5.3134]	± 49.8972

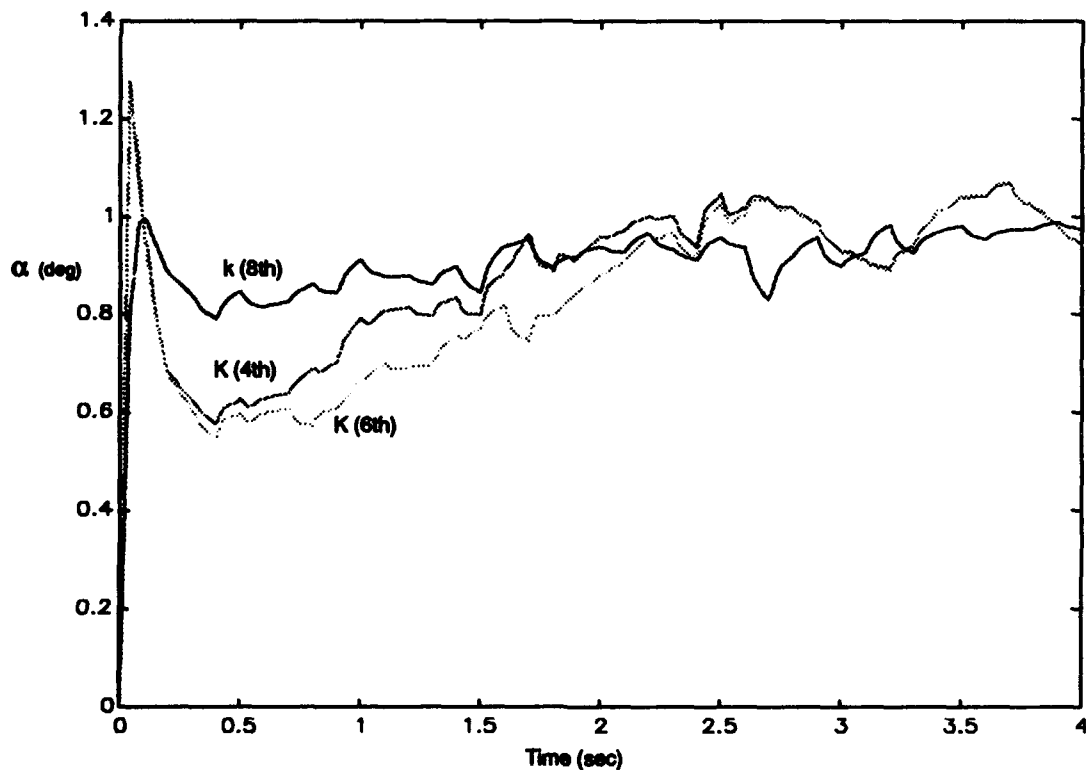


Figure 6-34 Time response, α command

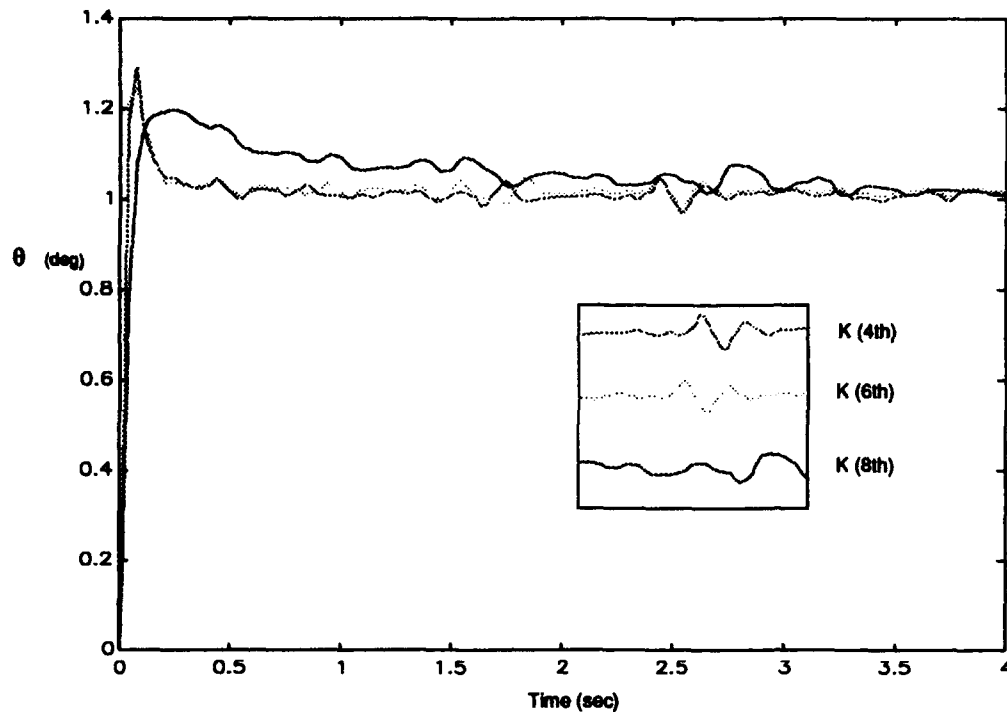


Figure 6-35 Time response, θ command

6.9 Summary

If the selection of the best controller has to be made, the question by itself is too complex, since many factors have to be considered. Table 6-11 summarizes the most important factors to consider in the selection of the controller. Consider the following factors (x in Table 6-11 if passed):

1. Satisfy Robust Stability (RS) at the input and output of the plant, and satisfy Nominal Performance (NP).
2. Satisfy RS and NP with high noise rejection
3. Satisfy Robust Performance < 1
4. Relax the Robust Performance $< 1/1.3404$
5. Relax the Robust Performance $< 1/5.4020$
6. Low overshoot

7. Low order controller that satisfies RS and NP

Table 6-11 (HIMAT) Selection of Controllers

Factor	1	2	3	4	5	6	7
Controller							
Mixed 4th (two H_{∞} Const.)	x				x		x
Mixed 8th (two H_{∞} Const.)	x	x		x	x		
Mixed 4th (three H_{∞} Const.)	x				x		x
Mixed 8th (three H_{∞} Const.)	x	x			x	x	
H_{∞} (8th)	x				x		
μ (20th)	x		x	x	x		

These are only a few factors to be considered. The selection will depend on how well we know the plant, and what factors are more important than others. The order of the controller is very important when it has to be implemented; therefore, the mixed H_2/H_{∞} control problem with multiple H_{∞} constraints will have great importance in low order controller design.

VII. Summary, Conclusions and Recommendations

Summary

The main objective of this thesis was to investigate the mixed H_2/H_∞ with multiple H_∞ constraints control problem. A SISO and a MIMO problem were solved. Successful strategies for obtaining measures of performance and robustness were presented in most designs.

The initial chapter gave a limited synthesis history that represented the motivation for the use of multiple H_∞ constraints in the mixed problem. Chapter II discussed the three base methodologies (H_2 , H_∞ , and μ -synthesis), and a review of the related design examples. Chapter III discussed the mixed H_2/H_∞ problem with a non-singular H_∞ constraint and with a single singular H_∞ constraint. Also, the new numerical method was explained. Chapter IV developed the mixed H_2/H_∞ problem with multiple H_∞ constraints, and discussed how the new numerical method can be used to solve this problem.

Chapter V presented the F-16 short period approximation (plus first order servo and Padé approximation) SISO example. The SISO example represented an introduction to this new design technique. First, an H_2 design was accomplished, and then two mixed problems with one H_∞ constraint were solved. The H_∞ constraints were weighted input sensitivity and weighted input complementary sensitivity. The trade off between both H_∞ constraints was observed. Finally, the mixed H_2/H_∞ with multiple H_∞ constraints problem was solved. Two methods were applied: the grid method and the direct method. A surface was created using the grid method, and it showed possible boundaries between H_∞

constraints when they are close to optimal values. The direct method was shown to be a better method, since it permitted selection of the direction of minimization.

Chapter VI presented the HIMAT problem (MIMO). Using the HIMAT problem, the following were solved:

- An H_2 design.
- Two mixed H_2/H_∞ designs, each with one H_∞ constraint. The H_∞ constraints addressed Robust Stability and Nominal Performance independently.
- A mixed H_2/H_∞ design with two H_∞ constraints. The constraints addressed Robust Stability and Nominal Performance, but now the trade off between them was manipulated.
- An H_∞ -synthesis and μ -synthesis (using D-K iteration), for the augmented system (the two H_∞ constraints wrapped in one block) were solved.
- Finally, a three H_∞ constraint problem was solved. The constraints addressed Robust Stability at the input and output of the plant, and Nominal Performance.

Different order mixed controllers were produced, with good results in most of them. A μ analysis was done on the mixed controller, and this was compared with the H_∞ optimal controller and the μ -synthesis controller. Table 6-11 summarizes some of the major results.

Conclusions

The conclusions of this thesis are:

- i). This new numerical technique permits minimization of the two norm of T_{zw} subject to single or multiple H_∞ constraints.
- ii). The H_∞ constraint can be regular or singular.

- iii). As the order of the controller was increased, better results were obtained.
- iv). The mixed H_2/H_∞ optimization with multiple singular H_∞ constraints permits the designer control over the level of Robust Stability and Nominal Performance, and also to fix the level of other H_∞ constraints. This means that the trade off between design requirements in terms of H_∞ constraints can be freely chosen by the designer.
- v). The main idea to include other H_∞ constraints, that are not specified as a Nominal Performance or Robust Stability requirement, is that the system could meet Robust Stability, Nominal Performance and even Robust Performance for a certain number of uncertainty blocks and performance requirements, yet fail when the number of uncertainty blocks or performance requirements are increased. Therefore, this technique can keep the level of Robust Stability and Nominal Performance for the original blocks, and can control the level in terms of H_∞ magnitude for those that the system does not meet.

Table 7-1 summarizes the improvement of this new nonconservative method, compared with other control design methods.

Table 7-1 Comparison of different Control Law Designs

	H_2	H_∞	μ (D-K)	Mixed H_2/H_∞
Handle white Gaussian noise (WGN)	x			x
Robust Stability, Nominal Performance		x	x	x
Robust Performance			x	
Trade off between RS and NP freely				x
WGN and RS, NP				x
Reduced order controller				x

Recommendations

- i) Improve the numerical method, especially around the knee of the α vs. γ curve.
- ii) Investigate the "relationship" between the diagonal and cross terms in mixed H_2/H_∞ with multiple H_∞ constraints, and how this relationship could affect Robust Performance.
- iii) A faster computer is needed in order to obtain a large number of controllers, so that various trade-offs can be examined quickly and efficiently.
- iv) Since the numerical method runs with any order controller, investigate results using any order stabilizing controller, including order less than the underlying H_2 plant (if it exists).
- v) Remove the restriction that the H_∞ constraints must be satisfied with equality through the use of constrained optimization. This has already been done [Wal94], and the results in this thesis are being reworked using sequential quadratic programming rather than DFP.

APPENDIX A.

HIMAT PROBLEM

A.1 Weighted Input Complementary Sensitivity Constraint

4th order controller

$\ T_{zw}\ _2$	$\ W_{del}T_i\ _\infty$	$\ W_pS_o\ _\infty$	$\ W_{del}T_o\ _\infty$
4.6970	37.0427	52.1864	0.6856
4.6970	34.1942	51.7626	0.6602
4.7031	28.1678	51.9762	0.5881
4.8223	22.2256	44.8161	0.6134
4.8698	19.5766	41.2103	0.5564
5.0489	16.3526	33.9038	0.5556
5.2281	13.4063	23.7194	0.6010
5.4864	7.4497	15.1682	0.6236
6.3685	2.1831	21.3140	0.6466
6.4369	1.8485	22.9333	0.6571
6.5611	1.4709	20.3251	0.6554
6.7332	1.0585	26.1706	0.6613
6.9970	0.6413	34.6669	0.6784
7.7440	0.4956	48.7810	0.7959
7.1843	0.4918	51.2928	0.6487
7.1759	0.4920	51.7376	0.6478

6th order controller

$\ T_{zw}\ _2$	$\ W_{del}T_i\ _\infty$	$\ W_pS_o\ _\infty$	$\ W_{del}T_o\ _\infty$
4.6970	37.0427	52.1864	0.6856
4.6970	34.1941	51.7622	0.6603
4.7064	28.2220	50.7688	0.5726
4.7365	25.3941	48.4703	0.6247
5.0925	16.4510	37.8934	0.5719
5.3813	13.1794	32.9813	0.5940
5.5764	10.7019	24.2157	0.6249
6.3416	4.6897	23.0864	0.6366
6.5190	2.0029	24.0980	0.6154
6.4690	1.8122	24.9896	0.6316
6.4751	1.5727	25.0295	0.6737
6.3395	1.4366	21.4272	0.7059
6.3674	1.2844	25.4598	0.7302
6.4721	1.1122	28.0406	0.7332

6.6457	0.8946	31.8055	0.7371
6.8571	0.7113	36.4956	0.7552
7.0705	0.5177	45.8587	0.6423
7.2149	0.5548	48.3201	0.7947
7.6167	0.5095	56.5616	0.8143
7.0705	0.5177	45.8587	0.6423

A.2 Weighted Output Sensitivity Constraint

4th order controller

$\ T_{zw}\ _2$	$\ W_{del}T_i\ _\infty$	$\ W_pS_o\ _\infty$	$\ W_{del}T_o\ _\infty$
4.6970	37.0427	52.1864	0.6856
4.6990	25.9277	48.2140	0.5763
4.6994	24.5831	44.2054	0.5439
4.7002	23.8210	40.2266	0.5406
4.7007	22.8746	36.2079	0.5410
4.7019	22.0211	32.2226	0.5440
4.7027	21.2916	28.2454	0.5509
4.7042	20.3073	24.2368	0.5628
4.7062	18.7839	20.2418	0.5714
4.7129	16.0872	12.2381	0.6305
4.7327	15.2283	8.3599	0.7095
4.7498	10.7949	4.2906	0.9023
5.1901	5.3058	1.0481	1.1369
5.2453	4.9608	1.0108	1.1111
5.2584	4.8214	0.9905	1.0972
5.2617	4.8043	0.9887	1.0960

6th order controller

$\ T_{zw}\ _2$	$\ W_{del}T_i\ _\infty$	$\ W_pS_o\ _\infty$	$\ W_{del}T_o\ _\infty$
4.6970	37.0427	52.1864	0.6856
4.6984	25.6282	48.2167	0.5744
4.6999	23.7559	40.2441	0.5407
4.7010	22.9563	36.2181	0.5412
4.7012	21.2190	28.2184	0.5525
4.7063	18.3781	20.2468	0.5713
4.7097	17.1423	16.2076	0.5955
4.7134	15.4557	12.1765	0.6364
5.1647	11.3612	1.4016	1.4939
5.2568	7.0627	1.2114	1.0669
5.3035	4.6762	1.1291	1.0641
5.6429	4.5730	0.8311	0.9451

A.3 Weighted Output Sensitivity and Weighted Input Complementary Sensitivity Constraints

4th order controller

$\ T_{zw}\ _2$	$\ W_{del}T_i\ _\infty$	$\ W_pS_o\ _\infty$	$\ W_{del}T_o\ _\infty$	
4.6970	37.0491	52.1574	0.6853	
4.9689	25.9037	37.9268	0.7416	
4.9747	17.5703	25.2809	0.5761	
5.0639	9.0661	13.1080	0.6197	
5.1136	7.2982	10.1080	0.6549	
5.2435	5.6649	7.3953	0.6874	
5.3986	1.5091	1.0073	1.0344	
5.5195	1.2231	0.9592	1.0137	
5.5208	1.2231	0.9365	1.0137	
5.5636	1.1034	0.9542	1.0154	
5.5827	1.0989	0.9178	1.0175	
5.5834	1.0982	0.9174	1.0167	
5.5884	1.0981	0.9159	1.0139	
5.6837	1.0009	0.9229	1.0225	
5.6883	0.9938	0.9234	1.0159(Case 1)
6.0137	0.8467	0.9146	1.0036	
6.0963	0.8278	0.9099	0.9985	
6.1099	0.8234	0.9122	1.0000	
6.1161	0.8215	0.9106	0.9983	
6.1101	0.8244	0.9102	0.9987	
6.1091	0.8244	0.9100	0.9986	
6.1322	0.8172	0.9110	0.9971(Case 2)
6.2257	0.8039	0.9154	0.9990	
6.8656	0.6933	1.0612	0.9698	
6.9195	0.6916	1.0474	0.9710	
6.9908	0.6895	1.0600	0.9732	

6th order controller

$\ T_{zw}\ _2$	$\ W_{del}T_i\ _\infty$	$\ W_pS_o\ _\infty$	$\ W_{del}T_o\ _\infty$	
4.6970	37.0491	52.1574	0.6853	
4.7468	34.0391	46.8218	0.7340	
4.7762	29.5118	41.4565	0.6448	
4.8104	26.3026	37.0553	0.6860	
4.9899	8.1814	10.7511	0.6518	
5.3292	1.5742	1.4497	0.9343	
5.7274	1.0706	0.9707	1.0010	
5.7311	0.9978	0.9574	0.9826(Case 1)
5.9607	0.8712	0.9581	0.9832	
6.0292	0.8512	0.9596	0.9819	

6.0274	0.8519	0.9579	0.9828(Case 2)
6.0341	0.8161	0.9764	1.0039	
6.3459	0.7776	1.0317	0.9624	
6.9503	0.7459	1.2159	0.9175	
5.7020	1.0383	0.9481	0.9748	
5.7287	1.1739	0.9177	0.9909	
5.4175	1.6316	0.8939	0.9889	
5.3692	1.7694	0.8891	0.9475	
5.3261	3.2591	0.8712	0.9776	

8th order controller

$\ T_{zw}\ _2$	$\ W_{del}T_i\ _\infty$	$\ W_pS_o\ _\infty$	$\ W_{del}T_o\ _\infty$	
4.6970	37.0491	52.1574	0.6853	
4.7023	32.0126	47.1634	0.6277	
4.7148	27.0366	42.0854	0.6006	
5.2319	0.9532	1.8408	1.2752	
5.2336	0.9613	1.6649	1.3010	
5.2324	0.9742	1.6543	1.3037	
5.7912	0.7939	0.7414	0.8783	
5.8145	0.7438	0.7644	0.7030(controller **)
5.7949	0.7872	0.7281	0.8540	
6.0145	0.7866	0.6897	0.7882	
5.9967	0.7946	0.6878	0.7870	
6.0252	0.7931	0.6867	0.7860	
5.7059	0.6251	0.7353	0.7195	
5.7159	0.6240	0.7326	0.7174	
5.6926	0.6109	0.7270	0.6707	
5.2319	0.9532	1.8408	1.2752	
5.6862	0.6148	0.7374	0.6710	
5.6926	0.6109	0.7270	0.6707(Case 2)
6.0252	0.7931	0.6867	0.7860	
6.0276	0.7961	0.6863	0.7857	
6.0270	0.7961	0.6862	0.7858	
6.0142	0.8078	0.6856	0.7924	
5.9267	0.9214	0.6857	0.7564	
5.9228	0.9220	0.6845	0.7560(Case 1)
5.9197	0.9218	0.6853	0.7565	
5.8233	0.9331	0.6939	0.7206	
5.7243	0.8906	0.7027	0.7403	

A.4 Weighted Output Sensitivity .Weighted Input Complementary Sensitivity. and Weighted Output Complementary Sensitivity Constraints

Case 1 and Case 2 for the 4th and 6th order controllers are almost identical, as there is not a substantial reduction of the infinity norms below one, as will be shown in Figure A-1.

4th order controller

$\ T_{zw}\ _2$	$\ W_{del}T_i\ _\infty$	$\ W_pS_o\ _\infty$	$\ W_{del}T_o\ _\infty$
5.6011	1.0653	0.9586	1.0523
5.5654	1.0937	0.9386	1.0431
5.5627	1.0934	0.9396	1.0430
5.5632	1.0914	0.9378	1.0429
5.7476	0.9423	0.9423	1.0423
6.6207	0.7618	0.9693	0.9683
6.3762	0.7790	0.9464	0.9900
7.9001	0.6586	1.4409	1.0213
6.5600	0.7599	1.0430	0.9423
6.7315	0.7444	0.9824	0.9323
6.4187	0.7662	1.0009	0.9370
5.7426	0.9197	0.9623	1.0059
6.0272	0.8155	0.9606	0.9805
6.4323	0.7484	0.9405	0.9873
6.4323	0.7484	0.9405	0.9873
6.5415	0.7584	0.9283	0.9975
6.4429	0.7592	0.9274	1.0006
6.4165	0.7590	0.9277	0.9999

6th order controller

$\ T_{zw}\ _2$	$\ W_{del}T_i\ _\infty$	$\ W_pS_o\ _\infty$	$\ W_{del}T_o\ _\infty$
4.6970	37.0491	52.1574	0.6853
4.8225	26.8937	37.4109	0.5390
4.8936	11.8365	16.1882	0.6239
5.1569	7.7096	10.9946	0.6614
5.2006	1.8236	2.3868	0.9725
5.2373	1.6559	1.7414	1.0336
5.3071	1.5121	1.4009	1.0226
5.3888	1.3224	1.0848	1.0750
5.4499	1.2454	0.9865	1.0689
5.7320	1.0089	0.9862	1.0345

5.8071	1.0188	0.9481	1.0278
5.8117	1.0203	0.9470	1.0276
5.8871	1.0433	0.9346	1.0282
5.8901	1.0429	0.9345	1.0279
5.8905	1.0445	0.9342	1.0275
5.9694	0.9521	0.9429	1.0186
6.3540	0.8750	0.9280	1.0122
6.5775	0.8029	0.9416	0.9894
7.3778	0.7032	1.0638	0.9695

8th order controller

$\ T_{zw}\ _2$	$\ W_{del}T_i\ _\infty$	$\ W_pS_o\ _\infty$	$\ W_{del}T_o\ _\infty$	
4.6970	37.0427	52.1864	0.6856	
4.7191	26.9350	40.0723	0.6345	
4.8990	19.7854	25.6832	0.6575	
5.0856	2.7212	1.8812	1.0661	
5.1065	2.4514	1.5789	1.0288	
5.1205	2.3120	1.4950	1.0391	
5.3710	0.8648	1.1453	0.7335	
5.3482	0.8183	0.9068	0.6471	
5.3238	0.7452	0.8444	0.6824(Case 2)
5.2582	0.9260	0.7405	0.5939	
5.2653	0.9189	0.6865	0.5956(Case 1)
5.2890	0.9292	0.6904	0.6086	
5.3413	0.9494	0.7701	0.7328	
5.3499	0.9399	0.7732	0.7371	
5.3634	0.9043	0.8438	0.8897	
5.9354	0.9563	0.7650	0.9622	
6.1497	0.9541	0.7366	0.9535	
6.0447	0.9538	0.7247	0.9533	
6.0827	0.9540	0.7145	0.9510	
6.0502	0.9542	0.7121	0.9510	

The following figures map the boundaries for the fourth and eight order controllers for two and three H_∞ constraints. As was shown in Chapter 6, the third H_∞ constraint (a weighted output complementary sensitivity) was not dominant, and therefore we can combine the results of the mixed controller with two H_∞ constraints and the controller with three H_∞ constraints of the same order. This is shown in Figure A-1 for the 4th order controller and Figure A-2 for the 8th order controller.

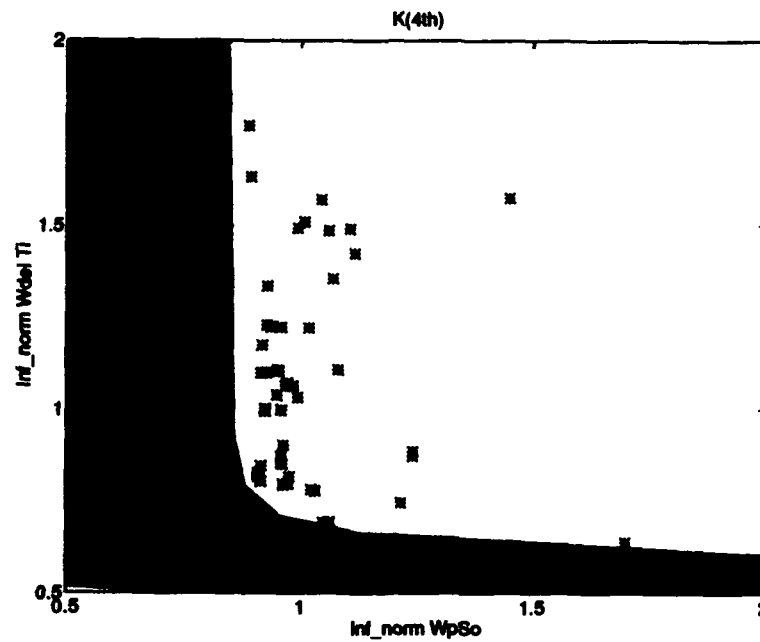


Figure A-1 Boundary for the fourth order controller with two and three H_∞ constraints

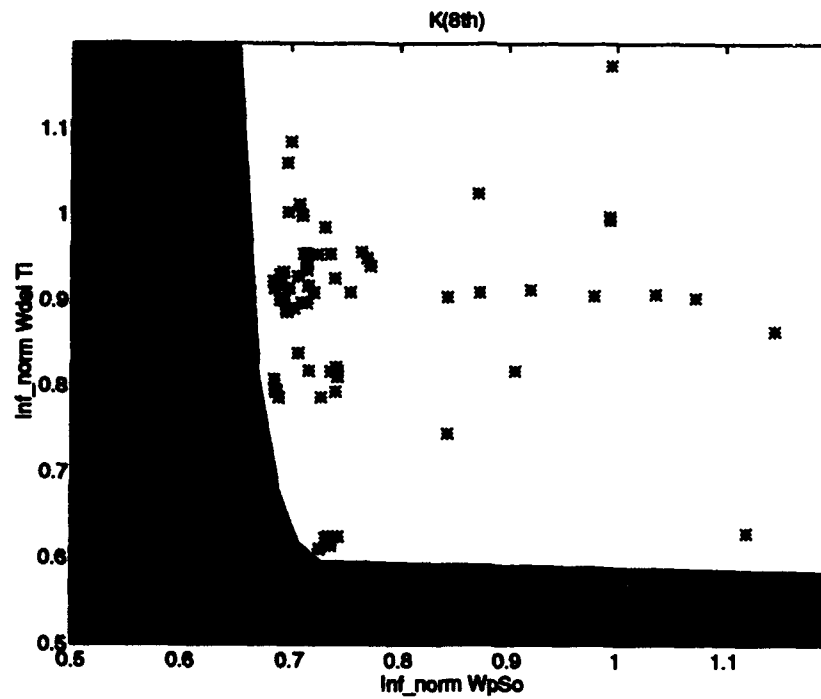


Figure A-2 Boundary for the eight order controller with two and three H_∞ constraints

Bibliography

- [ABSB92] Adams, R., Buffington, J., Sparks, A. and Banda, S. (1992). "An Introduction to multivariable flight control system design", WL-TR-92-3110.
- [BDGPS91] Balas, G., Doyle, J., Glover, K., Packard, A. and Smith, R (1991). *μ -Analysis and Synthesis Toolbox*, The Mathworks. Inc.
- [BH89] Bernstein, D.S. and Haddad, W.H. (1989). "LQG control with an H_{∞} performance bound: A Riccati equation approach", *IEEE Trans. Auto. Control* AC-34(3):293-305.
- [Dai90] Dailey, R. (1990). "Lectures notes for the workshop on H_{∞} and μ Methods for robust control", *American Control Conference*, San Diego, CA.
- [Doy82] Doyle, J. (1982). "Analysis of feedback systems with structured uncertainty", *IEEE Proceedings*, Vol. 129, Part D, no. 6, pp.242-250.
- [Doy85] Doyle, J. "Structured uncertainty in control system design", *Proc. of IEEE Conference on Decision and Control*, Fort Lauderdale, FL. Dec 1985, pp. 260-265
- [DD93] Dahleh, M. and Diaz, I. (1993). "Control of Uncertain Systems". Preprint.
- [DFT92] Doyle, J., Francis, B. and Tannenbaum, A. (1992). "Feedback Control Theory", Macmillan Publishing Company.
- [DGKF89] Doyle, J., Glover, P., Khargonekar, P. and Francis, B. (1989). "State-Space solutions to standard H_2 and H_{∞} control problems", *IEEE Trans. Auto. Control*, Vol. 34, no. 8:831-847.

- [DWS82] Doyle, J., Wall, J. and Stein, G. (1982). "Performance and robustness analysis for unstructured uncertainty", *Proceeding of the 20th Conference on Decision and Control*, pp. 629-636.
- [DZB89] Doyle, J., Zhou, K., and Bodenheimer, B. (1989). "Optimal Control with mixed H_2 and H_∞ performance objectives", *Proceeding of the American Control Conference*, Pittsburgh PA, pp. 2065-2070.
- [GL93] Giesy, D. and Lim, K. (1993). " H_∞ norm sensitivity formula with control system design applications", *Journal of Guidance, Control, and Dynamics*, **16**(6):1138-1145.
- [KDGB90] K.Zhou, Doyle, J., Glover, K. and Bodenheimer, B. (1990). "Mixed H_2 and H_∞ control", *Proceeding of the American Control Conference*, San Diego CA, pp. 2502-2507.
- [KR91] Khargonekar, P. and Rotea, M. (1991). "Mixed H_2/H_∞ control: A convex optimization approach", *IEEE Trans. Auto. Control* AC-36(7):824-837.
- [Mat] MatLab and Simulink software. The MathWorks, Inc.
- [MG88] Mustafa, D. and Glover, K. (1988). "Controllers which satisfy a closed-loop H_∞ -norm bound and maximize an entropy integral", *Proceeding of the 27th Conference on Decision and Control*, Austin TX, pp. 959-964.
- [MG90] Mustafa, D. and Glover, K. (1990). "Minimum entropy H_∞ control", *Lectures Notes in Control & Information Sciences*, Springer-Verlag.
- [PD93] Packard, A. and Doyle, J. (1993). "The complex structured singular value", *Automatica*, Vol. 29, no. 1 pp:71-109.
- [Rid91] Ridgely, D. (1991). "A nonconservative solution to the general mixed H_2/H_∞ optimization problem". Ph.D. dissertation. MIT, Cambridge MA.
- [RMV92] Ridgely, D., Mracek, C. and Valavani, L. (1992). "Numerical solution of the general mixed H_2/H_∞ optimization problem", *Proceedings of the American Control Conference*, Chicago, IL, pp. 1353-1357.

- [RVDS92] Ridgely, D., Valavani, L., Dahleh, M. and Stein, G. (1992). "Solution to the general mixed H_2/H_∞ control problem-necessary conditions for optimality", *Proceeding of the American Control Conference*, Chicago, IL, pp. 1348-1352.
- [SLH81] Safonov, M., Laub, A. and Hartman, G. (1981). "Feedback properties of multivariable system: The role and use of the return difference matrix", *IEEE Transactions on Automatic Control*, Vol. AC-26, no. 1.
- [UWR94] Ullauri, J., Walker, D. and Ridgely, D. (1994). "Reduced order mixed H_2/H_∞ optimization with multiple H_∞ constraints", To appear in *AIAA Guidance, Navigation and Control Conference*, August.
- [Wal94] Walker, D (1994). " H_2 Optimal Control with H_∞ , μ and L_1 Constraints". Ph.D. dissertation. Air Force Institute of Technology, WPAFB OH.
- [WR94a] Walker, D. and Ridgely, D (1994). "Reduced order mixed H_2/H_∞ optimization with a singular H_∞ constraint", To appear in the *Proceedings of the 1994 American Control Conference*.
- [WR94b] Walker, D. and Ridgely, D (1994). "Mixed H_2/μ Optimization", Submitted to the *13th Symposium on Automatic Control in Aerospace(1994)*.
- [WR94c] Walker, D. and Ridgely, D (1994). "Uniqueness of the General Mixed H_2/H_∞ Optimal Controller", Submitted to the *33rd conference on Decision and Control*.
- [YBC90] Yeh, H., Banda, S., and Chang, B. (1990). "Necessary and sufficient conditions for mixed H_2 and H_∞ optimal control", *Proceedings of the 29th Conference on Decision and Control*, Honolulu HI, pp. 1013-1017.

REPORT DOCUMENTATION PAGE			Form Approved OMB No. 0704-0188	
<small>Public reporting burden for this collection of information is estimated to average 1 hour per response, including the time for reviewing instructions, searching existing data sources, gathering and maintaining the data needed, and completing and reviewing the collection of information. Send comments regarding this burden estimate or any other aspect of this collection of information, including suggestions for reducing this burden, to Washington Headquarters Services, Directorate for Information Operations and Reports, 1215 Jefferson Davis Highway, Suite 1204, Arlington, VA 22202-4302, and to the Office of Management and Budget, Paperwork Reduction Project (0704-0188), Washington, DC 20503.</small>				
1. AGENCY USE ONLY (Leave blank)	2. REPORT DATE June 1994	3. REPORT TYPE AND DATES COVERED Master's Thesis		
4. TITLE AND SUBTITLE MIXED H_2/H_∞ OPTIMIZATION WITH MULTIPLE H_∞ CONSTRAINTS		5. FUNDING NUMBERS		
6. AUTHOR(S) Julio C. Ullauri, 1Lt, Ecuador AF				
7. PERFORMING ORGANIZATION NAME(S) AND ADDRESS(ES) Air Force Institute of Technology, WPAFB OH 45433		8. PERFORMING ORGANIZATION REPORT NUMBER AFIT/GAE/ENY/94J-04		
9. SPONSORING / MONITORING AGENCY NAME(S) AND ADDRESS(ES) Mr Marc Jacobs AFOSR/NM Bolling AFB, MD 20332-0001		10. SPONSORING / MONITORING AGENCY REPORT NUMBER		
11. SUPPLEMENTARY NOTES Approved for public release; distribution unlimited				
12a. DISTRIBUTION / AVAILABILITY STATEMENT			12b. DISTRIBUTION CODE	
13. ABSTRACT (Maximum 200 words) A general mixed H_2/H_∞ optimal control design with multiple H_∞ constraints is developed and applied to two systems, one SISO and the other MIMO. The SISO design model is normal acceleration command following for the F-16. This design constitutes the validation for the numerical method, for which boundaries between the H_2 design and the H_∞ constraints are shown. The MIMO design consists of a longitudinal aircraft plant (short period and phugoid modes) with stable weights on the H_2 and H_∞ transfer functions, and is linear-time-invariant. The controller order is reduced to that of the plant augmented with the H_2 weights only. The technique allows singular, proper (not necessarily strictly proper) H_∞ constraints. The analytical nature of the solution and a numerical approach for finding suboptimal controllers which are as close as desired to optimal is developed. The numerical method is based on the Davidson-Fletcher-Powell algorithm and uses analytical derivatives and central differences for the first order necessary conditions. The method is applied to a MIMO aircraft longitudinal control design to simultaneously achieve Nominal Performance at the output and Robust Stability at both the input and output of the plant.				
14. SUBJECT TERMS Optimization, Optimal Control, H_2 , H_∞ , μ , Mixed H_2/H_∞ , Single and multiple H_∞ constraints, SISO, MIMO, F-16, HIMAT			15. NUMBER OF PAGES 131	
			16. PRICE CODE	
17. SECURITY CLASSIFICATION Unclassified	18. SECURITY CLASSIFICATION OF TITLE Unclassified	19. SECURITY CLASSIFICATION OF ABSTRACT Unclassified	20. LIMITATION OF ABSTRACT UL	

GENERAL INSTRUCTIONS FOR COMPLETING SF 298

The Report Documentation Page (RDP) is used in announcing and cataloging reports. It is important that this information be consistent with the rest of the report, particularly the cover and title page. Instructions for filling in each block of the form follow. It is important to *stay within the lines* to meet optical scanning requirements.

Block 1. Agency Use Only (Leave blank).

Block 2. Report Date. Full publication date including day, month, and year, if available (e.g. 1 Jan 88). Must cite at least the year.

Block 3. Type of Report and Dates Covered. State whether report is interim, final, etc. If applicable, enter inclusive report dates (e.g. 10 Jun 87 - 30 Jun 88).

Block 4. Title and Subtitle. A title is taken from the part of the report that provides the most meaningful and complete information. When a report is prepared in more than one volume, repeat the primary title, add volume number, and include subtitle for the specific volume. On classified documents enter the title classification in parentheses.

Block 5. Funding Numbers. To include contract and grant numbers; may include program element number(s), project number(s), task number(s), and work unit number(s). Use the following labels:

C - Contract	PR - Project
G - Grant	TA - Task
PE - Program Element	WU - Work Unit Accession No.

Block 6. Author(s). Name(s) of person(s) responsible for writing the report, performing the research, or credited with the content of the report. If editor or compiler, this should follow the name(s).

Block 7. Performing Organization Name(s) and Address(es). Self-explanatory.

Block 8. Performing Organization Report Number. Enter the unique alphanumeric report number(s) assigned by the organization performing the report.

Block 9. Sponsoring/Monitoring Agency Name(s) and Address(es). Self-explanatory.

Block 10. Sponsoring/Monitoring Agency Report Number. (If known)

Block 11. Supplementary Notes. Enter information not included elsewhere such as: Prepared in cooperation with...; Trans. of...; To be published in.... When a report is revised, include a statement whether the new report supersedes or supplements the older report.

Block 12a. Distribution/Availability Statement. Denotes public availability or limitations. Cite any availability to the public. Enter additional limitations or special markings in all capitals (e.g. NOFORN, REL, ITAR).

DOD - See DoDD 5230.24, "Distribution Statements on Technical Documents."

DOE - See authorities.

NASA - See Handbook NHB 2200.2.

NTIS - Leave blank.

Block 12b. Distribution Code.

DOD - Leave blank.

DOE - Enter DOE distribution categories from the Standard Distribution for Unclassified Scientific and Technical Reports.

NASA - Leave blank.

NTIS - Leave blank.

Block 13. Abstract. Include a brief (*Maximum 200 words*) factual summary of the most significant information contained in the report.

Block 14. Subject Terms. Keywords or phrases identifying major subjects in the report.

Block 15. Number of Pages. Enter the total number of pages.

Block 16. Price Code. Enter appropriate price code (*NTIS only*).

Blocks 17. - 19. Security Classifications. Self-explanatory. Enter U.S. Security Classification in accordance with U.S. Security Regulations (i.e., UNCLASSIFIED). If form contains classified information, stamp classification on the top and bottom of the page.

Block 20. Limitation of Abstract. This block must be completed to assign a limitation to the abstract. Enter either UL (unlimited) or SAR (same as report). An entry in this block is necessary if the abstract is to be limited. If blank, the abstract is assumed to be unlimited.